Ministry of Higher Education and Scientific Research

Al-Karkh University of Science

College of Remote Sensing and Geophysics

Department of Geophysics

Methods in Geophysical Data Interpretation

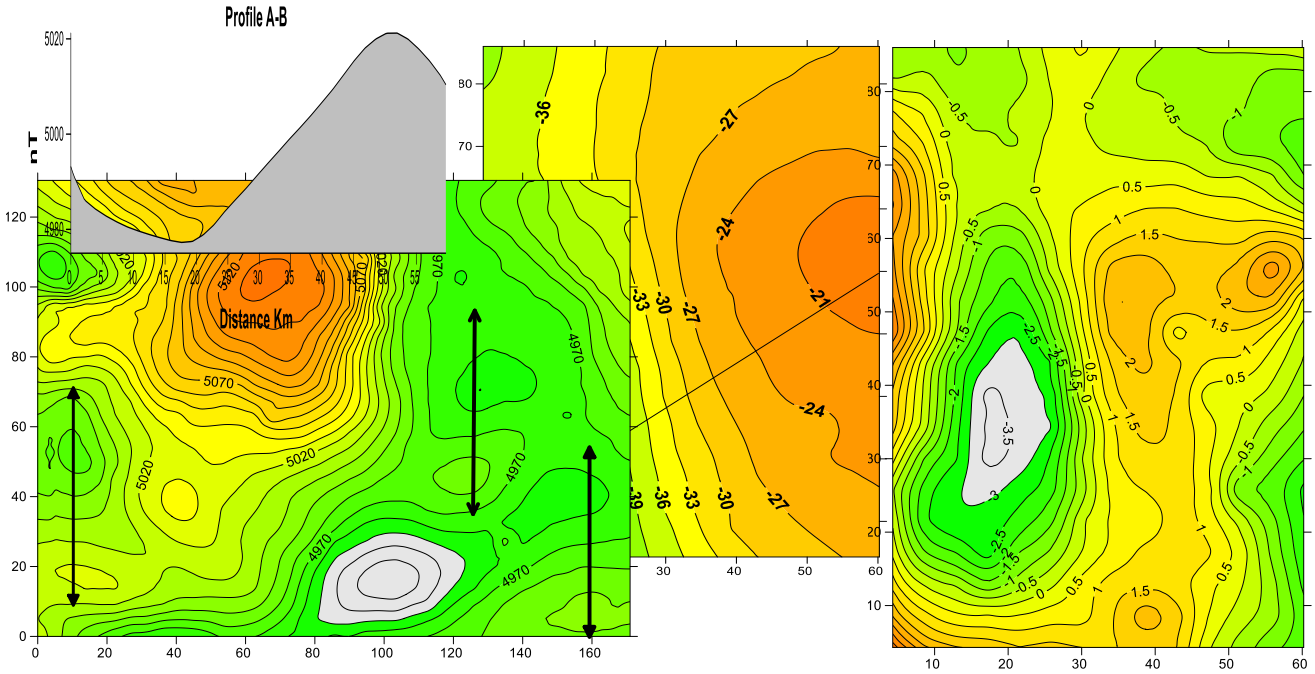

4th Level Lectures Edited by:

Assistant Professor Dr. Wadhah Mahmood Shakir Al-Khafaji

Introduction

In this course the geophysics students learn how to deal with geophysical data processing and interpretation in a way that considers the reduction of ambiguity which accompanies interpretation as much as possible. There are several geophysical methods applied on field according to the aim or target that geophysists is looking for. Most of oil exploration geophysical investigation surveys use the seismic reflection method. Other methods like seismic refraction are more suitable for environmental and engineering purposes. The geoelectrical investigations mostly depends on the electrical resistivity and self potential methods in application, especially when it is concerned about the detection for groundwater aquifer subsurface properties including ground water table level , aquifers thickness and the reserving rocks effective porosity and permeability…etc.. The magnetic method is rather more applicable for subsurface metallic mineral ores detection also for subsurface geological structures exploration. The electromagnetic (EM) and Induced Polarization method is more suitable for near surface sulfide ores detection and archaeological sites investigation. In this context, it is important to know about the methods of interpretation which used in processing geophysical data in order to decide which one is more suitable to be used in field according to what is going to be measured from the surface, also to the target or the goal behind achieving the concerned geophysical surveys.

In the last decades, geophysical prospecting applied to the subsurface characterization has been of an increasing interest, particularly in Soil Science. Major advances in this technological domain can be attributed to the development of integrated measure systems, increasing computing power, equipment portability and hardware/software diffusion. In this context, two kinds of technological

platforms can be involved: ground based and proximal technologies, respectively working from the surface and from a flight airborne vector.

Ground-based geophysical instruments are now equipped with digital signal processing and recording capabilities previously restricted to large corporate computing centers. This improved computational capacity has provided investigators with near real-time results that, in turn, drive improvements in instrument sensors and processing algorithms. Identically, recent airborne geophysics sparked off a strong interest due to the possibilities of flights with civil airplanes equipped with optical, thermal or hyper spectral sensors. The most common methods which took advantages of these enhancements and the related parameters are listed in Table 1.

Table (1): Main ground-based and airborne geophysical methods and related physical measured parameters.

Geophysical methods	Physical parameters
Ground-penetrating radar (GPR):	Dielectric permittivity, electric conductivity, magnetic permeability, frequency dependence of these electromagnetic properties
Seismic reflection and refraction:	Volume and shear-wave velocities
Electromagnetic induction (EMI):	Electrical resistivity (electric conductivity and frequency dependence)
Electrical resistivity (geoelectric):	Electrical resistivity (almost zero-frequency)
Gravity:	*Density*
Magnetics:	Magnetic susceptibility and viscosity
Airborne thermic:	*Surface temperature*
Airborne hyperspectral:	Spectral reflectance
Gammametry:	*Gamma spectrum (U, K, Th)*

Electrical resistivity method

Concept :

Electrical methods represent one of four principal groups of geophysical exploration techniques. The other three are: seismic, gravimetric and magnetic. The latter two differ in that they depend on naturally occurring physical fields. The seismic and most of electrical methods make use of artificial sources; the added control over source position and characteristics offers important advantages. Since each of the four techniques measure the effect of different physical properties of the subsurface materials, each has its field of application. Often a combination of techniques is more effective than one alone (Orellana and Mooney, 1966). Resistivity method has its origin in the 1920's due to the work of Schlumberger brothers. In this method the midpoint of the electrode array remains fixed, but the spacing between the electrodes increased to obtain more information about deeper sections of Subsurface. The most commonly used methods for measuring earth resistivity are those of four electrodes. Current is driven through one pair of electrodes and the potential is measured with second pair of electrodes (Keller and Frischknecht, 1970).

There are a number of ways in which electric current can be employed to investigate subsurface conditions in a certain area. In the most commonly used method the current is driven through the ground by using a pair of electrodes, and the resulting distribution of the potential in the ground is read by using another pair of electrodes connected to a sensitive voltmeter.

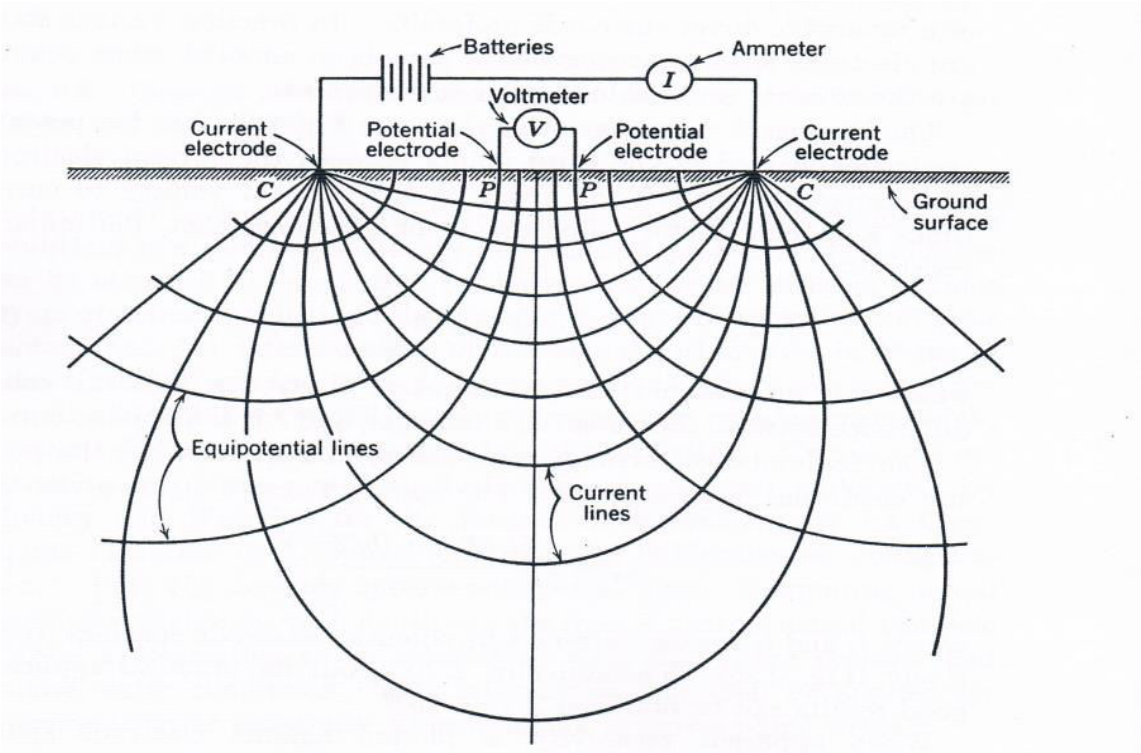

Figure (1): The geometry of current distribution within homogeneous and isotropic subsurface media (Todd, 1959).

From the magnitude of the current applied and from the knowledge of the current electrode separation it is possible to calculate the potential distribution and the path of the current flow if the underground materials were homogeneous. Anomalous conditions or inhomogeneities within the ground, such as electrically better or poorer conducting layers, are inferred from the fact that they deflect the current and distort the normal potentials. This represents briefly the principle of measuring subsurface variation in the electrical resistivity, which is the (reciprocal of conductivity) within the earth. In 1920's the technique of the method was perfected by Conrad Schlumberger, who conducted the first experiments in the field of Normandy (Sharma, 1986).

Geophysical surveys are not always the most effective methods of obtaining the information needed. For example, in some areas auger or drill holes may be more effective way of obtaining near-surface information than geophysical surveys. In some investigations a combination of drilling and geophysical measurements may provide the optimum cost benefit ratio. Geophysical surveys are not practical in all ground-water investigations, but this determination usually can be made only by someone with an understanding of the capabilities, limitations, and costs of geophysical surveys. A clear definition of the geologic or hydrologic problem and objectives of an investigation is important in determining whether exploration geophysics should be used and also in designing the geophysical survey. The lack of a clear definition of the problem can result in ineffective use of geophysical methods. The proper design of a geophysical survey is important not only in insuring that the needed data will be obtained but also in controlling costs, as the expense of making a geophysical survey is determined primarily by the detail and accuracy required (Zohdy, et.al.,1990).

The electrical methods of geophysical exploration include a variety of techniques employing both natural and artificial sources, of which the latter has wider application. Within the artificial source group a distinction may be made between inductive and conductive methods. The inductive methods uses frequencies up to a few thousands cycles per second and the measurement of the electromagnetic field set up by the induced earth currents. The conductive methods involve the use of direct current (DC), or alternating current (AC) with frequencies up to few tens of cycles per second to study the electrical field (Orellana and Mooney, 1966).

Rocks Electrical Conductivity

With the exception of clays and certain metallic ores, the passage of electricity through rocks takes place by way of the groundwater contained in the pores and fissures, while the rock matrix being non conducting. All other factors being constant an increase in the concentration of dissolved salts in the groundwater leads to decrease in resistivity. In general way the resistivity is also controlled by the amount of water present. The more porous or fissured a rock the lower the resistivity. Degree of saturation also affects resistivity which increases with decrease in the amount of water in the pore spaces and fissures (Griffiths and King, 1981).

Most rocks conduct electricity only because of mineralized water in pores and fissures (Brine). This property is called (electrolytic conductivity). Their conductivity depends on the conditions of contained water, the amount of water that is contained, and the manner in which the water is distributed (Kunetz, 1966).

Rocks Bulk or Total Resistivity (ρ_s)

Rocks bulk or total resistivity of rocks (ρ_s) could be expressed as a function of many variables as following:

$$\rho_s = f(c,n,S_w,T_p,Q,\rho_m,\rho_w)$$

Where: c=clay content, n = porosity , S_w=degree of rock saturation with brine, T_p= temperature, Q= Ionic exchange, ρ_m= solid part or rock grains resistivity, $\rho_{w=}$ Brine resistivity.

Current Behavior In Homogeneous Ground

The property of the electrical resistance of a material is usually expressed in terms of its resistivity. If the resistance between opposite faces of a conductive cylinder of length (L) and cross sectional area (A) is (R), (Figure (2)), the resistivity (ρ) is expressed as:

$$\rho = R\ A/L$$

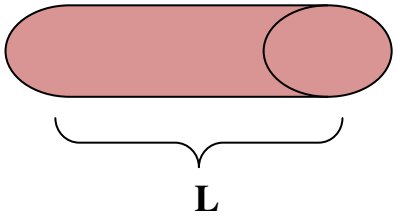

Figure (2): The resistivity of a conductive cylindrical body.

The simplest approach to the theoretical study of the current flow in the earth is to consider first the case of completely homogeneous isotropic earth layer of uniform resistivity. For a quantitative treatment, let us consider a homogeneous layer of length (L) and resistance (R) through which a current (I) is flowing. The potential difference across the ends of the resistance is given by Ohm's law and is:

$$\Delta V = RI$$

While: $\rho = R\ A/L$

The resistance, R, of the layer is specified by its length (L), of cross section area (A), and the resistivity (ρ). By definition: $R = \rho\ L / A$, and, therefore the equation can be written as the following:

$$\Delta V / L = \rho\ I / A$$

Where: I= current in Ampere (A) or mille Ampere (mA), L= length of the bead or layer, ΔV= potential difference in Volts (V)

The current density for each cross-sectional unit could be defined as (i), and the potential gradient could be expressed as (grad V), where:

$$\text{Grad } V = \rho i$$

If a semi-infinite conducting layer of uniform resistivity bounded by the ground surface and a current strength (+I) enters at point (A) on the ground surface, (Figure 3).The current will flow away radially from the point of entry and at any instant its distribution will be uniform over a hemispherical surface of the underground resistivity (ρ).

At a distance (r), away from the current source, the current density (i) would be (Sharma, 1986):

$$i = I / 2\pi r^2$$

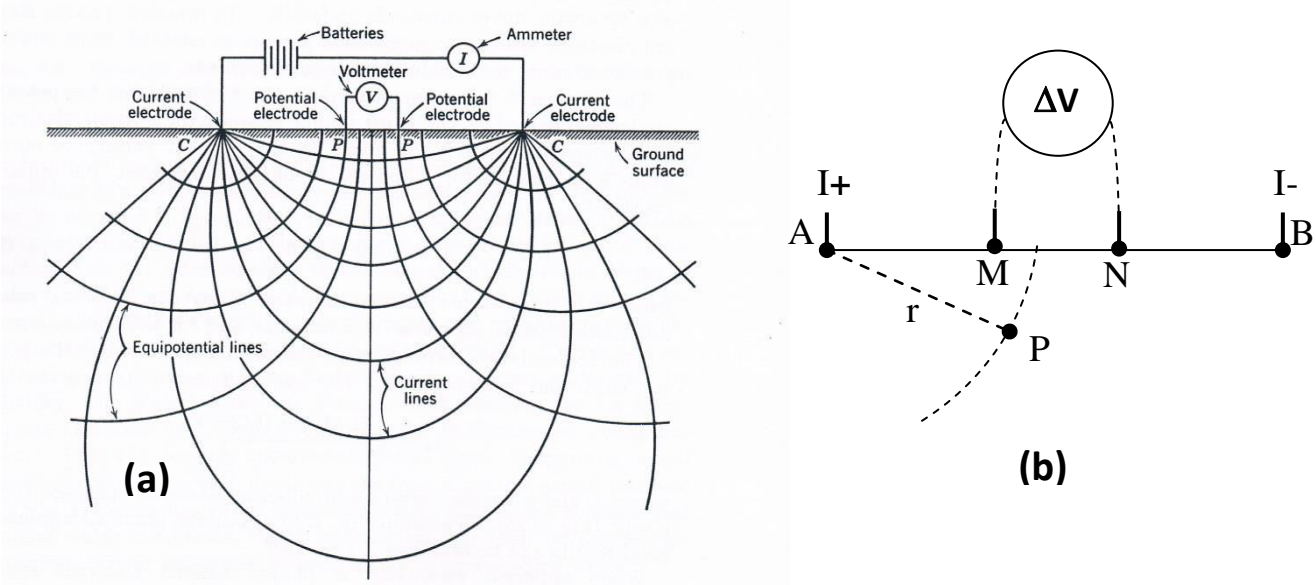

Figure (3): (a) The geometry of current distribution within homogeneous and isotropic subsurface media (Todd, 1959).

(b) Method of calculating potential distribution due to a current source in a homogeneous medium (Sharma, 1986).

as: Grad V = ρi

The potential gradient $-\frac{\delta V}{\delta r}$ associated with the current is given by:

$$-\frac{\delta V}{\delta r} = \rho i = \rho I / 2\pi\ r^2$$

By integration we get:

$$V = \rho I / 2\pi\ r$$

The potential at distance (r) (e.g., at point (P) in figure (3,(b)) , is obtained by integrating the previous equation and is :

$$V_M^A = \rho I / 2\pi\, r$$

This is the basic equation which enables the calculation of the potential distribution in a homogeneous conducting semi-infinite medium.

The potential difference (ΔV) between the potential electrodes M and N , Figure(3,(b)) which caused by current (+I) at the source entry point (A) is:

$$\Delta V_{MN}^A = \frac{\rho I}{2\pi}\left(\frac{1}{AM} - \frac{1}{AN}\right)$$

In the same manner, the potential difference (ΔV) between the points M and N , caused by (-I) current at the (sink) or exit point (B) is :

$$\Delta V_{MN}^B = \frac{-\rho I}{2\pi}\left(\frac{1}{BM} - \frac{1}{BN}\right)$$

The total potential difference between M and N is therefore, given by the sum of the right-hand sides of the previous two equations, and is:

$$\Delta V_{MN}^{AB} = (\Delta V_{MN}^A + \Delta V_{MN}^B)$$

Or

$$\Delta V_{MN}^{AB} = \frac{\rho I}{2\pi}\left(\frac{1}{AM} - \frac{1}{AN} - \frac{1}{BM} + \frac{1}{BN}\right)$$

$(\frac{1}{AM} - \frac{1}{AN} - \frac{1}{BM} + \frac{1}{BN})$ is called the geometrical factor (G).

Then the potential difference between M and N could be written as:

$$\Delta V_{MN}^{AB} = \frac{\rho IG}{2\pi}$$

A more simple way to write the previous equation is:

$$\Delta V\ 2\pi = \rho IG$$

Or:

$$\rho = 2\pi \frac{\Delta V}{I} * \frac{1}{G}$$

(ρ) Will be constant in homogenous and isotropic Medias even if the electrode array or the geometrical factor (G) is changed.

It's common in the geoelectrical – hydrogeological studies to use the Ohm resistivity meter as a field instrument and Schlumberger configuration as a ground electrodes array, (Figure (4)).

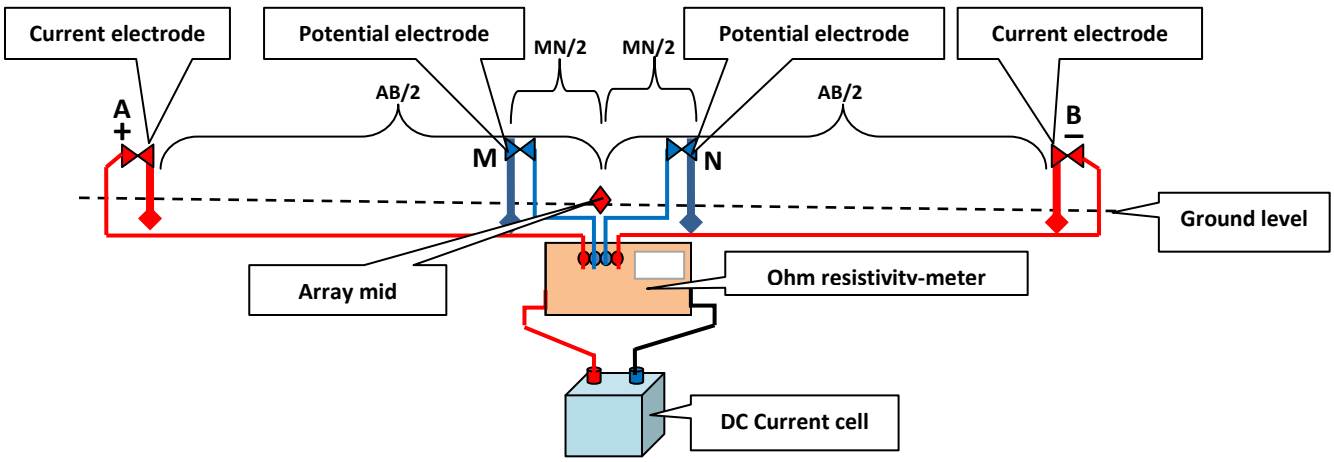

Figure (4): The electrode array for Schlumberger configuration at field resistivity survey, (AL-Khafaji 2014).

Electrode configurations:

From the nature of the method it could be deduced that it is better suited to resolve conductive features than the high resistivity ones. After all, the resistivity method was originally designed for an ore prospection. Nevertheless, the high resistivity anomalies could be detected when an electrode array is carefully selected and the field layout is sufficiently dense. Up to now, we were not considering any special electrode arrangement. Essentially, four electrodes are necessary, however, their positioning substantially influence the results and could be the factor determining whether the survey is successful or not. The different arrays have different sensitivities for the subsurface inhomogeneities and also a different resistance to a noise. In general, the more sensitive array the more prone to a noise it is.

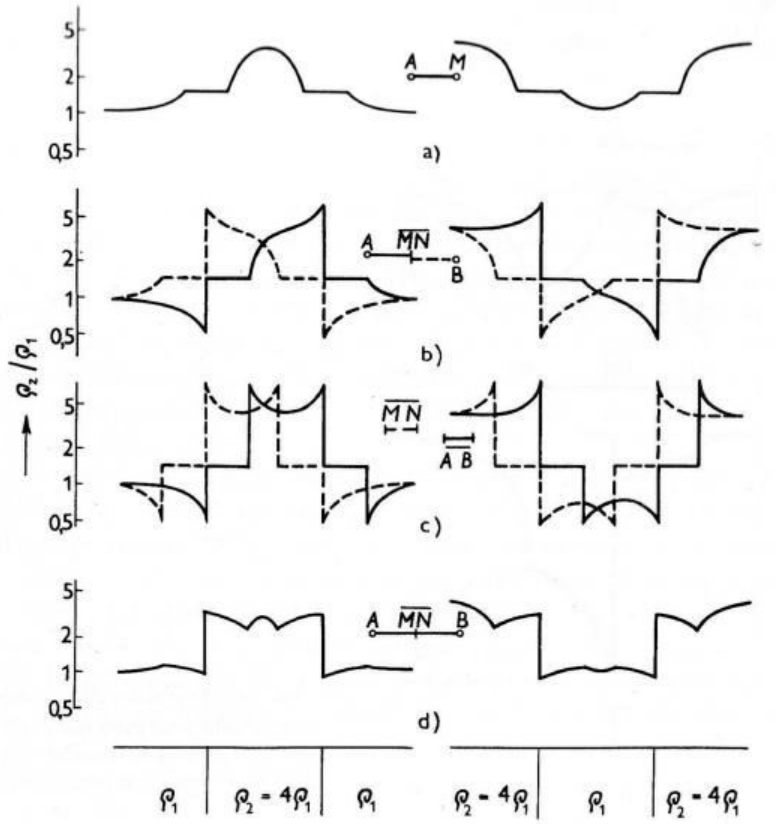

Figure: Apparent resistivity (ρa) curves over a thick dyke (Mareš and Tvrdý 1984). a) Potential array. b) Pole-dipole and reversed pole-dipole array. c) Dipole-dipole array. d) Schlumberger array. The reference point (the point at which the measured resistivities are plotted) is in the middle of the potential dipole (or at the potential electrode in case of the potential array).

The electrode configuration inevitably influences the current and potential readings. To be able to compare measurements with different electrode arrays, the measured values must be corrected for the effect of electrode configuration. This is carried out by multiplying readings with a constant of the array, k:

$$\rho = k\frac{\Delta V}{I}.$$

The constant of the array depends only on the distances between individual electrodes:

$$k = \frac{2\pi}{\frac{1}{C_1P_1} - \frac{1}{C_1P_2} + \frac{1}{C_2P_2} - \frac{1}{C_2P_1}}.$$

Hence the farther the current electrodes are the smaller potential is read. When the potential is too small to be read accurately then, either a better electrode grounding and more powerful electrode source is needed, or increasing the distance between the potential electrodes is necessary. Also, using different electrode array could help, however, changing the array inevitably changes parameters of the whole survey. The most common electrode arrays are demonstrated in the next figure.

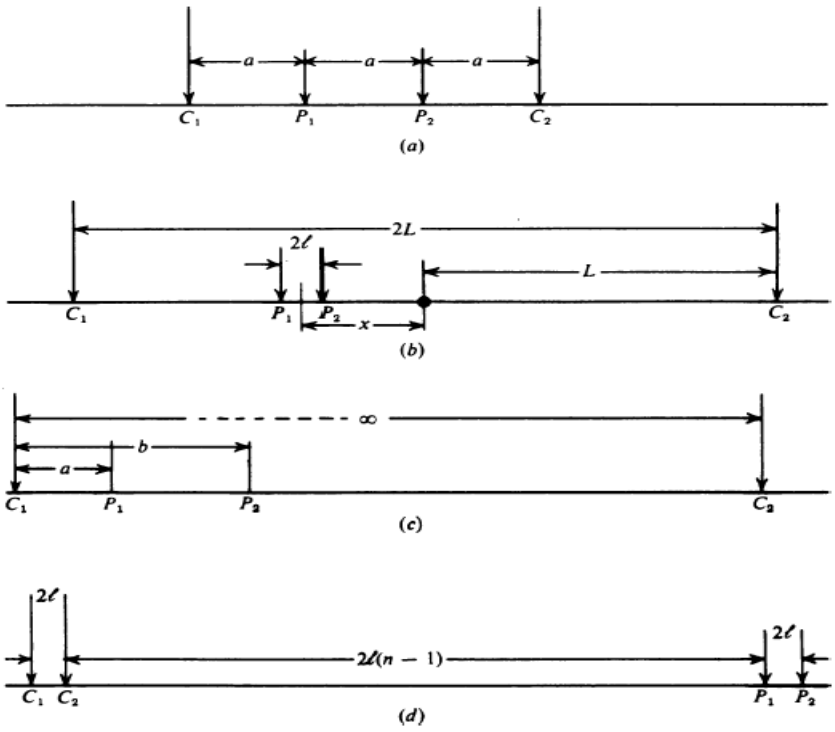

Figure: Commonly used electrode arrays (Telford et al. 1990). (a) Wenner (potential) array. All the distances between electrodes are equal. (b) Schlumberger (gradient) array. The distance between the potential electrodes is much smaller than the distance between the potential and current electrodes. The most common configuration is to put the measuring dipole in the center of the array. (c) Pole-dipole array. One of the current electrodes is much further from the measuring dipole than the second one. (d) Dipole-dipole array. The measuring dipole is remote from the current electrodes.

They can be divided into three basic groups: potential, gradient and dipole arrays. The potential arrays measure potential between two relatively distant electrodes, the values of voltages read are large (due to the large distance between potential electrodes) and hence this type of arrays is suitable for surveys with difficulties with grounding of electrodes or where the noise level is high. The gradient arrays measures potential difference between two closely spaced electrodes. If this spacing is sufficiently small (zero distance in theory) we can assume that we measure the gradient (the first derivative of potential). Therefore, the measured changes of resistivities will be sharper at boundaries of anomalous bodies. On the other hand, the recorded values of voltages are lower than in the case of potential arrays and the noise level is higher. The dipole arrays are the most sensitive, but

also the most affected by the noise and also the resistivity curve could be overcomplicated in case of complex geological conditions.

The properties of the most common electrode arrays are summarized below:

Wenner array: This potential array has a relatively large distance between the potential electrodes compared with the distance between the potential and current electrodes. Hence the potential readings would be reasonably large and the array is suitable for areas with poor grounding conditions or areas where a high amount of noise is expected.

Schlumberger array: This is a very versatile array. Since it is a gradient array, the measured anomalies are narrower and better localized than in the case of the Wenner array. This configuration is often used in sounding.

Pole-dipole array: This is a three electrode gradient array. One of the current electrode is placed in a large distance (in infinity") from the array and does not move with it. The necessary distance is at least five times the distance between the remaining current electrode and the measuring (potential) dipole. In this case, the effect of the distant electrode is negligible and the electric field of the near electrode resembles that of a point source rather than the field of a dipole. Often used configuration is a combination of two pole-dipole arrays – forward and reversed one. The potential dipole is common for both and the forward dipole has a current electrode on one side of the potential dipole whereas the reversed dipole on the other side. The current electrode in the "infinity" is, again, common for both. Two measurements are taken on each point – forward and reversed, employing both of the current electrodes (an average of these two readings gives the value that would be read if the Schlumberger array would be used). The main benefit is in

profiling, where changes in resistivities are clearly mapped. It has a good ratio between the sensitivity and noise.

Dipole-dipole array: This is the most sensitive array of those mentioned, however, also the most prone to the noise. The measured resistivity values clearly delineate subsurface structures, but the image produced is complicated, with side lobes, etc., which makes things complicated when a complex geology is encountered. The depth estimate with this configuration could be approximately the one fourth the distance the centers of the dipoles. However, the maximal recommended separation between the dipoles is a fifth or six times the distance between electrodes in the dipole. If the distance is larger, too low voltages are read and an error of measurements rapidly increases. If a larger depth of penetration is required, larger separation of electrodes in the dipoles is needed.

Potential array: One of the potential and one of the current electrodes are far way (in "infinity") and only one potential and one current electrode is moving along the profile. The advantage is that only two persons are required for operating the array. The serious disadvantage, however, is that the long wire between potential electrodes induces a lot of noise.

Vertical electrical sounding

A vertical electrical sounding (VES) is a resistivity method enabling detection of changes of resistivities with depth. Resistivities in different depth levels are measured by increasing a distance between current electrodes, while potential ones remains at one place. The result is changes of resistivities below the measurment point. This is similar to, say, a borehole with the difference that one VES measurement is much quicker and cheaper. On the other hand, the geophysical measurement suffers from non-uniqueness and also the geophysical parameters not

necessarily correspond to the geological ones. Hence the best way is to carry out the geophysical research and subsequently verify the results with several boreholes on selected places. The VES measurements are most often used for assessing interfaces within the sedimentary basins – geological mapping, hydrogeological applications (mapping of potential aquifers), find depth to bedrock for the constructions industry, etc.

As was stated earlier, the most common electrode array for the VES measurements is the Schlumberger array. the main reason is that for changing the depth reach only the current electrodes needed to be moved (in contrast to Wenner or dipole-dipole array). Hence, to measure the VES point, the electrodes are positioned at the desired point and the current and voltage values for the first current electrode separation (depth level) are measured. The resistivity is computed and plotted into the log-log graph as it shown in the next figure.

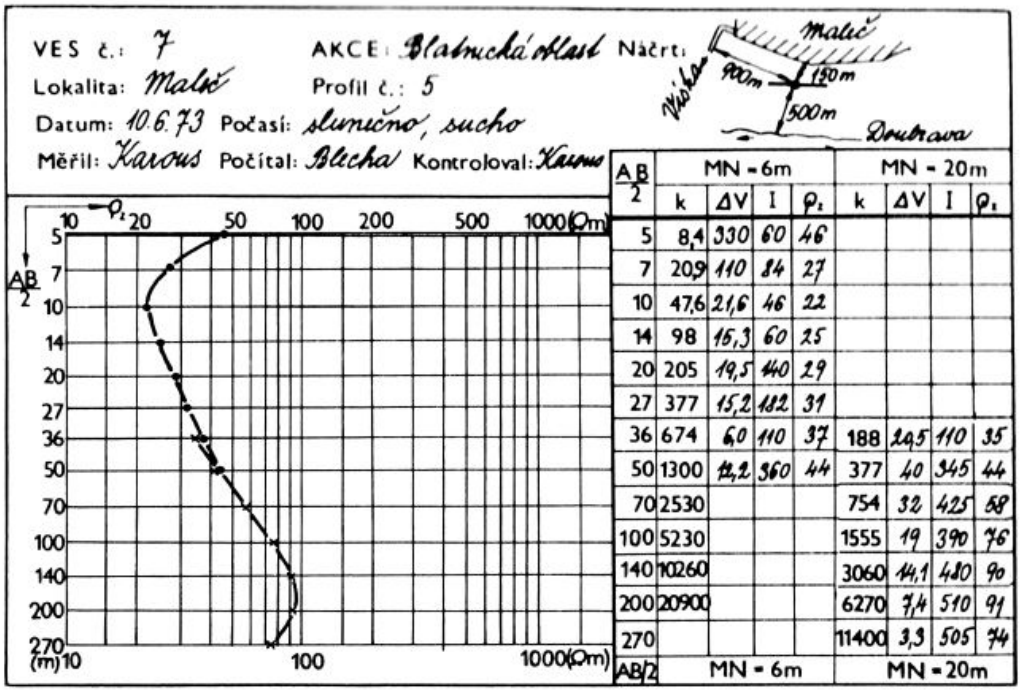

AB/2	MN = 6m k	ΔV	I	ρ_1	MN = 20m k	ΔV	I	ρ_1
5	8,4	330	60	46				
7	20,9	110	84	27				
10	47,6	21,6	46	22				
14	98	15,3	60	25				
20	205	19,5	440	29				
27	377	15,2	182	31				
36	674	6,0	110	37	188	24,5	110	35
50	1300	12,2	360	44	377	40	345	44
70	2530				754	32	425	58
100	5230				1555	19	390	76
140	10260				3060	14,1	480	90
200	20900				6270	7,4	510	91
270					11400	3,3	505	74
AB/2	MN = 6m				MN = 20m			

Figure: An example of the VES terrain chart (Mareš and Tvrdý 1984). For surveys mapping the near surface in more detail the first AB/2 (half of the current electrode separation) is usually 1m and the starting MN (potential electrodes) distance is also 1 m. Note that the AB/2 distances are equidistantly sampled in a log scale. This is due to the exponential decrease of resolution with depth.

Then the current electrodes are moved to the next position, values measured, plotted, etc. When the measured potential becomes too low, it is necessary to increase the distance between the potential electrodes. In this case it is necessary to measure several points with both potential dipole separations to be able to connect both sets of measurements, see the next figure.

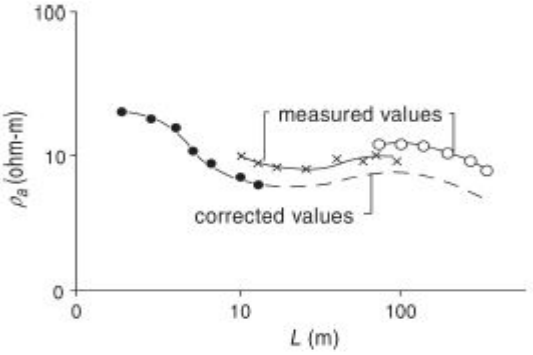

Figure: The individual branches of the resistivity curves could have offset if different potential electrode separations are used. Measuring several points with both offsets gives the redundancy necessary for correction. (Musset and Khan 2000.)

Finally, when all the desired points are measured the resistivity curve is checked for smoothness. Any outliers are most likely errors and should be measured once more. To convert measured apparent resistivities to resistivities and current electrode separations into depth of interfaces nowadays an inversion process is carried out on the computer. In past, a set of master curves like the ones shown in the next figure was used for this task.

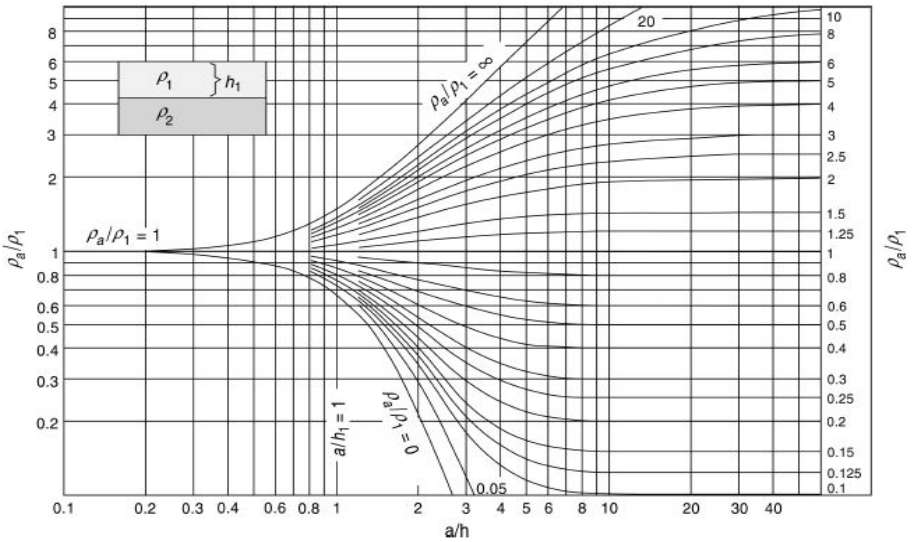

Figure: Wenner array master curves for two layers (Musset and Khan 2000).

Anyway, even a computer modelling requires certain experience with assessing layers to field data However, first of all the principle of equivalence have to be mentioned.

The principle of equivalence limits the uniqueness of the interpretation for thin layers. If there is a thin layer with resistivity much higher than the surrounding layers (see the next figure) then replacing the layer with another one with the same product of (t.ρ) has a negligible effect on readings (t being a thickness of the layer). Conversely, if the thin layer has the resistivity lower then layers having the same ratio of (t/ρ) will appear the same.

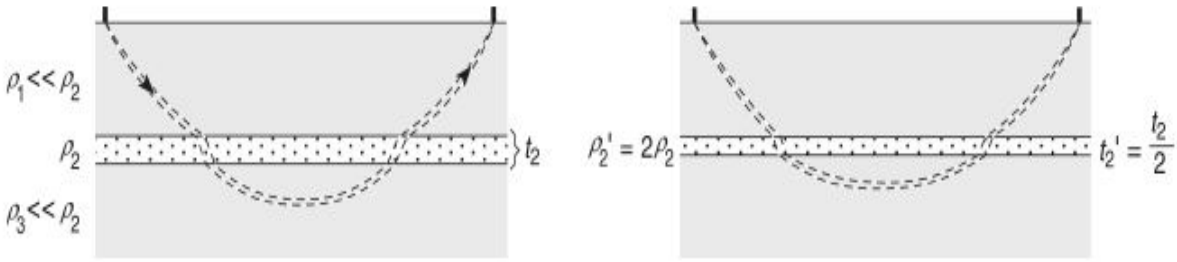

Figure: Principle of equivalence (Musset and Khan 2000).

To assess the starting model for further inversion, first of all, one have to decide, how many layers are present. Every change of the direction of the measured resistivity curve indicates a layer that could be detected. For the two layer case the curves looks as those on the master curve diagram. They start at the resistivity of the upper layer and slowly changes to the value of resistivity of the bottom layer (asymptotically – it will reach that value at infinity). In case three layers are present, the resulting model consists of two two-layer cases (see the following figure).

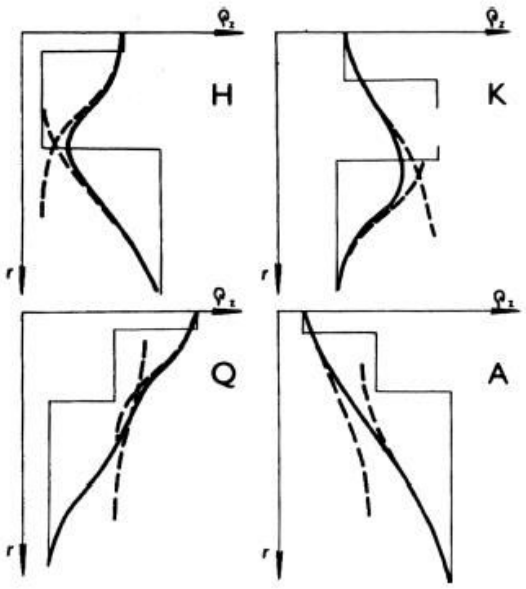

Figure: The four types of three layer curves and corresponding two layer cases (Mareš andTvrdý 1984).

Curves start at the resistivity value of the uppermost layer, then slowly changes to the resistivity values of the second layer, but will not reach it, and, finally, turns to the resistivity value of the third layer. The more complex models could be constructed in a similar way.

When the starting model is completed, the computer is used to fine-tune the model to fit the data (see the following figure).

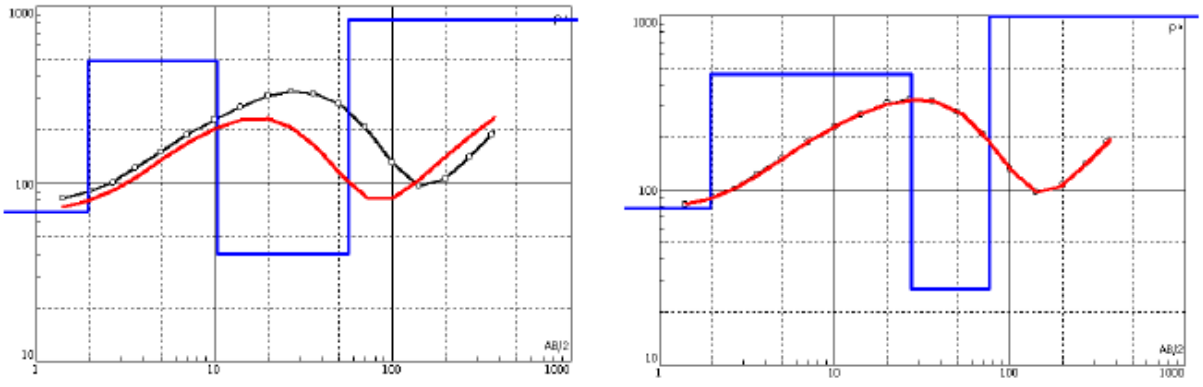

Figure: Example of a VES curve inversion. The approximate starting model (left) is adjusted to a perfectly fitting model (right).

The presented layer model is useful, when the survey is carried out in the area with layered geology (e.g. sedimentary basins). In case, there is a gradual change of

rocks (e.g. a weathered crystalline complex – the weathered clayey rocks near the surface are becoming less weathered with increasing depth up to the sound rock at large depths), the layer model might not be sufficient. In such case, the model could consists of a large number of layers – each measured point would represent one layer (see the next figure). The large number of thin layers simulates the desired smooth change.

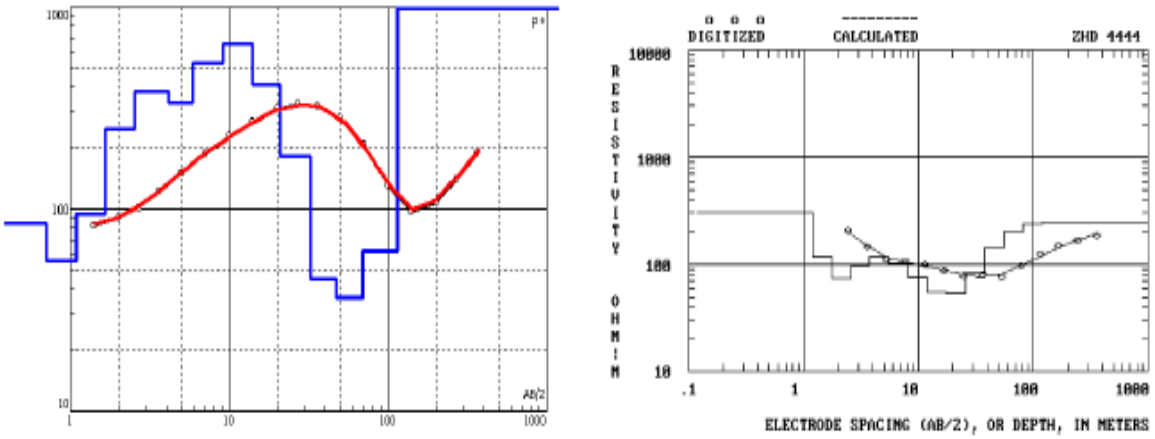

Figure: The VES curve from the previous figure interpreted using a gradient model (left) and a field example of the gradient environment (right) – a VES curve over a weathered granite. Each measured resistivity point represents one layer.

If there are several VES measurements on the profile, the measured apparent resistivity values can be plotted against certain depth estimate (e.g. AB/4 – one fourth of the current electrode distance) to form a resistivity pseudosection (see the following figure). Next, individual sounding curves are interpreted and a geological section could be constructed in a similar way as if the sounding curves were boreholes.

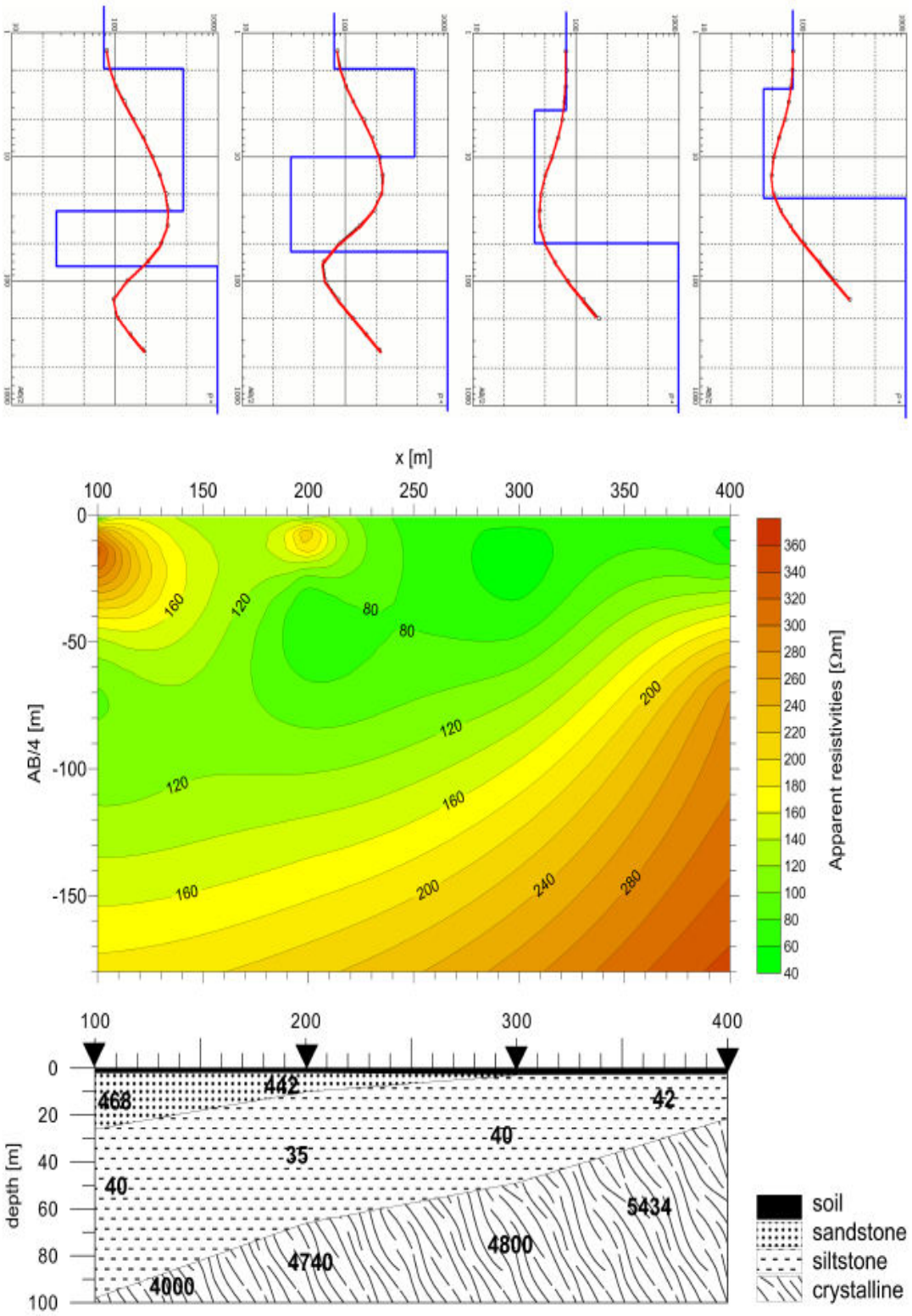

Figure: Four VES curves measured on a profile with a hundred meter distance (top). A resistivity pseudosection (middle) and an interpreted geological section (bottom) created from four VES curves on profile. The distance between individual VES points was 100 m. Interpreted resistivity values are added to the geological section.

Resistivity profiling

In contrast to the sounding examining a resistivity-depth distribution, the resistivity profiling maps lateral distribution of resistivities. The method is very versatile and hence used for various tasks, scales and depths. The depth of investigation is selected by the distance of current electrodes and character of measured anomalies (complexity, precision of anomaly indicators, etc.) depends on the electrode configuration. The small inter-electrode distances could provide a very detailed image of near-surface inhomogeneities for archaeological prospection. In contrast, large inter-electrode distances easily maps depths of tens of meters.

The selection of the electrode array is determined by target structures and desired outputs. If a thin structure (e.g. a fault or a vein) is to be found by several profiles, the best is to use some of the high-resolution arrays, like pole-dipole or dipole-dipole (see the following two figures).

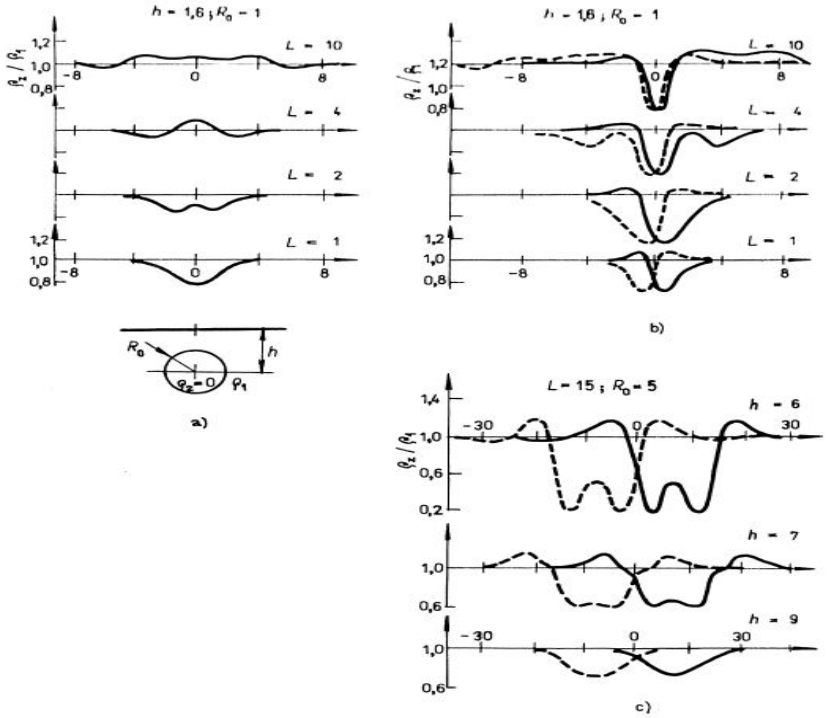

Figure: Resistivity curves over a conductive sphere (Mareš and Tvrdý, 1984). a) Potential array. b) Pole-dipole and reversed pole-dipole. Station is a midpoint of potential electrodes. c) Dipole-dipole array. Station is a midpoint of potential electrodes. R_0 is a diameter of the sphere and h is the depth of its center.

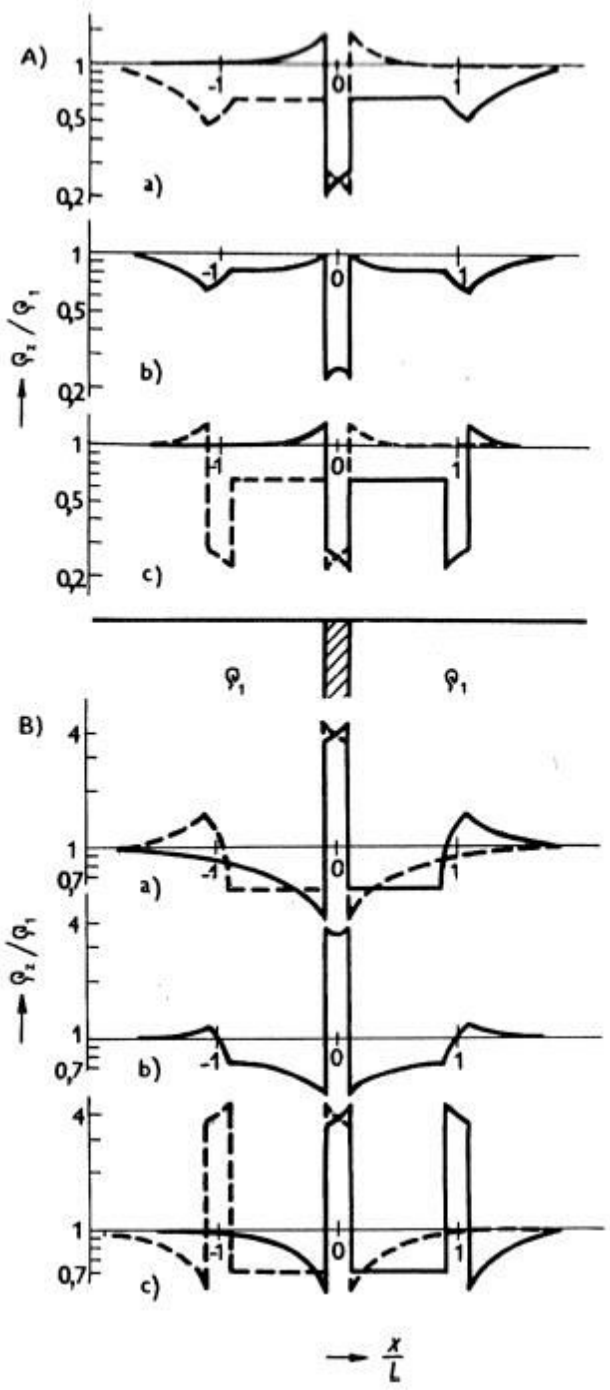

Figure: The resistivity curves over a thin dyke (Mareš and Tvrdý, 1984). a)Pole-dipole and reversed pole-dipole array. b)Schlumberger array. c) Dipole-dipole array.A) The case of a low resistivity dyke. B) The case of a high resistivity dyke. L is the lengthof the array.

On the other hand, if a distribution of resistivities is to be mapped for, e.g. a lateral distribution of fluvial sediments or an archaeological prospection (see the next figure), it is better to choose an array with a simple and clear image – a Wenner or a Schlumberger array.

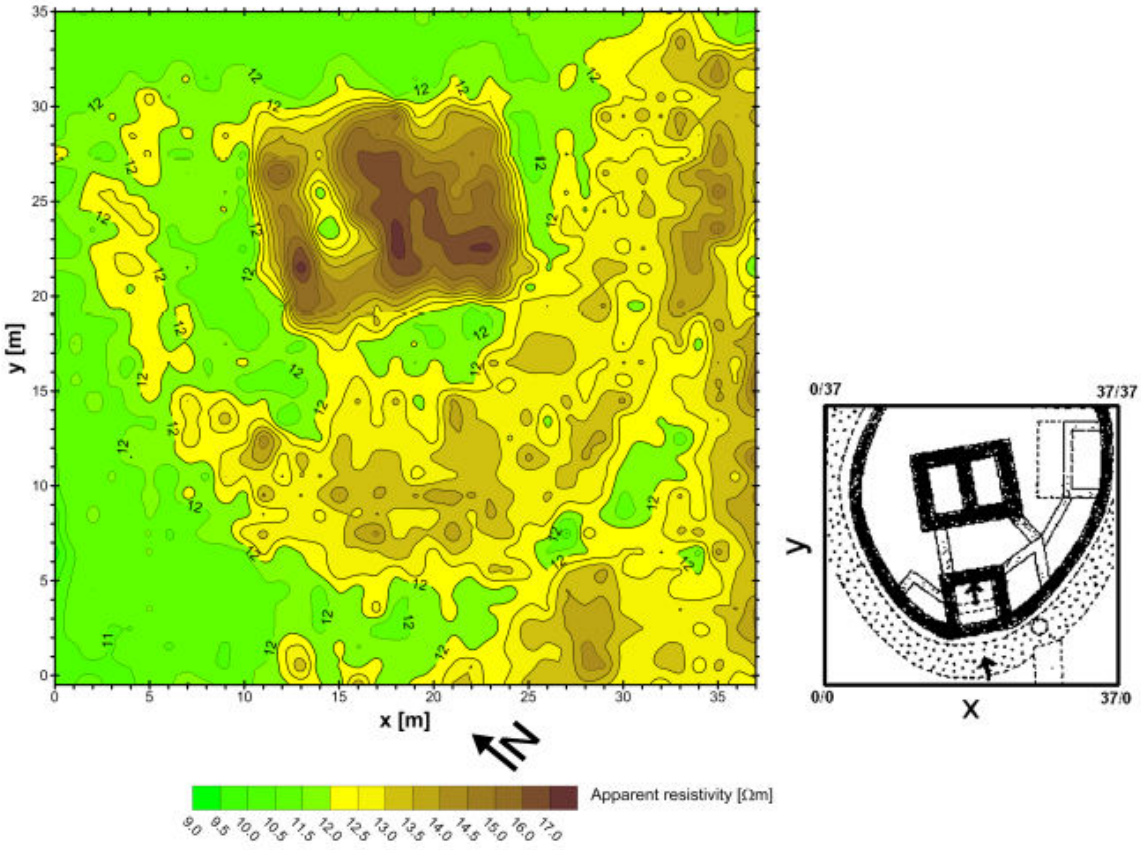

Figure: Resistivity survey over the former medieval fortress, Czech Republic. Wenner array with a 1m inter-electrode distances was used, the resistivities were mapped in the 1_1m grid. The map of apparent resistivities (left) indicates the remnants of masonry as zones with increased resistivities. The interpreted ground-plan (right) shows the central tower, entrance with a gate, fortifications with adjacent smaller buildings and a ditch (dotted).

For the precise location of (relatively) thin objects there is a graphical "trick" for the pole-dipole and dipole-dipole configurations. The reference point is the middle of the potential dipole for both configurations. During the pole-dipole survey, the values for the pole-dipole and reversed pole-dipole are measured and plotted into one graph. Both of the curves have slightly different character when crossing the

boundaries of bodies and the curves intersect just in the middle of the vertical dykes, sphere or cylinders (see the following figure).

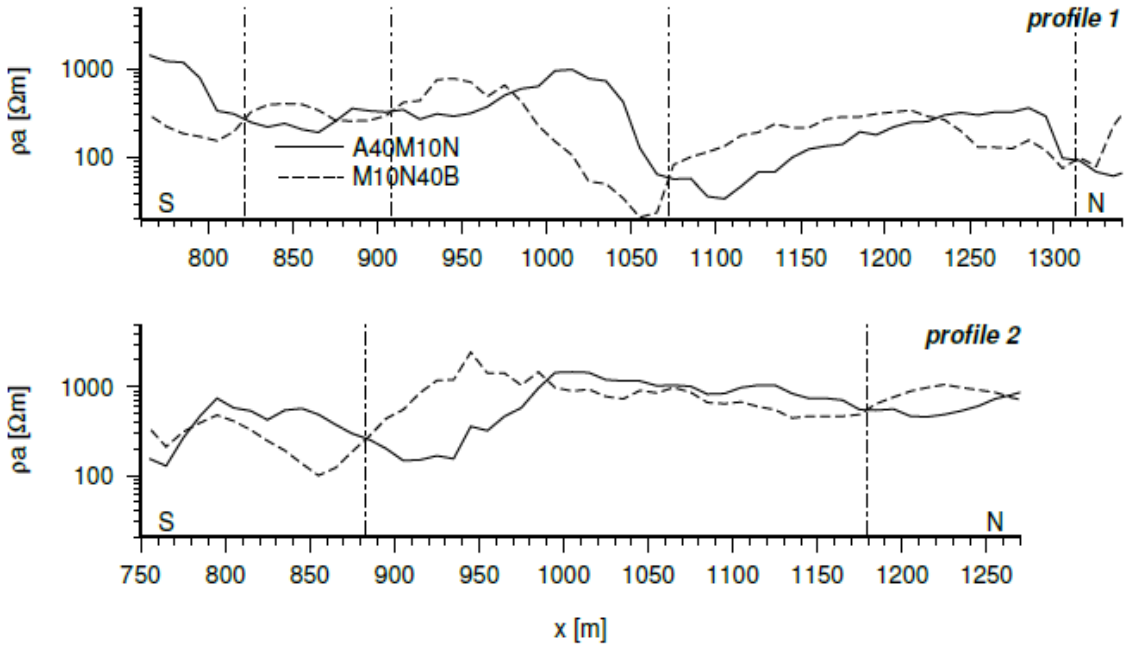

Figure: Pole-dipole survey over the Pošumavský Fault (the Onen Svet site), Czech Republic. The geological media is formed by a different types of gneiss. A reference point is in the middle of the potential dipole (MN). Full line AMN (pole-dipole) resistivity plot, dashed line MNB (reversed pole-dipole) resistivity plot. Dot-and-dashed vertical lines indicate the conductors – fault zones. The legend shows inter-electrode distances in metres (hence also specifying the electrode array). Note the logarithmic scale for apparent resistivities.

For the dipole-dipole arrays the "trick" is similar. The reference point is in the middle of the potential dipole and the resistivity curve is plotted. Now, due to the reciprocity of the electrodes (the resistivity curves are the same if we swap current and potential electrodes), we can assign the reference point to the middle of the current dipole and plot the curve for this point. Hence we get two resistivity curves shifted for the length of the array. Both resistivity curves intersect in the middle of the bodies again (see the following figure).

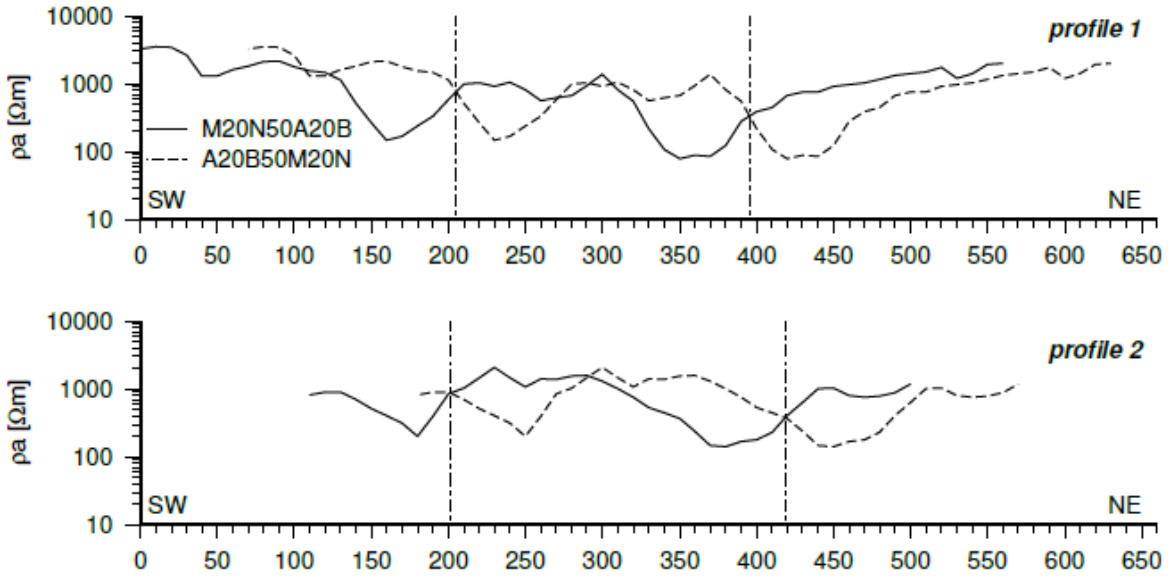

Figure: Dipole-dipole survey over the Pošumavský Fault (the Pstružný site), Czech Republic. The geological media is formed by a gneiss. Two resistivity curves are plotted for the measured configuration (a reference point is in the middle of potential dipole MN) and reciprocal configuration (swapped current and potential dipoles, the reference point is now in the middle of current dipole AB). Hence the two resistivity curves are shifted for the length of the array. Dot-and-dashed vertical lines indicate the conductors – fault zones. The legend shows inter-electrode distances in metres (hence also specifying the electrode array). Note the logarithmic scale for apparent resistivities.

The best suited targets for the resistivity methods are conductive anomalies (ore veins, fault zones, etc.), however, the high resistivity bodies could be mapped as well. It was mentioned that fault zones could be mapped as low resistivity anomalies. The rocks within the fault zone are usually fragmented, which increases a degree of weathering and amount of clay in the affected volume. The increased content of clay decreases the resistivity significantly and hence the low resistivity anomaly is measured. The faults are detected either as a conductive zone (due to the presence of clay particles) or as a resistivity contrast (due to the different lithology on both sides of the fault). The most common arrays for the fault mapping are the pole-dipole and dipole-dipole arrays. The latter is suitable for simple geological conditions, whereas the former could be recommended on most of the cases. The potential and gradient arrays are often used in a prospection when

a complex distribution of resistivities is expected – an archaeological prospection, leaking of contaminants from waste dumps, etc. The improvement of technology of geophysical instruments was fast, for example Vertical Electrical Sounding VES and Horizontal Electrical Profiling HEP surveying techniques was very commonly used by using the 1D resistivity meters until the nineties of the last century, figure (5) shows the ABEM SAS 1000 , 1D resistivity and Induced polarization surveys instrument .

Figure (5): The ABEM 1000 Terrameter system which used in the 1D resistivity survey.

later , the 2D electrical surveys appeared, its faster in application and more costly effective, in a addition to the application of the new technique of ERT electrical Resistivity Tomography which is nowadays very common in application for groundwater , hydrogeological , environmental and engineering geophysics surveys. The instrument became more developed that it includes an auto switching measurement system and built in computer and processor which automated the style of readings. Furthermore, a multi electrode cable is used in 2D and 3D resistivity surveys, and this changed the style of surveying technique either. The new resistivity meters like (ABEM Terrameter LS) , figure(6) is more fast and effective in covering large areas with less possible surveying time, especially when

it becomes possible to check the results in field by the PC laptop which linked to the device directly. So it is possible, with the assistance of processing sophisticated software, to transfer readings and save them and processing them immediately in field to see interpretation results in the shape of 2D sections of what called subsurface resistivity tomography.

Figure (6): The ABEM Terrameter LS system which used in the 2D and 3D electrical resistivity tomography surveys.

Figure (7), showing the on field setting of the 2D electrical resistivity surveying and figure (8) shows the resulted 2D colored resistivity pseudosection and depth section.

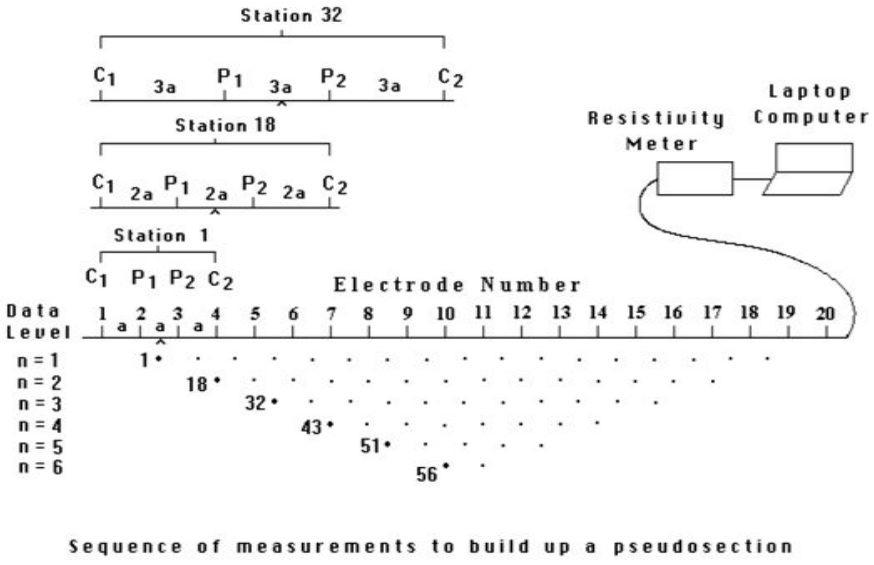

Figure (7): The on field setting of the 2D resistivity tomography survey.

Geophysical Exploration 2011-GE-56

FINAL MODELS FOR RESISTIVITY SURVEY IN UET GROUND:

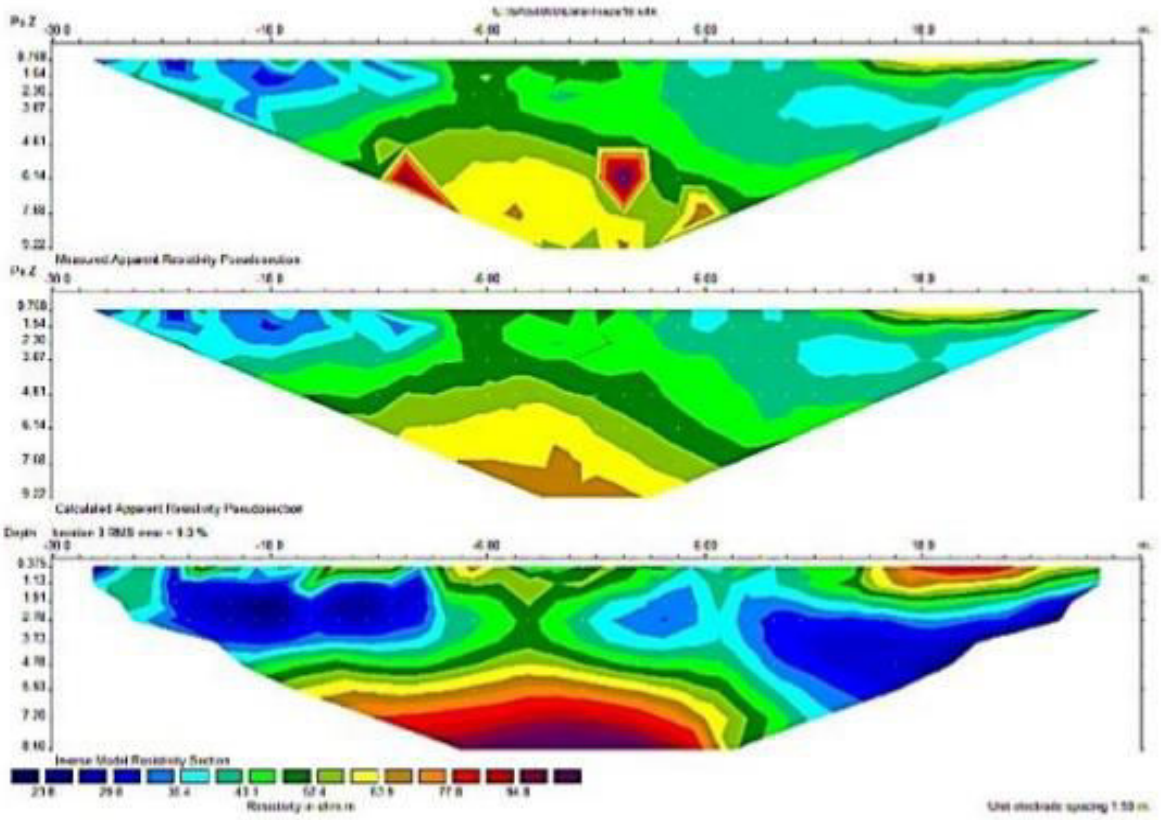

INTERPRETATION:

There are four layers identified from the data (from 3.7m to 6m), The different colour in the image shows different resistivity levels. Also with the increase in depth the resistivity is increasing which shows that either there exists lower moisture content or anomalies are present. There is an error of 9% which shows that the data is not a good one but may be acceptable.

PRECAUTIONS:

- The surface should not be too dry or too wet
- The electrodes should be connected properly
- Battery should be fully charged

REFRENCES:

Instruction manual of ABEM Terrameter SAS 4000 / SAS1000

Figure (8): The 2D resistivity pseudo sections and the true resistivity depth section.

Several 2D sections may achieved in field to cover the whole surveyed area spatially , then with assistant of a sophisticated software it is possible to conduct a 3D model for the subsurface actual resistivity lateral variation and resistivity variation with the actual depth as it appear in the figure (9).

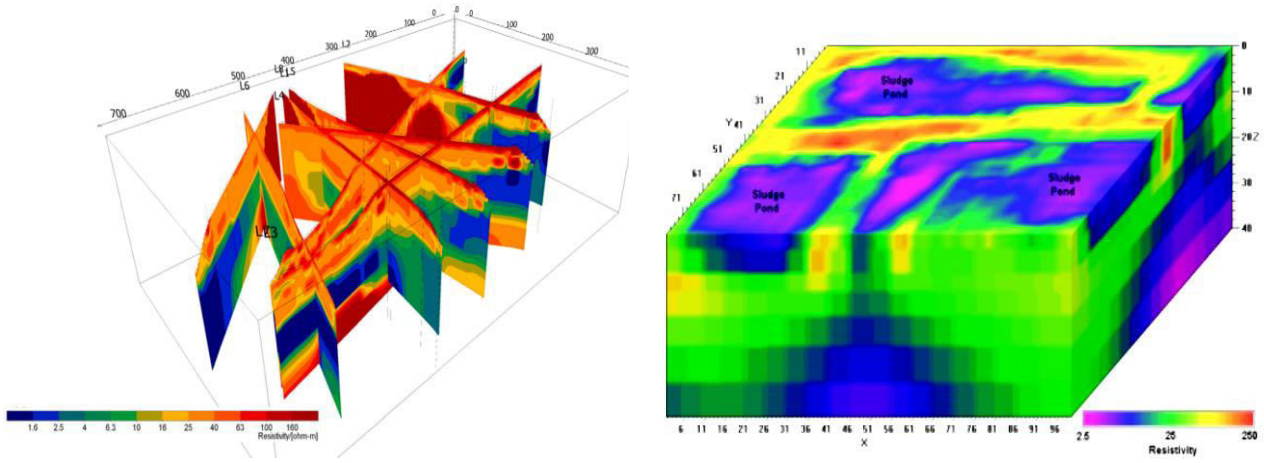

Figure (9): The 2D resistivity sections which covers an area is transformed to a 3D colored resistivity block diagram by using a special software in order to visualize the subsurface resistivity variation in any direction or depth of the region .

Gravity Geophysical Method

Newton's Law of Gravitation

Everyone is familiar with the Earth pull or attractive force. It causes thing s to fall and is also responsible for a pretty hard work if we need to carry stones to build a house. The man who discovered that every mass attracts another one was Sir Isaac Newton. In 1687 he formulated his discovery into the equation called the Newton's Law of Gravitation:

$$F = \gamma \frac{m_1 m_2}{r^2},$$

Where F denotes the gravitational force, is the universal gravitational constant (6.673×10^{-11} $N(m/kg)^2$), m are weights of attracting bodies and r is the distance between them. This equation enables us to calculate a gravitational force the Earth is pulling e.g. a rock on the Earth surface:

$$F = \gamma \frac{M_E m_r}{R_E^2}$$

Where M_E is the weight of the Earth, m_r is the weight of the rock and R_E is the diameter of the Earth. We can see that it is inconvenient to use and measure the gravitational force, since it depends on weights (masses) of both bodies M_E and m_r. Dividing both sides of equation by m_r we get:

$$\frac{F}{m_r} = \gamma \frac{M_E}{R_E^2}$$

Since the force is computed as (weight x acceleration) , we can transform the equation into:

$$g = \gamma \frac{M_E}{R_E^2}$$

Defining the acceleration caused by the Earth. The acceleration g is called the "acceleration due to gravity" or "acceleration of gravity". The value of g on the Earth surface is 9.80665 m/s^2 which is often simplified to 10 m/s^2. The unit of

acceleration of gravity (1 cm/s^2) is also referred to as Galileo or Gal, in honor of Galileo Galilei, who was the first who measured its value. The modern gravimeters are capable of readings with the precision of 0.001 mGal (0.01 $\mu m/s^2$),

1 Gal = 1000 mGal.

Gravity field of the Earth and data reduction

Because the Earth is not a perfect homogeneous sphere, the gravitational acceleration is not constant over the whole Earth's surface. Its magnitude depends on five following factors: latitude, elevation, topography of the surrounding terrain, earth tides and density variations in the subsurface.

Within the geophysical prospection, we are interested in the last one, which is usually much smaller than the latitude and altitude changes. The removal of unwanted components is often referred to as reduction.

Drift and Tidal Correction: The gravity measurement value which taken for a certain station at ground surface differs with time during the same day after some hours, this effect is called the **drift effect**. Gravitational readings are also influenced by the tides which produced by the gravitational attraction force of the sun and moon's to the mass of the Earth during the hours of a day. It is possible to eliminate this effect by correcting our readings according to what called **base stations**. The base station is a gravity station in which gravity measurement value is known on the bases of day and hours. The correction could be done by plotting a drift curve and by using data of the nearby base stations which considered as a reference to correct this drift, figure 18. It is intended to refer to the nearby base station every hour, two or three hours according to the distance of the reference station from the point of measurement.

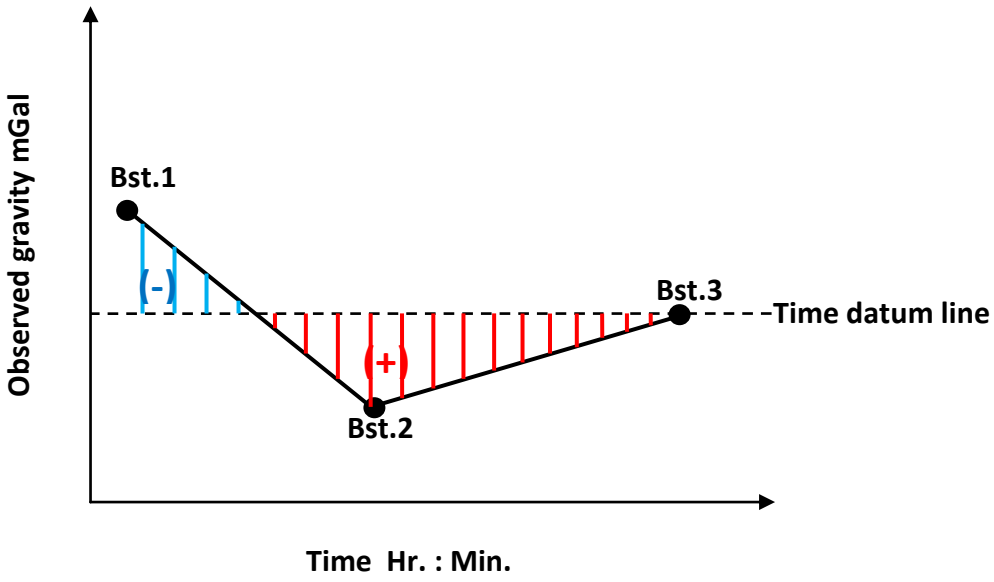

Figure: Gravity readings Drift graph , the black points represent the base stations, the disconnected line represents the time datum line taken from the Bst.3 and used as an index line to correct the normal stations measurements, short vertical lines over the datum line represent the increasing drift values at normal stations, while the below datum line represent the decreasing drift values at normal stations.

The figure above shows the drift correction graph. It represents an experimental relation between the observed gravity values which measured at normal and base stations. One of the base stations (Bst.3) considered drawing the time datum line which represents the reference line in correcting the other stations drift. The drift that happened in gravity readings for the normal stations represents the vertical short lines. Short lines over the datum line represent the unwanted positive drift which must be subtracted from the station observed reading, while the short lines below the datum line represents the unwanted negative drift which should be added to the station observed reading.

Free-air correction: This is the first step of reducing topography effects. It simply corrects for the change in the elevation of the gravity meter, considering only air (hence a free-air) being between the meter and selected datum. To get the change in gravity acceleration with height we can use the following equation:

$$\frac{\Delta g_{FA}}{\Delta R} = -2\gamma\frac{M_E}{R^3} = -\frac{2g}{R}\ \text{mGal/m}.$$

This correction takes into account the decrease of gravity vertically by increasing the elevation of the measurement station above sea level. This will cause the increase of distance from the center of the earth and the measurement station. The amount of decrease is about (-0.3086 mGal) for every one elevated meter above the sea level. The correction is done by returning readings to a reference level (Datum plane or the reference ellipsoid), which is often the sea level, see the figure below.

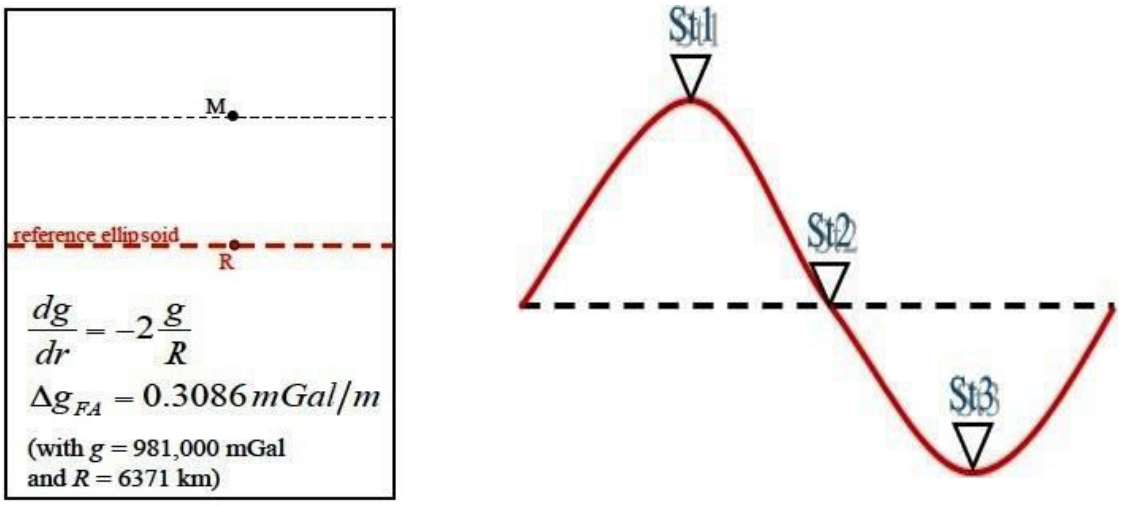

Figure: The free Air effect on gravity measurement at three stations, St.1 is located over the sea level datum which (decrease in gravity), St.3 is located below sea level (increase in gravity), and St.2 is located within the sea level (no effect in gravity).

The free Air effect on gravity measurement on earth surface could be expressed by the equation:

$$\textbf{Free Air effect (mGal)} = \pm 0.3086 \times h$$

Were (h): is the measurement station elevation above sea level.

Raising the gravity meter (e.g. extending its tripod) decreases the measured gravity values by 0.3086 mGal/m. Hence to measure with an accuracy of 0.01 mGal we have to measure the elevation of the gravity meter with an accuracy of 3 cm.

Bouguer Correction: This type of correction is concerned with the attraction of rock materials which located between the reference level (reference ellipsoid), and the measurement station at the earth surface, see the next figure. It is proposed that these rock materials represent a horizontal plate (Horizontal slab) which extends to infinity and its thickness is equivalent to the height difference between the measurement station and the reference level. The Bouguer effect is based on the assumption that the station is subjected to a downward gravimetric attraction due to the rocks mass and density in addition to the opposite force upward which caused by the Free Air effect.

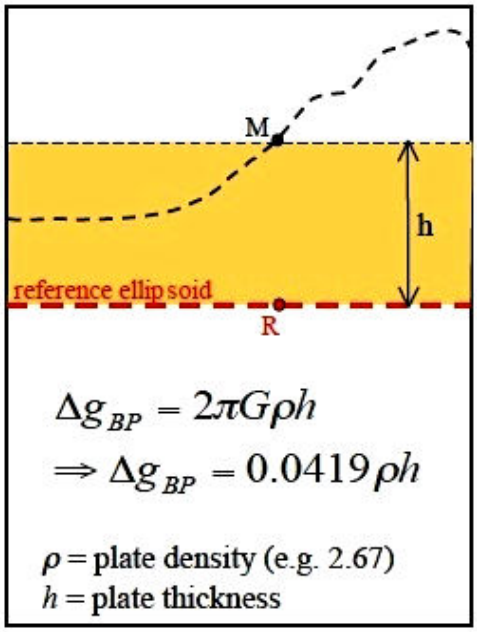

Figure (20): The Bouguer effect or correction at the surface gravity measurement station (M).

The Bouguer effect is expressed by the following equation:

$$\textbf{Bouguer effect (mGal)} = \pm 0.0419 \times \rho \times h$$

Where : (ρ) is the rocks density of the horizontal slab extending to infinity with a thickness equivalent to the difference between the reference level and the measurement station location, its unit is $(g \setminus Cm^3)$ or $(Kg \setminus m^3)$.

(h): is the elevation above sea level.

The Bouguer correction takes both (h) and (ρ) into account. This correction effect value is negative for the stations which are located above the reference level and usually get subtracted from the station observed reading. Vice versa happens for the stations located below the reference level where Bouguer effect value is positive and usually get added to the station observed reading.

Since (Free Air and Bouguer) effects or corrections are both dependant on the elevation above sea level (h), then the both effects are able to be calculated in one equation and this is what called (Total Elevation Correction), In other words the equations of total Elevation effect could be written as:

For the stations located above the reference level:

$$\textbf{Total Elevation Effect (mGal)} = \textbf{(Free air effect)} - \textbf{(Bouguer effect)}$$

For the stations located below the reference level:

$$\textbf{Total Elevation Effect (mGal)} = -\textbf{(Free air effect)} + \textbf{(Bouguer effect)}$$

Or

$$\textbf{Total Elevation Effect (mGal)} = (0.3086 \pm 0.0419\ \rho)\ h$$

Latitude correction: The reason for the latitude correction is two-fold. First of all, it is caused by the Earth's centrifugal force being added to the gravitational force (vector sum). This decreases the gravitational force with an increase of a radius of rotation. Hence the smallest gravitational force is on the equator (maximal centrifugal force) and the largest is on the pole. Second, the gravitational force is further affected by the fact that the Earth is not spherical but ellipsoidal. This further decreases the gravitational force on the equator. Both of these effects could be removed by the International Gravity Formula:

$$g_\lambda = 978031.8(1 + 0.0053024 \sin^2 \lambda - 0.0000059 \sin^2 2\lambda)\,\text{mGal}$$

It is clear that the centrifugal force changes only in the N–S direction, not in the W–E. As we have seen from the Newton's Law of Gravity equation, the gravity decreases with the square of distance. Hence, if we lift the gravimeter from the surface (or any other datum), the gravity will change. To be able to compare data measured in different elevations we have to reduce them to a common datum.

The value of gravity increases as we move from the equator toward the poles because of earth low rotation velocity and the decrease of centrifugal force at the poles. Furthermore, Earths radius at the northern and southern poles is less than that at the equator with the amount of about 21 Km, this produces a gravity value difference between Earth poles and equator of about (5172) mGal or (5.1) Gal. Gravity increases gradually when we move from the equatorial regions toward polar regions with latitude at average increase rate of (w), where:

W = 0.8122 sin2Θ mGal / km , W =1.307 sin2Θ mGal / mile

W: The average increase or decrease rate of gravity with latitude.

Θ: is the latitude angle in degrees.

If the vertical distance away from the equator toward north or south is known then, the latitude effect of gravity could be expressed by the following equation:

$$\textbf{Latitude Effect mGal} = \textbf{w} \times \textbf{distance}$$

The theoretical gravity value (g_ϕ) is the gravity value of the reference ellipsoid which mentioned previously. The **International Gravity Formula** is used to find the (g_ϕ) in the unit of (Gal) for any station located at earth surface, this formula is:

$$g_\phi = g_0 (1+a \sin^2\Theta - b \sin^2 2\Theta)$$

Where: g_0 is the gravity at the equator

a and b : constants which depend on the tilting of earth rotation axis, the angular velocity of Earth rotation and earth flattening as shown in the next figure.

Θ: is the latitude angle value in degrees.

Therefore, the final shape of the international gravity formula is:

$$g_\phi = 978.049 (1+0.0052884 \sin^2\Theta - 0.0000059 \sin^2 2\Theta) \quad \text{Gal}$$

The theoretical gravity value (g_ϕ) which calculated by the above equation is in the unit of (Gal) , so it must be multiplied by 1000 to convert it to the unit of (mGal). It is worth to mention that:

g_ϕ when $\Theta = 0°$ is 978.049Gal at the Equator

g_ϕ when $\Theta = 90°$ is 983.221Gal at the Pole

g_ϕ when $\Theta = 45°$ is 980.629Gal at the middle distance between equator and pole.

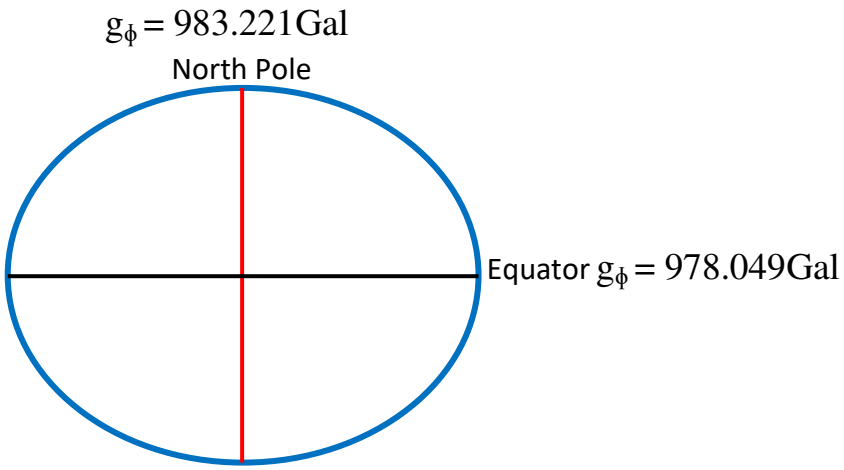

Figure: The difference in the theoretical gravity value (g_ϕ) between the earth's equator and pole.

Terrain Correction: This type of correction is concerned with the tangential pulling attraction force which produced by different terrains such as valleys and hills in the areas surrounding the measurement station. This attraction force affects the measured gravity value which supposed to be vertical and toward the center of the earth. This effect is related to the topography rocks mass which adds unwanted effect to the gravity measurement value, see the figure below.

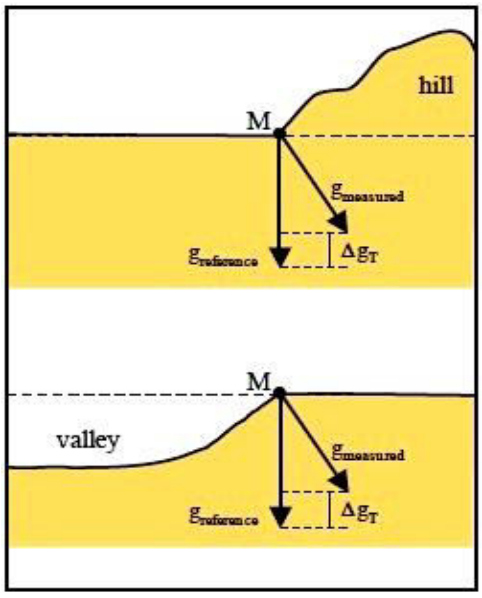

Figure: The effect of terrain or topography on the measured gravity at station (M) in the case of surrounding by a hill or valley.

The terrain or topographic effects should be taken in consideration by calculating the gravity of rock blocks which will be added to the valleys below the measurement level or that will be subtracted from the hills above the measurement level.

Terrain corrections is achieved by using a special calibration models and tables designed for this purpose and called (**Hammer`s circles**),figure 23, which is a group of concentric circles with lines or rays emanating from the center point and divided these circles into a group Zones, and be either A circle or half circle drawn in two dimensions (x, y), see the figure below.

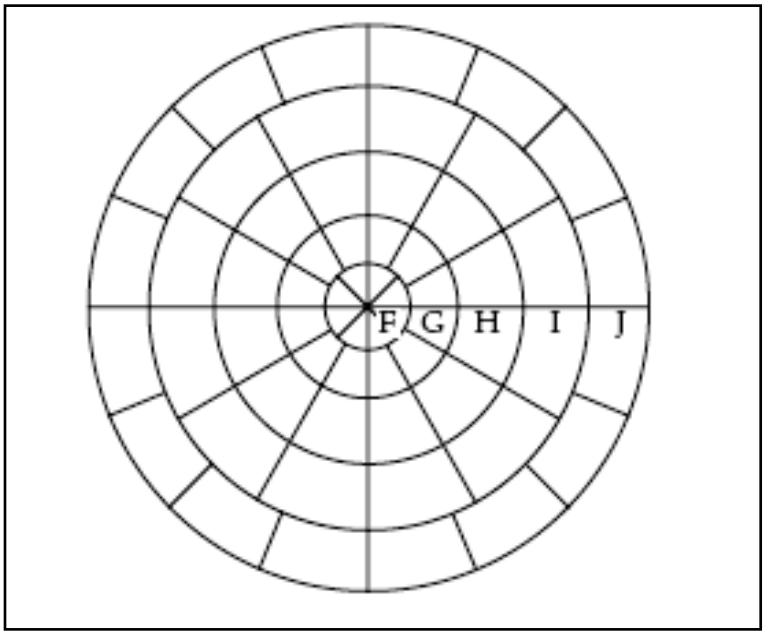

Figure :The standard Hammer`s circles which used in gravity terrain correction.

The center of these circles is superimposed at the measurement point of the topographic map for the surveyed area, which must has the same drawing scale for these circles (drawn on a transparent sheet), then we calculate the average elevation for each band. The correction value for each range is obtained from the standard tables (Hammer`s Table), after that these correction values are collected

to obtain the total correction value which is added to the gravity reading of the measurement station.

By observing the figure below one can configure the importance of applying the terrain correction on the observed gravity data in order to eliminate the terrains effect on gravity readings.

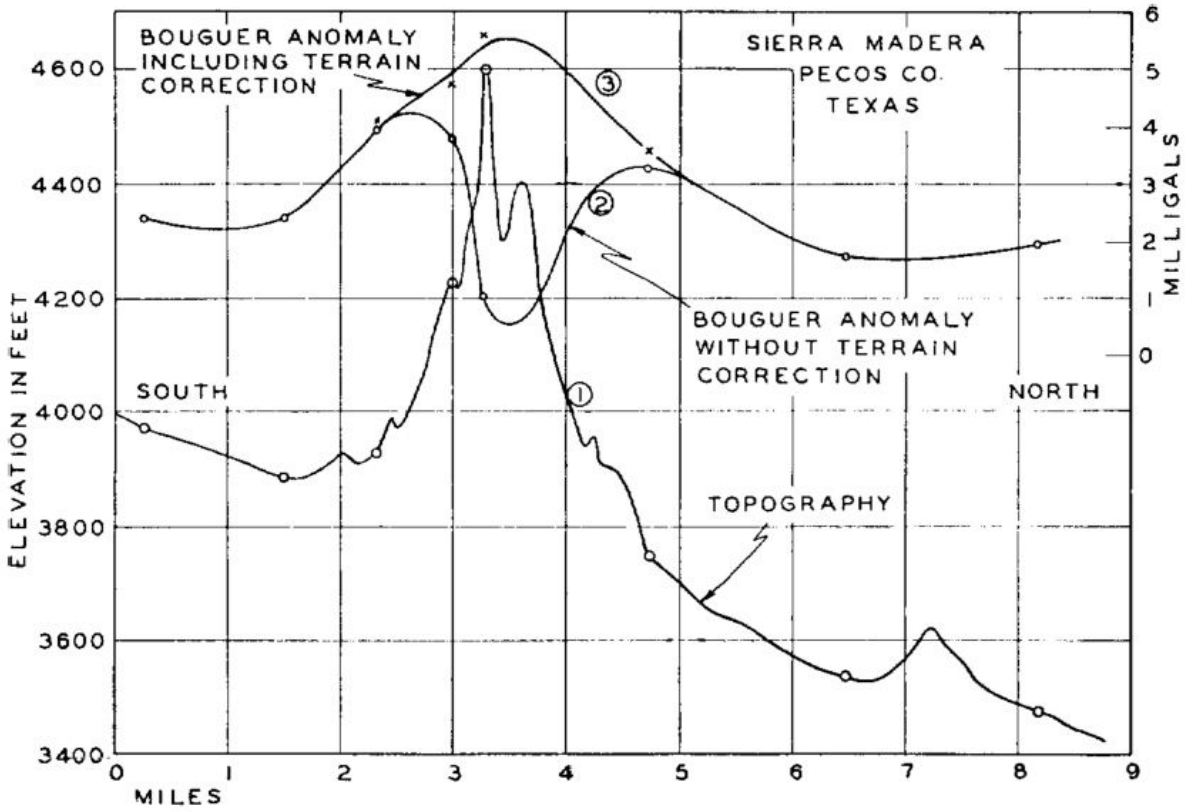

Figure: Gravimeter profile across Sierra Madera, Pews County, Texas, illustrating the importance of terrain corrections (Hammer 1939).

Isostatic Correction: It is carried out in large areas of regional gravity studies and cannot be carried out in local gravity explorations. This correction reduces the effect of unbalanced rock blocks of earth crust which related to the theory of Isostasy and the mechanical properties of the lithosphere.

The calculation of Bouguer Anomaly value

In all gravity and geodetic studies, Bouguer gravity anomaly value represent the difference between the observed gravity value which measured in the field (after making all the necessary corrections) and the theoretical gravity value (g_ϕ) which obtained by applying the international gravity equation (International Gravity Formula) for the same measurement station. The Bouguer anomaly value could be obtained from the following formula:

Boug.Anom.Value mGal = (observed gravity station reading± all corrections) - g_ϕ

After calculating the Bouguer anomaly values for every station in the area they superimposed on the base map and a contour map of Bouguer anomaly is drawn, figure 16. The Bouguer anomaly contour map considered as the raw material for both descriptive and qualitative interpretation, figure 17.

Gravity Data Interpretation

The final outcome of the gravitational field survey after applying all the necessary corrections is a contour map of Bouguer anomalies which representing the anomalies that produced by all subsurface objects. The depth, location and shape of subsurface structures could be estimated by identifying the characteristics of the anomalies (such as amplitude, shape, sharpness), after making a cross sections or profile across the Bouguer map pass through the anomalies. The main thing reflected in this map is the heterogeneity of the densities in both the horizontal and vertical directions.

The interpretation process is more complex than some thought and is called ambiguity in the interpretation of **gravity ambiguity**.

The reasons behind gravity ambiguity are:

1- The gravitational field measured at any point on the Earth's surface represents the sum of the gravitational pull of all sources from the Earth's surface downward rather than to the single structure or object to be determined. Sometimes the process of separating this body from the rest of the objects and varying its gravitational effect alone is very difficult or impossible.
2- Infinite numbers of subsurface structures can produce similar gravitational data on the surface. For example, embedded river channel and igneous objects that penetrate layers horizontally can be rounded to a simple geometric shape representing a horizontal cylinder, so it is sometimes difficult to determine which model is most acceptable. This requires the application of more than one model to get the most acceptable one.
3- Gravitational explanations are not conclusive or definitive, but require a great deal of speculation and assumptions, but it can be said in general if the anomalies drawn on the map sharp (Sharp) It indicates that the sources of these anomalies located at shallow depths (Shallow), and medium-sharp anomalies indicate Their sources which are geologically significant, while very broad anomalies point to deep regional sources such as the presence of basement rocks.

Assisting gravity interpretations with additional geological information like borehole information or by the results of additional geophysical methods like magnetic, seismic, electrical and well logging methods may eliminate the ambiguity.

The deep boreholes can provide valuable information about the depth and density of subsurface rocks. Core samples obtained from boreholes could be tested in the laboratory to study rocks density, porosity, permeability and other petro physical properties such information may help in reducing ambiguity to an acceptable rate.

Qualitative Interpretation

The Bouguer anomaly contour map considered as the tool for the qualitative interpretation of gravity field for a certain area. It represents a visualizing tool that shows the locations of positive anomalies (the high gravity values) as crests, also, it shows the negative anomalies (the low gravity values) as troughs. Positive gravity anomaly is usually produced by subsurface high density body if compared to the hosting rocks, or it may be related to the close to surface basement rocks (dense rocks). A negative anomaly refers to subsurface low density body or cavity surrounded by the hosting rocks, and it may refer to the high depth of the basement rocks. The figure 24, shows the Bouguer anomaly contour map and the location of the profile A-A$^{\backslash}$. The gravity profile for the total Bouguer anomaly represents a descriptive method to describe the lateral variation of subsurface densities along the profile line, like the profile A-A$^{\backslash}$ in figure 24.

Separating the residual gravity field from the total Field

The Total Bouguer anomaly map represents the total effect of deep and shallow subsurface rocks. It represents the summation of both the very deep dense basement rocks gravity and the near surface or shallow gravity field which related to the sedimentary cover. Therefore, it is required to separate the both effects, especially when we are looking for the specifications of a burred structure located within the residual anomaly which related to the sedimentary cover. Generally, a graphical method with the assistance of computer software is applied to the total

Bouguer anomaly by taking the 2nd order polynomial regression to obtain the regional field.

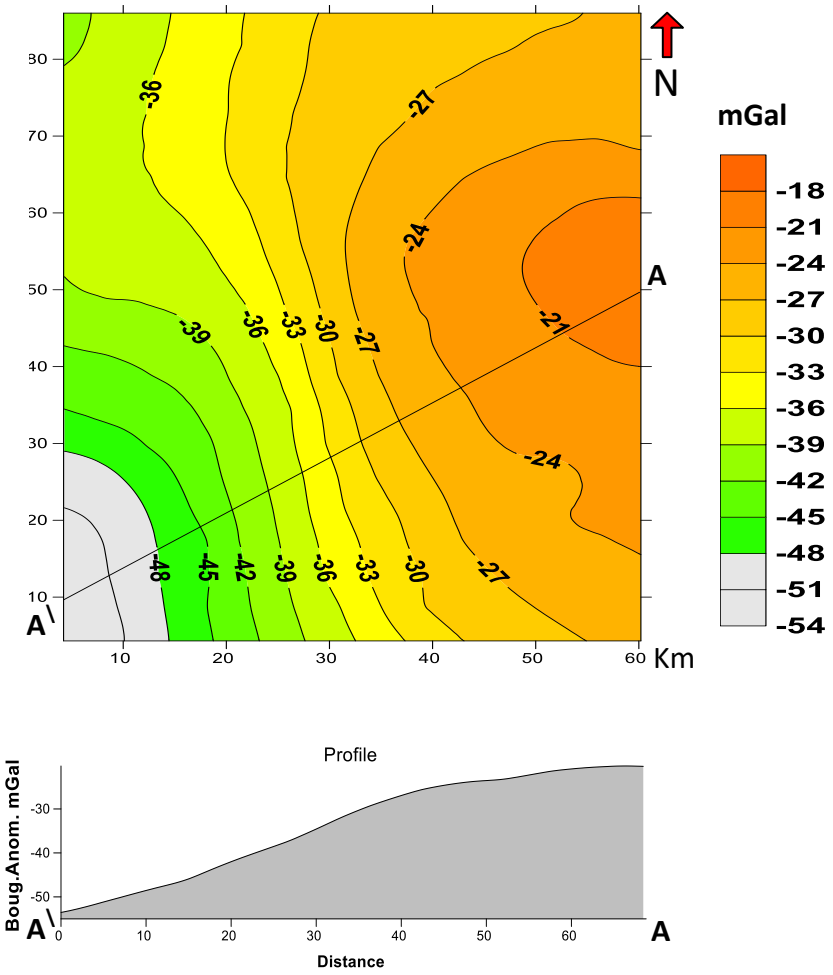

Figure (24): The total Bouguer anomaly contour map showing the locations of positive and negative anomalies, and the profile A-A\ is passing through both of them.

Figure 25-A, shows the regional field of the total Bouguer anomaly which is going to be used in obtaining the residual gravity field, figure 25-C. The residual gravity field is obtained by subtracting the regional field, figure 25-B, from the total field, figure 25-A.

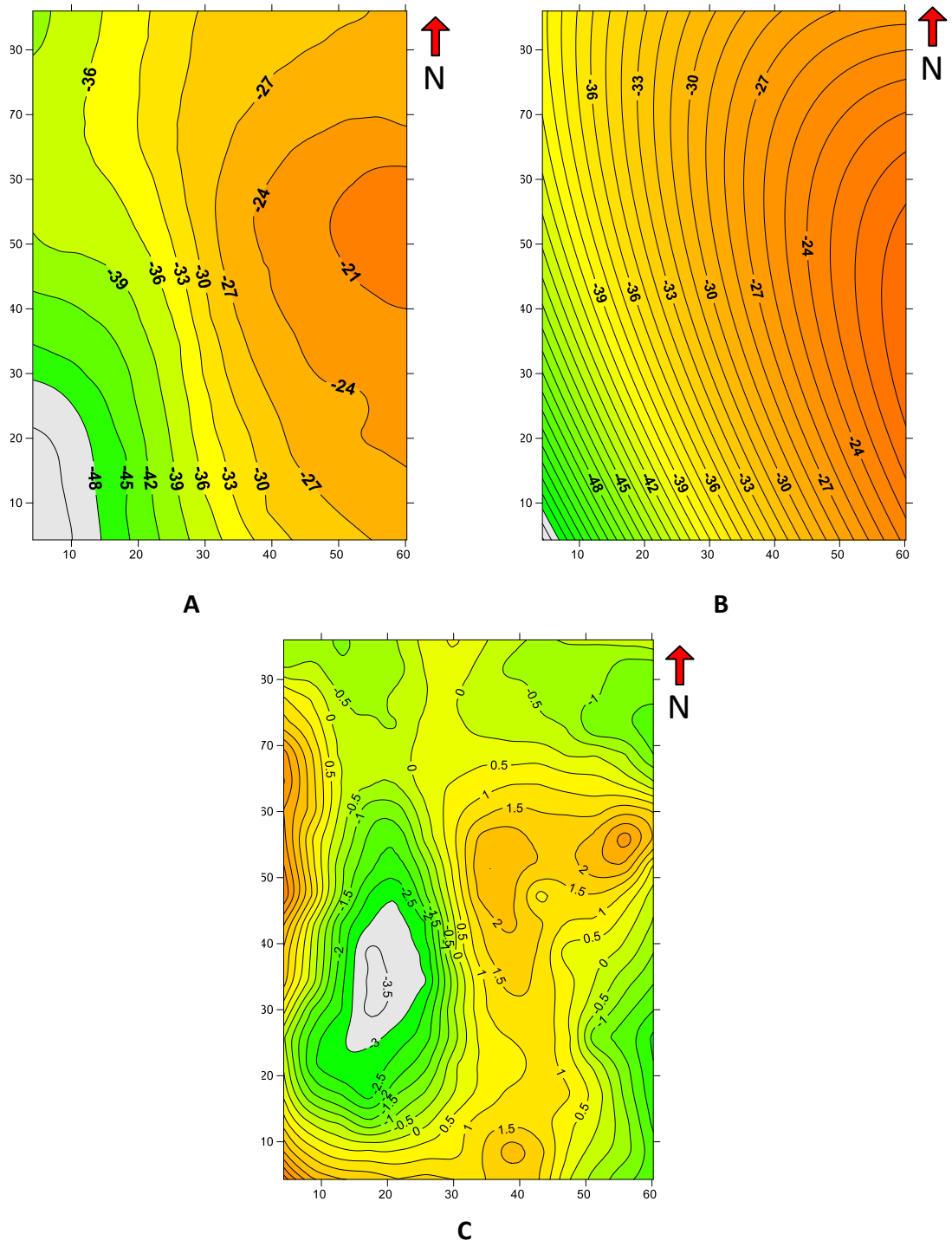

Figure (25): The Residual Bouguer Anomaly map (C), is obtained by subtracting the regional Bouguer field (B) from the total Bouguer field (A).

The residual Bouguer anomaly map, figure 25-C, considered as the raw material for the quantitative interpretation of the gravity data.

Quantitative Interpretation

Gravity profile could be drawn across the map of the residual gravity anomaly by making it passing through the concerned anomalies which required to be interpreted quantitatively like the profile A-A\ in figure 26.

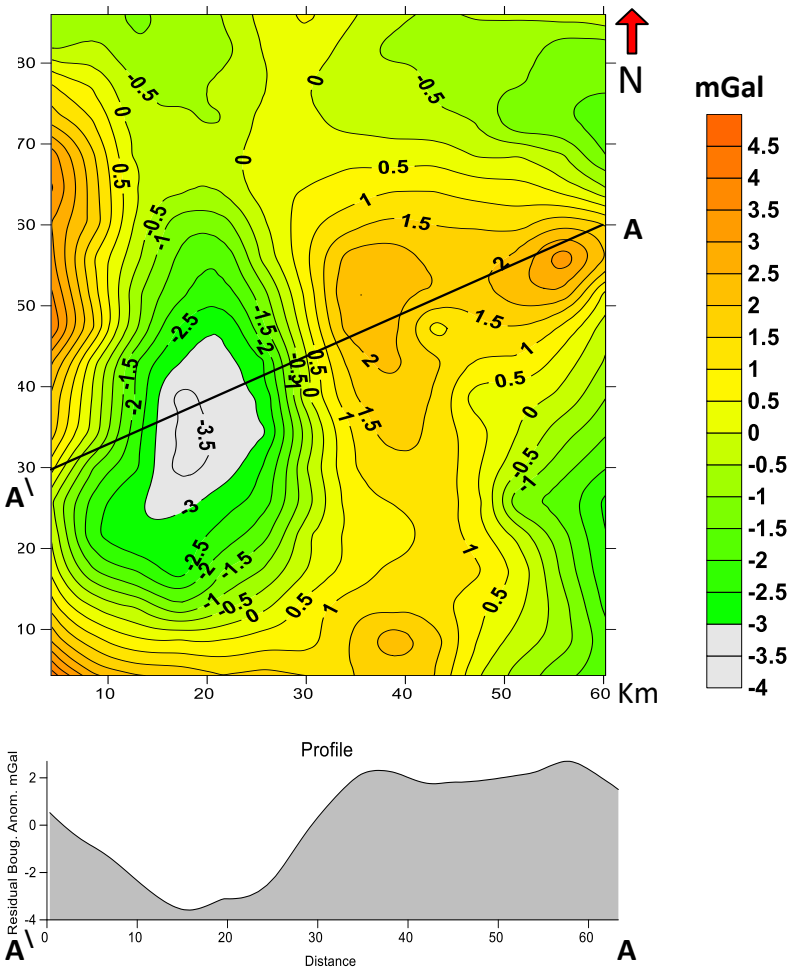

Figure (26): The Residual Bouguer Anomaly map and the profile line A-A\ which is ready to be interpreted quantitatively.

The quantitative interpretation is achieved by adopting a suitable geometrical modeling for the subsurface body which produced the anomaly. Therefore, the subsurface bodies shape is approximated to a geometrical body like: sphere, vertical or horizontal cylinder, sheet or slab and faulting case.

1- Sphere

Assume a ball with a mass (M) and a radius (R), its density (ρ), figure 27, then its mass = volume × density, if the center of the ball is at the depth (Z) below the earth surface, the force of gravity to the center of the ball to the mass unit at the surface at a horizontal distance (X) from the center will be:

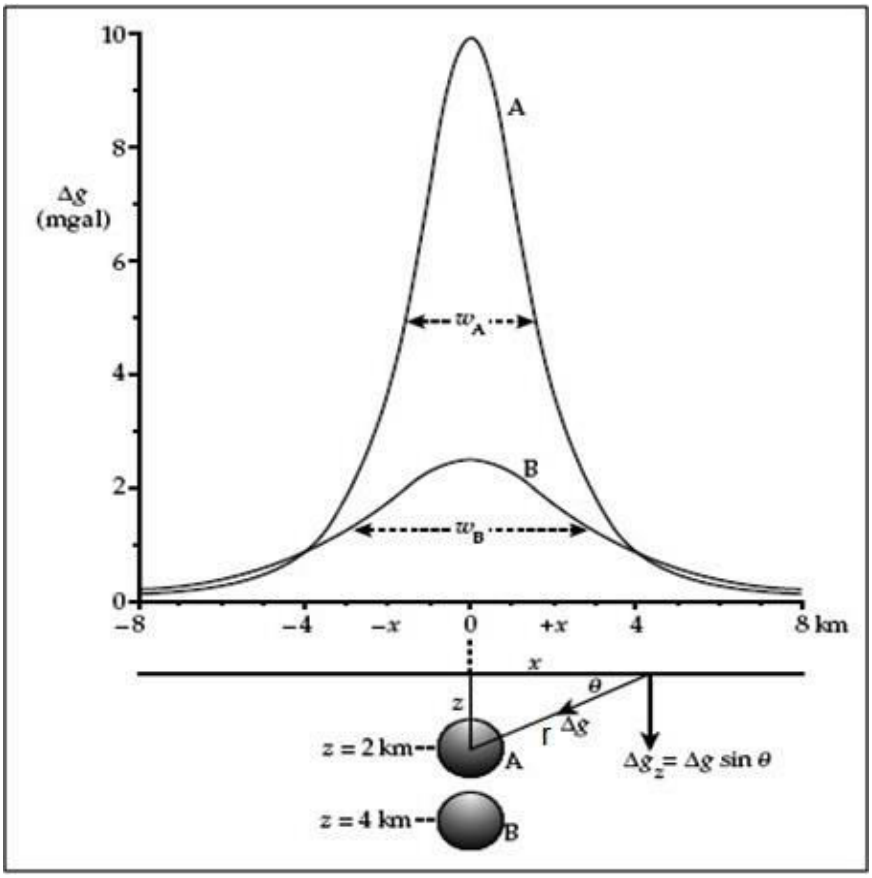

Figure (27): The gravity anomaly of a geometrical sphere.

The mass for the sphere: $M = \frac{4}{3}\pi R^3 \rho$

The gravimetric field produced by the sphere is:

$$g = G\frac{M}{r^2} = \frac{4\pi R^3 \Delta\rho G}{3(Z^2 + X^2)}$$

$\Delta\rho$: is the density contrast value between the sphere and the surrounding hosting rocks , G: the gravity constant.

$$r = \sqrt{Z^2 + X^2} \qquad r = (Z^2 + X^2)^{1/2}$$

$$\cos\theta = \frac{Z}{r} = \frac{Z}{(Z^2 + X^2)^{1/2}}$$

$$g_z = G\frac{M}{r^2}.\frac{Z}{r} = \frac{4}{3}\pi R^3 \Delta\rho \frac{Z}{(Z^2 + X^2)^{3/2}} \ldots\ldots (1)$$

Nettleton noted that the relationship (1) should be rearranged as follows:

$$g_x(\text{in mgals}) = \frac{8.53\,\Delta\rho\, R^3}{Z^2\left(1 + \frac{X^2}{Z^2}\right)^{3/2}} \ldots\ldots\ldots\ldots (2)$$

The values (X, R and Z) are measured in kilo feet = 1000 feet, and the density (ρ) is measured in units (g / Cm^3). 1Kilofeet = 3×10^4 Cm.

Equation (2) is better and more practical because it is possible to find the value of (g_z) at any distance (X) easily by multiplying the value of the maximum anomaly

peak by a factor based on the ratio (X / Z) only, that is, when the value of X = zero, then:

$$g_x(\text{in mgals}) = \frac{8.53\,\Delta\rho\,R^3}{Z^2}$$

Density Contrast represents the difference between the density of a buried mass underground and the density of surrounding materials. For example, salt domes always give negative anomalies because the density of salt rocks is less than the density of the hosting surrounding sedimentary formations. The magnitude of the expected gravity anomaly of a spherical salt dome can be estimated from the above equation.

2- Buried Horizontal Cylinder

Assume an infinite buried horizontal cylinder in length that has a radius of (R) embedded at a distance (Z) below the surface of the earth, figure 28, the vertical component (g_z) will be measured in mGal as follows:

$$g_z = \frac{2\,\pi\,R^2\,G\,\Delta\rho\,Z}{r^2} = \frac{2\,\pi\,R^2\,G\,\Delta\rho\,Z}{(X^2+Z^2)}$$

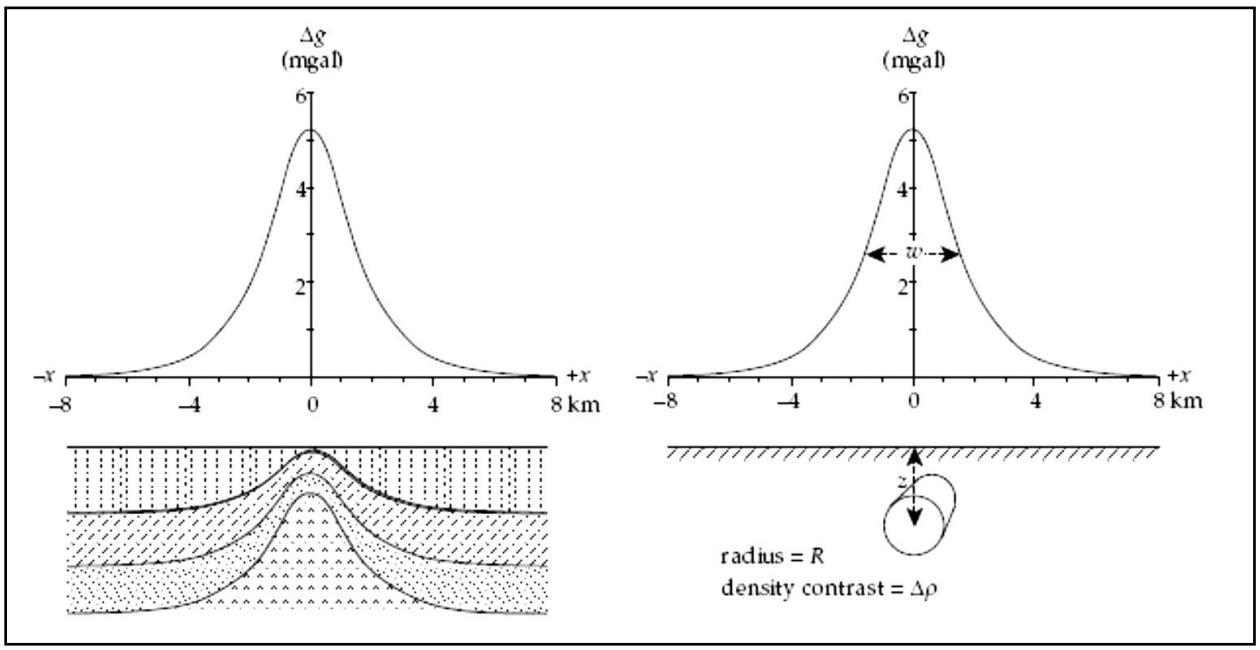

Figure (28): The gravity anomaly of a horizontal cylinder.

The gravity model of an endless horizontal cylinder represents the calculation of gravity anomaly which produced by anticline fold, figure 28.

3-Buried Vertical Cylinder

Suppose that there is a infinite embedded cylinder of length (L) and radius (r), whose upper base is embedded at a depth (d) from the Earth's surface (the depth of the cylinder), figure 29.

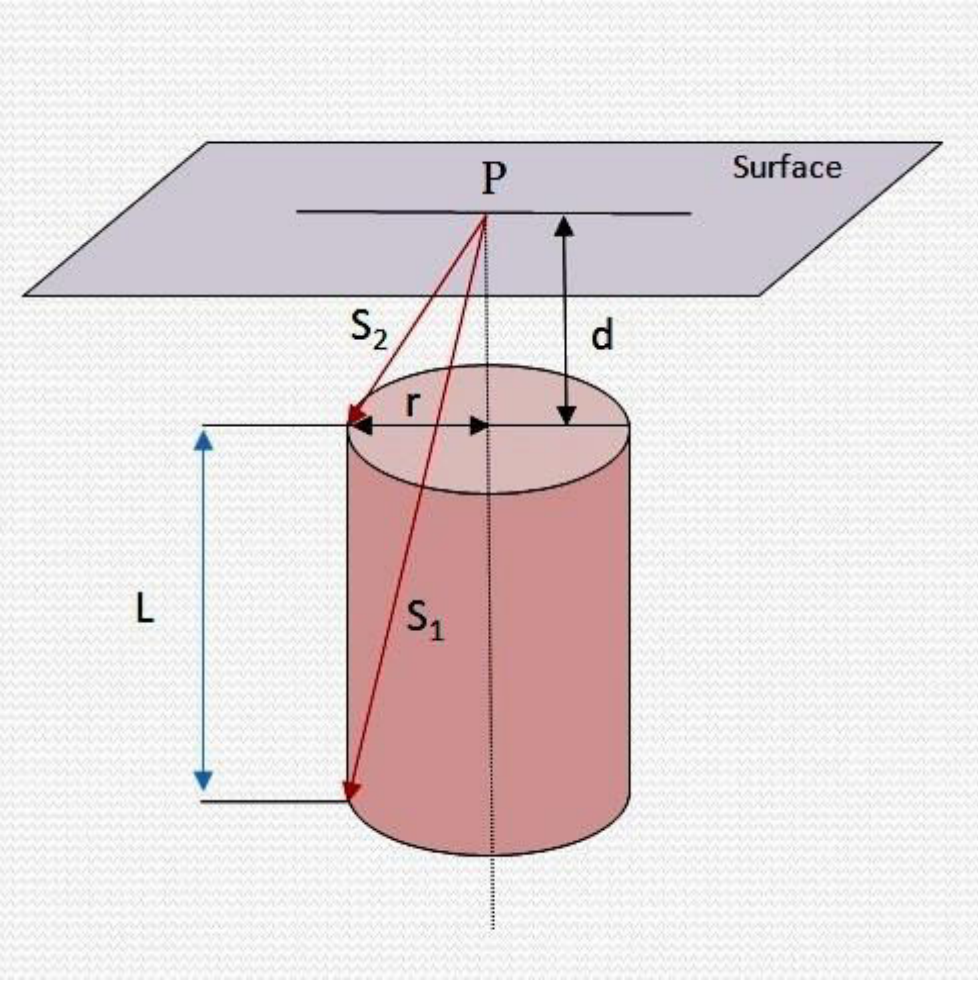

Figure (29): The vertical gravity component g_z of a vertical cylinder.

The vertical component of gravity (g_z) at the point (P) at earth's surface which passing through the cylinder axis is given by:

$$g_z = 2\,\pi\,G\,\Delta\rho\,(L\text{-}S_1\text{+}S_2)$$

$$g_z\ (in\ mgals) = 12.77\,\Delta\rho\,(L\text{-}S_1\text{+}S_2)$$

Where: Δρ is the density contrast value in g\Cm^3, between the cylinder and the hosting surrounding rocks density. The **(L, S_1, S_2, d)** distances are measured in kilo feet. If the cylinder has an infinite length then: $S_1 = L + d$,and the gravity equation will be written as:

$$g_z = 12.77\,\Delta\rho\ (\ L - (L - d\ ) + S2\ )$$

$$g_z\ (in\ mgals) = 12.77\,\Delta\rho\,(S_2\text{-}d)$$

According to the geological point of view, the buried vertical cylinder represents approximately the shape of buried salt domes and dike.

4-Buried Slab

Assume a buried plate or slab of dense rocks which has an infinite length and thickness (L), with a depth below ground surface (d), figure 30.

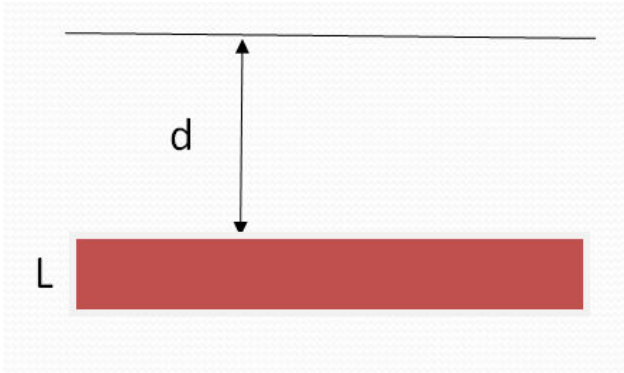

Figure (30): The vertical gravity component g_z of a buried slab.

Then the vertical component of gravity g_z which produced by this dense slab at a measurement point on earth surface is given by:

$$g_z = 12.77\ \Delta\rho\ L$$

g_z in this case depends on the thickness of the slab and not its length.

5-Faulted Horizontal Slab

Assume a buried infinite slab in length, its thickness is (t) and stroked by a fault (normal direction to the paper plane) figure 31, then the vertical component of gravity g_z which produced by this fault at the location of the fault plane is given by:

$$g_z\ (in\ mgals) = 4.05\ \Delta\rho\ t\ \left(\frac{\pi}{2} - \tan^{-1}\frac{X}{Z}\right)$$

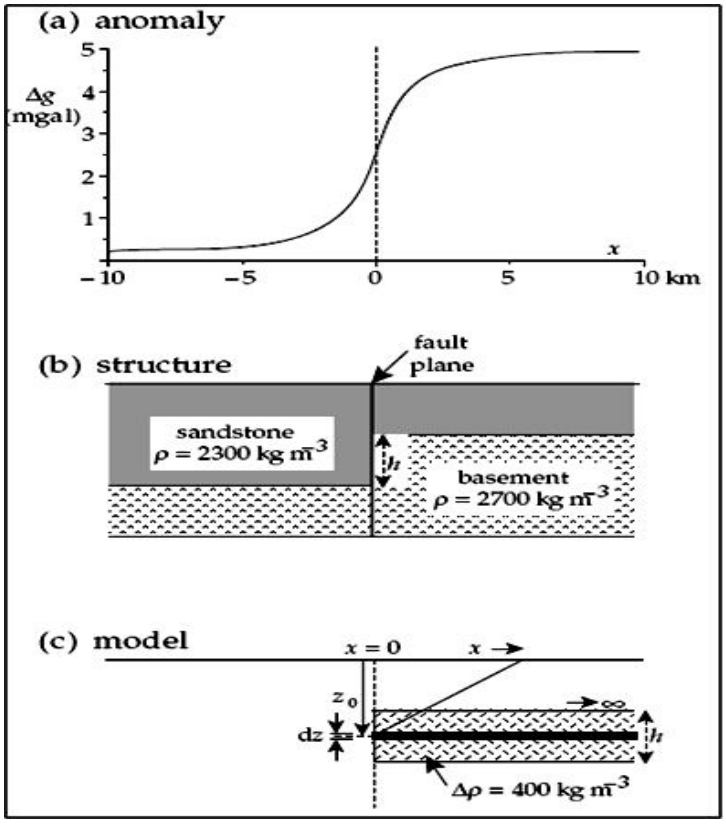

Figure (30): The vertical gravity component g_z over a faulted slab.

Magnetic Geophysical Method

The Earth's geomagnetic field

The Earth's magnetic field is more complicated than a simple dipole. It consists of:

a) The main field: This approximates to a non-geocentric dipole inclined to the Earth's spin axis. It can be modeled as polar and equatorial dipoles. A simple dipole is a good approximation for 80% of the Earth's field. The remainder can be modeled as dipoles distributed around the core/mantle boundary.

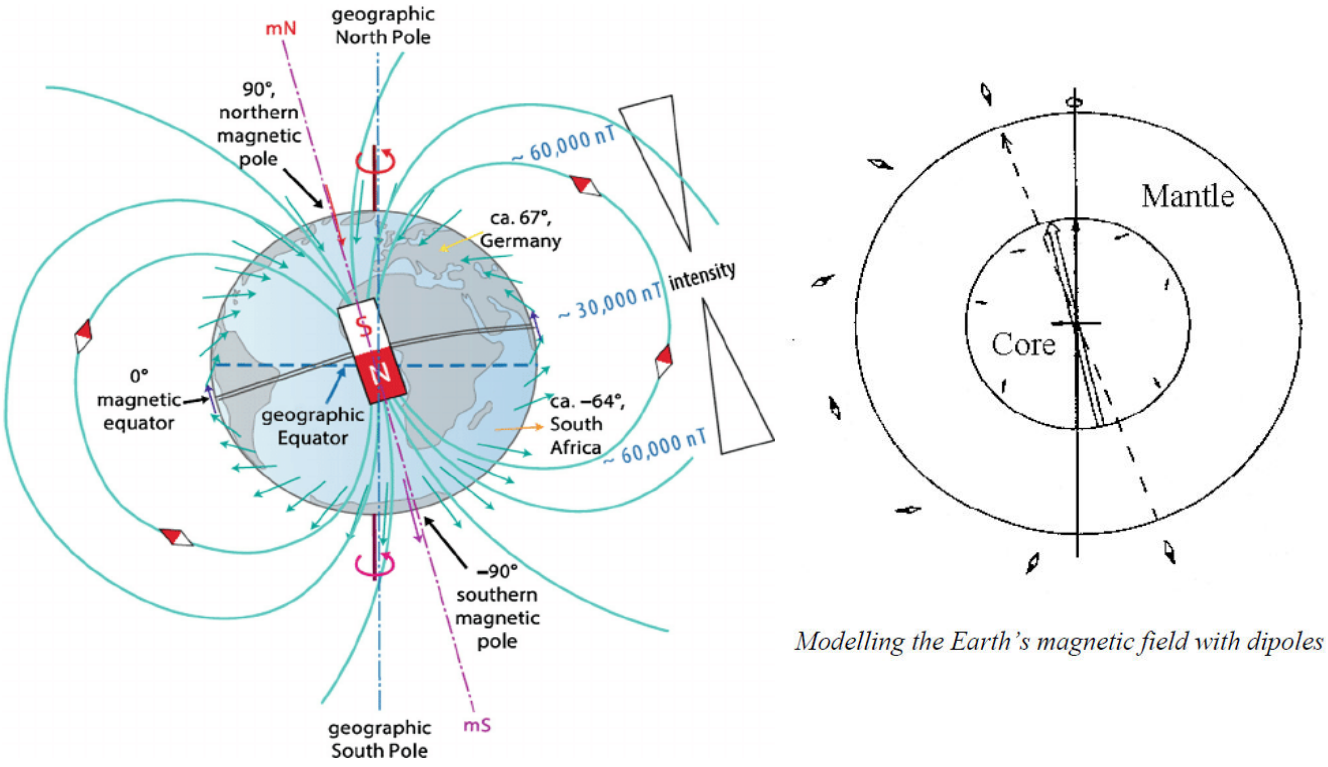

Modelling the Earth's magnetic field with dipoles

The origin of the Earth's field is known to be 99% internal and to be generated by convection in the liquid outer core, which drives electric currents. It cannot be due to magnetized rocks because it must be deep, and rocks lose all magnetization above the Curie temperature. The Curie temperature for magnetite is 578°C, whereas the temperature of the core is probably ~ 5,000°C.

b) The external field: This accounts for the other 1% of the Earth's field. It is caused by electric currents in ionized layers of the outer atmosphere. It is very variable, and has an 11-year periodicity which corresponds to sunspot activity. There is a diurnal periodicity of up to 30 γ, which varies with latitude and season because of the effect of the sun on the ionosphere. There is a monthly variation of up to 2 γ which is the effect of the moon on the ionosphere.

Superimposed on this are micro pulsations which are seemingly random changes with variable amplitude, typically lasting for short periods of time.

Magnetic storms are random fluctuations caused by solar ionospheric interactions as sunspots are rotated towards and away from the Earth. They may last a few days and have amplitudes of up to 1,000 γ within 60° of the equator. They are more frequent and of higher amplitude closer to the poles, *e.g.*, in the auroral zone. The possibility of magnetic storms must be taken into consideration in exploration near the poles, *e.g.*, in Alaska.

c) Local anomalies: These are caused by magnetic bodies in the crust, where the temperature is higher than the Curie temperature. These bodies are the targets of magnetic surveying.

Mathematical treatment of main field

The terms used are:

F = total field

H = horizontal component

Z = vertical component

I = inclination

D = declination

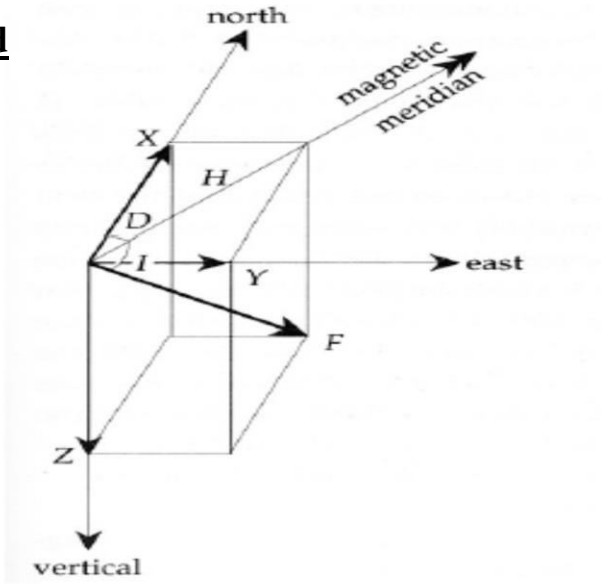

In surveying, ΔH, ΔZ or ΔF can be measured. It is most common to measure ΔF. Measurement of ΔH and ΔZ is now mostly confined to observatories.

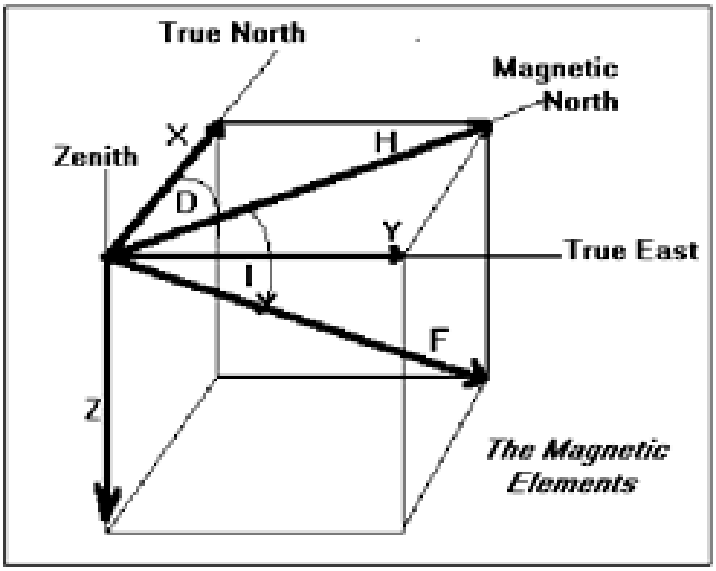

Components of Earth's Magnetic Field

Secular variations in the main field

These are very long period changes that result from convective changes in the core. They are

monitored by measuring changes in I, D and F at observatories. The Earth's field is also subject to *reversals*, the last of which occurred at 0.7 Mya (i.e., 0.7 million years ago). They appear to be geologically sudden, not gradual, and their frequency is very variable. They are used for palaeomagnetic dating. This is done by comparing the sequence of reversals in the field area of interest to the known, dated, geological record of reversals.

Diurnal variations

The Earth's magnetic field also varies because of changes in the strength and direction of currents circulating in the ionosphere. In the normal *solarquiet* (Sq) pattern, the background field is almost constant during the night but decreases

between dawn and about 11 a.m., increases again until about 4 p.m. and then slowly declines to the overnight value (see the following figure).

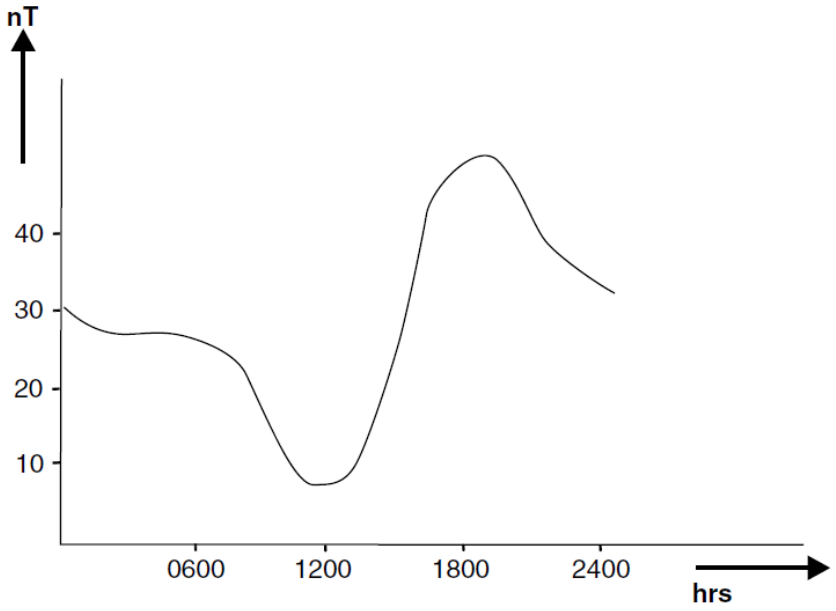

Typical 'quiet day' magnetic field variation at mid-latitudes.

Peak to-trough amplitudes in mid-latitudes are of the order of a few tens of nanoTesla. Since upper atmosphere ionization is caused by solar radiation, diurnal curves tend to be directly related to local solar time but amplitude differences of more than 20% due to differences in crustal conductivity may be more important than time dependency for points up to a few hundred kilometers apart. Short period, horizontally polarized and roughly sinusoidal *micro pulsations* are significant only in surveys that are to be contoured at less than 5 nT.

Within about 5◦ of the magnetic equator the diurnal variation is strongly influenced by the *equatorial electro jet*, a band of high conductivity in the ionosphere about 600 km (5◦ of latitude) wide. The amplitudes of the diurnal curves in the affected regions may be well in excess of 100 nT and may differ by 10 to 20 nT at points only a few tens of kilometers apart.

Many of the magnetic phenomena observed in polar regions can be explained by an *auroral electro jet* subject to severe short-period fluctuations. In both equatorial and polar regions it is particularly important that background variations be monitored continuously. Returning to a base station at intervals of one or two hours may be quite insufficient.

Magnetic storms

Short-term auroral effects are special cases of the irregular disturbances (Ds and Dst) known as *magnetic storms.* These are produced by sunspot and solar flare activity and, despite the name, are not meteorological, often occurring on clear, cloudless days. There is usually a sudden onset, during which the field may change by hundreds of nT, followed by a slower, erratic return to normality. Time scales vary widely but the effects can persist for hours and sometimes days. Micro pulsations are generally at their strongest in the days immediately following a storm, when components with periods of a few tens of seconds can have amplitudes of as much as 5 nT.

Ionospheric prediction services in many countries give advance warning of the general probability of storms but not of their detailed patterns, and the field changes in both time and space are too rapid for corrections to be applied. Survey work must stop until a storm is over. Aeromagnetic data are severely affected by quite small irregularities and for contract purposes *technical magnetic storms* may be defined, sometimes as departures from linearity in the diurnal curve of as little as 2 nT in an hour. Similar criteria may have to be applied in archaeological surveys when only a single sensor is being used (rather than a two-sensor gradiometer).

Geological effects

The Curie points for all geologically important magnetic materials are in the range 500–600 ◦C. Such temperatures are reached in the lower part of normal continental crust but below the Moho under the oceans. The upper mantle is only weakly magnetic, so that the effective base of local magnetic sources is the Curie isotherm beneath continents and the Moho beneath the oceans.

Massive magnetite deposits can produce magnetic fields of as much as 200 000 nT, which is several times the magnitude of the Earth's normal field. Because of the dipolar nature of magnetic sources these, and all other, magnetic anomalies have positive and negative parts and in extreme cases directional magnetometers may even record negative fields. Anomalies of this size are unusual, but basalt dykes and flows and some larger basic intrusions can produce fields of thousands and occasionally tens of thousands of nT. Anomalous fields of more than 1000 nT are otherwise rare, even in areas of outcropping crystalline basement. Sedimentary rocks generally produce changes of less than 10 nT, as do the changes in soil magnetization important in archaeology. In some tropical areas, magnetic fields of tens of nT are produced by maghemite formed as nodular growths in laterites. The nodules may later weather out to form ironstone gravels which give rise to high noise levels in ground surveys. The factors that control the formation of maghemite rather than the commoner, non-magnetic form of hematite are not yet fully understood.

Rock magnetism

Kinds of minerals magnetism

1-Diamagnetism: In diamagnetic minerals, all the electron shells are full, and there are no unpaired electrons. The electrons spin in opposite senses and the magnetic effects cancel. When placed in an external field, the electrons rotate to

produce a magnetic field in the opposite sense to the applied. Such minerals have negative susceptibilities, k. Examples of such materials are quartzite and salt. Salt domes thus give diamagnetic anomalies, i.e., weak negative anomalies.

2- Paramagnetism: Paramagnetic minerals are ones where the electron shells are incomplete. They generate weak magnetic fields as a result. When placed in an external field, a magnetic field in the same sense is induced, i.e., k is positive. Examples of materials that are paramagnetic are the Ca - Ni element series.

3- Ferromagnetism: Ferromagnetic minerals are minerals that are paramagnetic, but where groups of atoms align to make domains. They have much larger k values than paramagnetic elements. There are only three ferromagnetic elements – Iron, Cobalt and Nickel. Ferromagnetic minerals do not exist in nature.

Types of magnetism

1- Induced magnetism: This is due to induction by the Earth's field, and is in the same direction as the Earth's field. Most magnetization is from this source. It is important to appreciate that since the Earth's field varies from place to place, the magnetic anomaly of a body will vary according to its location.

2- Remnant magnetism: This is due to the previous history of the rock. There are various types:

a- Chemical remnant magnetization (CRM): This is acquired as a result of chemical grain accretion or alteration, and affects sedimentary and metamorphic rocks.

b- ***Detrital remnant magnetisation (DRM):*** This is acquired as particles settle in the presence of Earth's field. The particles tend to orient themselves as they settle.

c- Isothermal remnant magnetism (IRM): This is the residual magnetic field left when an external field is applied and removed, *e.g.*, lightning.

d- Thermoremnant magnetization (TRM): This is acquired when rock cools through the Curie temperature, and characterizes most igneous rocks. It is the most important kind of magnetization for palaeomagnetic dating.

e- Viscous remnant magnetism (VRM): Rocks acquire this after long exposure to an external magnetic field, and it may be important in fine-grained rocks.

Induced and remnant magnetism

The direction and strength of the present Earth's field is known. However, we may know nothing about the remnant magnetization of a rock. For this reason, and because in strongly magnetized rocks the induced field dominates, it is often assumed that all the magnetization is induced. The true magnetization is the vector sum of the induced and remnant components. However, the remnant magnetization be measured using a static or Spinner magnetometer, which measure the magnetism of samples in the absence of the Earth's field.

Rock susceptibility

These are analogous to density in gravity surveying. Most rocks have very low susceptibilities. The susceptibility of a rock is dependent on the quantity of ferrimagnetic minerals. *In situ* measurements of rock susceptibility may be made using special magnetometers but it is more common to measure a sample in the laboratory, *e.g.*, using an induction balance. The sample is placed in a coil, a current is applied and the induced magnetization is measured. It is usual to quote the strength of the field applied along with the result. If the applied field was very much greater than the Earth's field, the value obtained may not be suitable for interpreting magnetic anomalies. Another method of obtaining the susceptibility of a rock is to assume that all the magnetization is due to magnetite. The volume percent of magnetite is multiplied by the Susceptibility of magnetite. This method has produced good correlation with field measurements. Susceptibility (k), ranges

over 2-3 orders of magnitude in common rock types. Basic igneous rocks have the highest susceptibilities since they contain much magnetite. The proportion of magnetite tends to decrease with increasing rocks acidity, and thus k tends to be low for acid rocks such as granite. The susceptibility of metamorphic rocks depends on the availability of O_2 during their formation, since plentiful O_2 results in magnetite forming.

Sedimentary rocks usually have very low k, and sedimentary structures very rarely give large magnetic anomalies. If a large magnetic anomaly occurs in a sedimentary environment, it is usually due to an igneous body at depth.

The *susceptibility* of a rock usually depends on its magnetite content. Sediments and acid igneous rocks have small susceptibilities whereas basalts, dolerites, gabbros and serpentinites are usually strongly magnetic. Weathering generally reduces susceptibility because magnetite is oxidized to hematite, but some laterites are magnetic because of the presence of maghemite and remanently magnetized hematite. The susceptibilities, in rationalized SI units, of some common rocks and minerals are given in the following table.

Common rocks	
Slate	0–0.002
Dolerite	0.01–0.15
Greenstone	0.0005–0.001
Basalt	0.001–0.1
Granulite	0.0001–0.05
Rhyolite	0.00025–0.01
Salt	0.0–0.001
Gabbro	0.001–0.1
Limestone	0.00001–0.0001
Ores	
Hematite	0.001–0.0001
Magnetite	0.1–20.0
Chromite	0.0075–1.5
Pyrrhotite	0.001–1.0
Pyrite	0.0001–0.005

Common causes of magnetic anomalies

Dykes, folded or faulted sills, lava flows, basic intrusions, metamorphic basement rocks and ore bodies that contain magnetite all generate large-amplitude magnetic anomalies. Other targets suitable for study using magnetic method are disturbed soils at shallow depth, fire pits and kilns, all of which are of interest in archaeological studies. Magnetic anomalies can be used to get the depth to basement rocks, and hence sedimentary thickness, and to study metamorphic thermal aureoles.

Magnetometers and Magnetic Measurements

Magnetometer is a scientific instrument used to measure the strength and/ or direction of the magnetic field. Magnetism varies from place to place and differences in Earth's magnetic field can be caused by the differing nature of rocks and the interaction between charged particles from the Sun and the magnetosphere.

Magnetometer Types:

•**Scalar magnetometers** measure the total strength of the magnetic field to which they are subjected.

•**Vector magnetometers** have the capability to measure the component of the magnetic field in a particular direction, relative to the spatial orientation of the device.

Modern magnetometers

•**Rotating coil magnetometer**

•**Hall effect magnetometer**

•**Proton precession magnetometer**

•**Gradiometer**

•Fluxgate magnetometer

•Cesium vapor magnetometer

•Spin-exchange relaxation-free (SERF) atomic magnetometers

Rotating coil magnetometer

•The magnetic field induces a sine wave in a rotating coil. The amplitude of the signal is proportional to the strength of the field, provided it is uniform, and to the sine of the angle between the rotation axis of the coil and the field lines.

Hall Effect magnetometer

The most common magnetic sensing devices are solid- state Hall effect sensors. These sensors produce a voltage proportional to the applied magnetic field and also sense polarity, see figure 16.

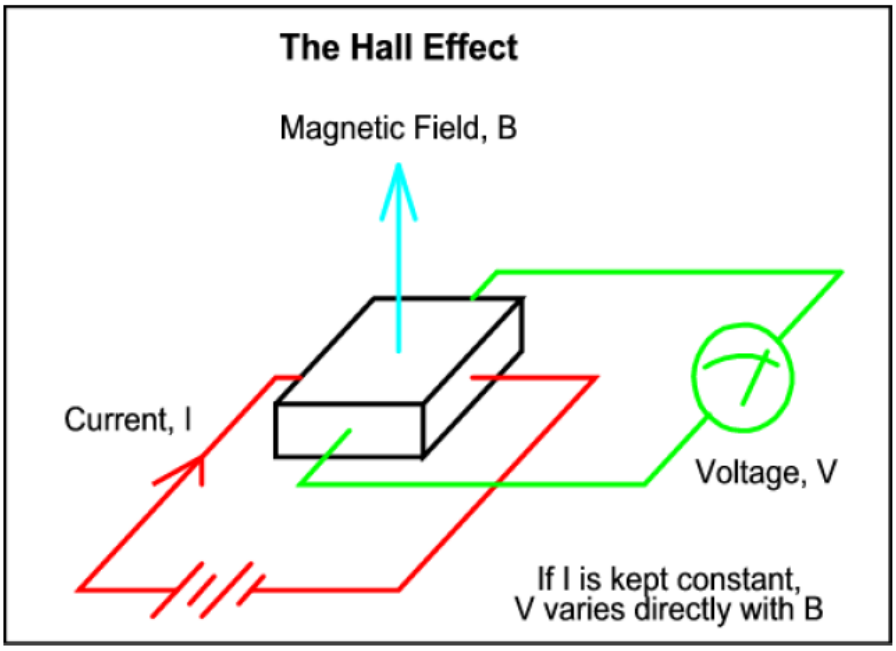

Figure (16): The Hall Effect Magnetometer diagram.

Proton precession magnetometer

•Proton precession magnetometers, also known as proton magnetometers, measure the resonance frequency of protons (hydrogen nuclei) in the magnetic field to be

measured, due to nuclear magnetic resonance (NMR). Because the precession frequency depends only on atomic constants and the strength of the ambient magnetic field, the accuracy of this type of magnetometer is very good, see figure 17.

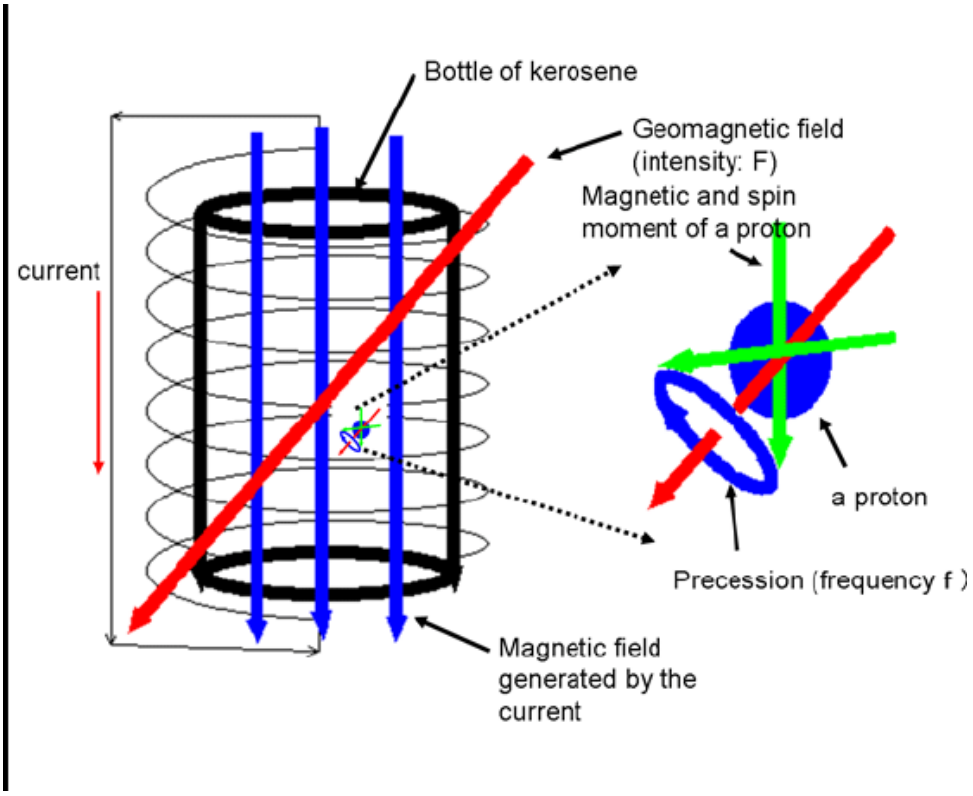

Figure (17): The principle of proton precession magnetometer operation .

Figure 18 , shows the geophysical ground surveying and taking magnetic measurements in field by using the proton precession magnetometer.

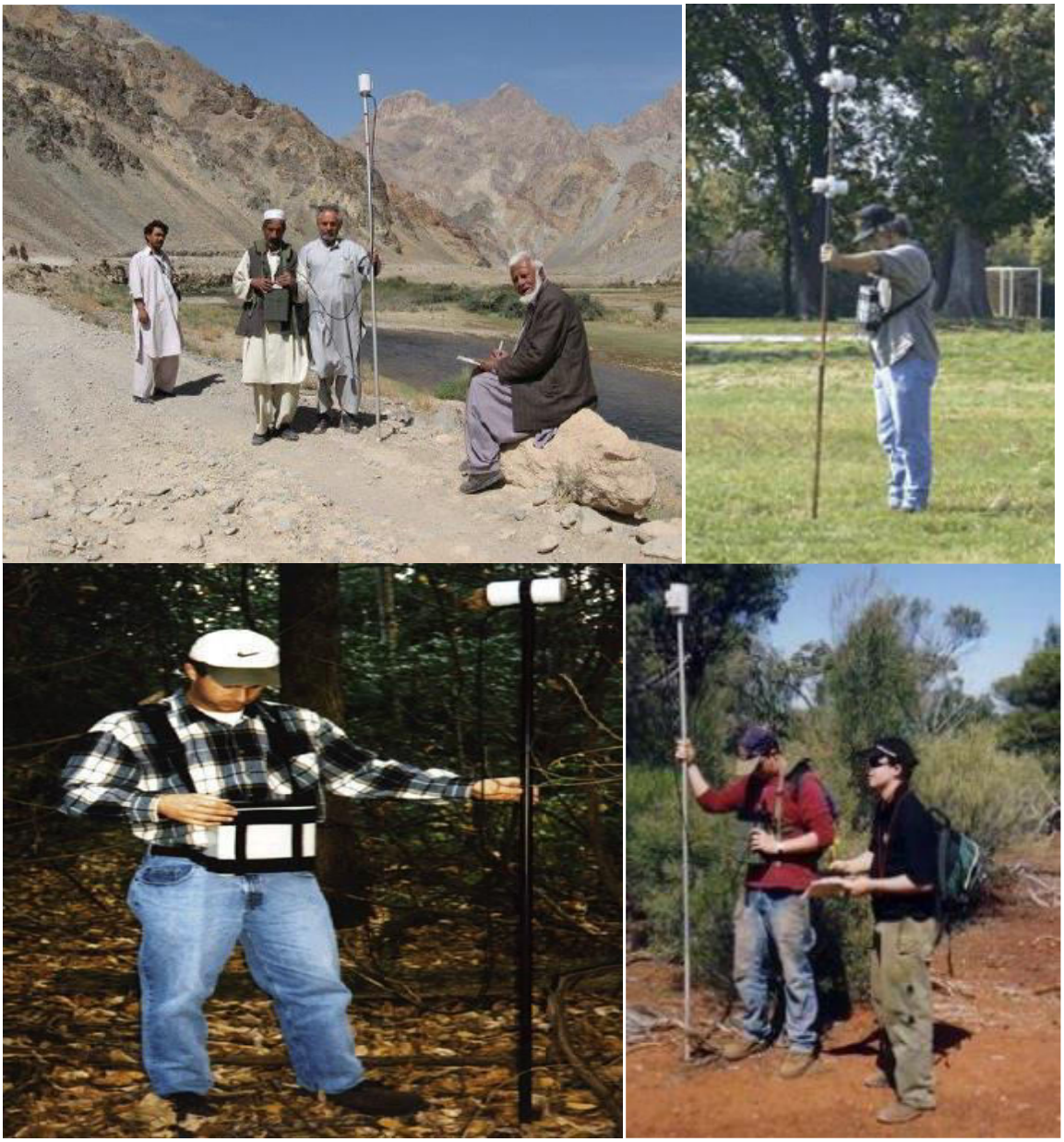

Figure (18): field magnetic surveying by using the proton precession magnetometer.

Gradiometer

•Magnetic gradiometers are pairs of magnetometers with their sensors horizontally separated by a fixed distance. The readings are subtracted in order to measure the difference between the sensed magnetic fields, which measures the field gradients caused by magnetic anomalies. This is one way of compensating both the variability in time of the Earth's magnetic field and for other sources of

electromagnetic interference, allowing more sensitive detection of anomalies , figure 19 , represents a diagram showing the principle of magnetic sensor for the proton precession magnetometer .

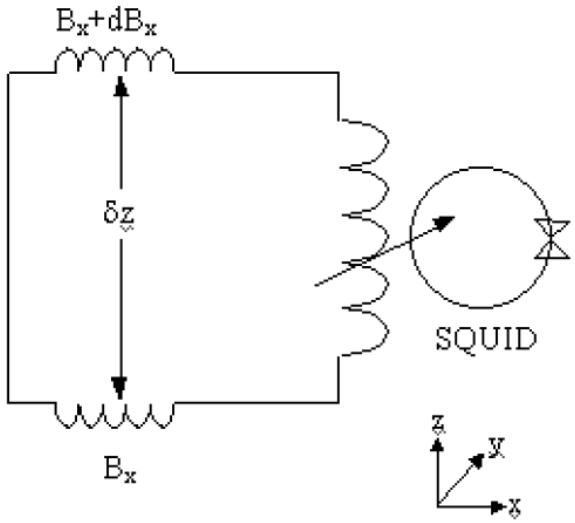

Figure (19): the precession proton magnetometer sensor components.

The figure 20, show the magnetic gradiometer which composed of two magnetic sensors with a constant distance between them which used in field to measure both vertical and horizontal magnetic gradient.

Figure (20): The magnetic gradiometer in use during field surveying.

Fluxgate magnetometer

•A fluxgate magnetometer consists of a small, magnetically susceptible, core wrapped by two coils of wire. An alternating electrical current is passed through one coil, driving the core through an alternating cycle of magnetic saturation. This constantly changing field induces an electrical current in this conducting coil, and this output current is measured by a detector, figure 21 shows the components of the fluxgate magnetometer.

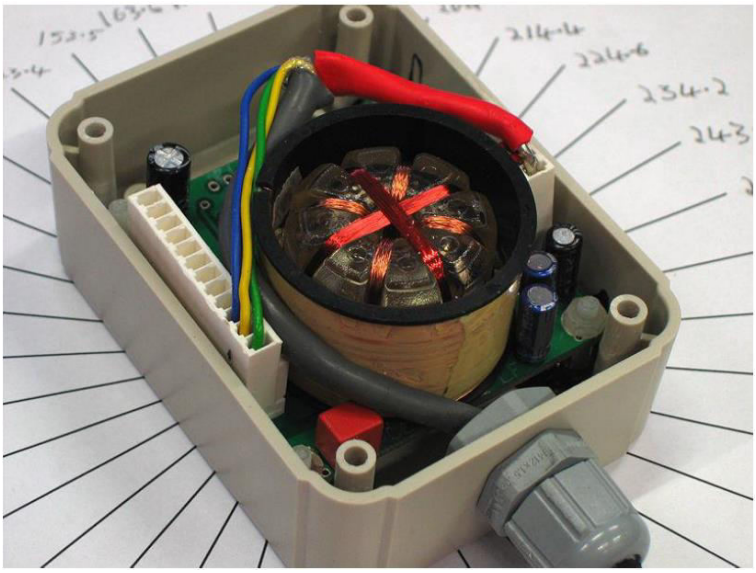

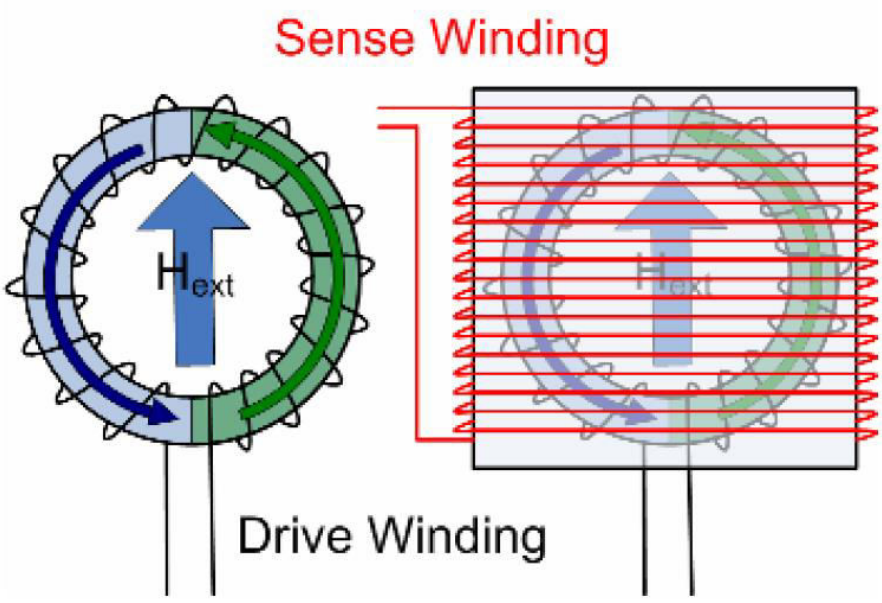

Figure (21): components of the fluxgate magnetometer.

Magnetic surveys

Magnetic surveys either directly seek magnetic bodies or they seek magnetic material associated with an interesting target. For example, magnetic minerals may exist in faults or fractures.

1- Land surveys:

These are usually done with portable proton precession magnetometers. Profiles or networks of points are measured in the same way as for gravity. It is important to survey perpendicular to the strike of an elongate body or two-dimensional modeling may be very difficult.

It is necessary to tie back to the base station at 2-3 hour intervals, or to set up a continually-reading base magnetometer. This will give diurnal drift and detect magnetic storms.

The operator must:

• Record the time, at which readings were taken, for drift correction,

• Stay away from interfering objects, e.g., wire fences, railway lines, roads.

• Not carry metal objects *e.g.*, mobile phones, and

• Take multiple readings at each station to check for repeatability.

Reduction of the observations is much simpler than for gravity:

1. The diurnal correction

This may be up to 100 γ. Observatory data may be used if the observatory is within about 100 km and no major magnetic bodies occur in between, which might cause phase shifts in the temporal magnetic variations. A magnetic storm renders the data useless.

2. Regional trends

These are corrected for in the same way as for gravity, i.e., a linear gradient or polynomial surface is fit to regional values, and subtracted. The UK regional

gradient is 2.13 γ/km N and 0.26 γ/km W. Another method is to subtract the predicted IGRF (International Geomagnetic Reference Field) which is a mathematical description of the field due to the Earth's core. There are several such formulae to choose from, all based on empirical fits to observatory orsatellite data. The other corrections made to gravity readings are not necessary in magnetic surveys. In particular, small elevation changes have a negligible effect on magnetic anomalies, and thus elevation-related corrections are not needed for most surveys.

Air Magnetic surveys

Most magnetic surveying is aeromagnetic surveying, and it may be done with either airplane or helicopter. Helicopters are more suitable for detailed or difficult access areas, though airplanes are cheaper. Usually a proton magnetometer is towed behind the helicopter, and thus discrete measurements are made. The magnetometer is then called the *bird*. It may also be mounted as a tail stinger on planes because of problems with sensor motion and cable vibrations that result from higher speeds. Wingtip mounting is also available. If the instrument is housed inboard, it is necessary to correct for the magnetic effect of airplane. It is also possible to measure vertical and longitudinal gradients and often several magnetometers are flown to maximize the use of the flight. Aeromagnetic surveying is not useful for surveys where great spatial accuracy or very dense measurements are required.

The use of aeromagnetic surveying is limited by navigation which is a first order problem for such surveys. Before the widespread use of the GPS this was done by radio beacon *e.g.*, Loran or aerial photography. Photography is not a solution sometimes, however, *e.g.*, over jungles or the sea where there are no landmarks. Doppler navigation was sometimes used.

This involves radio beams that are bounced off the ground both before and aft of the aircraft. This gives the speed of the aircraft accurately. The recent advent of the GPS has enabled Aeromagnetic surveys to be used more widely for sea surveys. Prior to the GPS, navigation accuracy was often no better than 100 m. The layout of the survey depends on target scale and anomaly strike. Usually a criss-cross pattern of perpendicular flight paths is adopted. The lines perpendicular to strike are more closely spaced, and the *tie lines* at right angles to these may be typically at 1/4 or 1/10 the density.

The optimum design of lines has been examined analytically to determine the optimum spacing for a given anomaly width. The difference in anomaly deduced from lines with spacing's of 0.5 and 0.25 miles is illustrated by a study of one of the largest sulphide deposits in Canada:

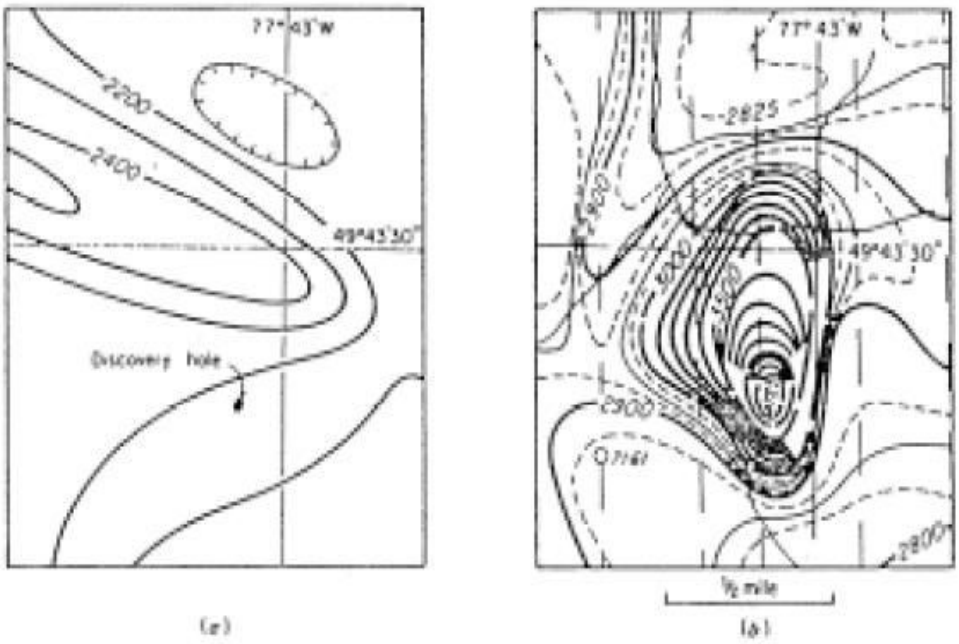

Results from sparse and dense flight lines

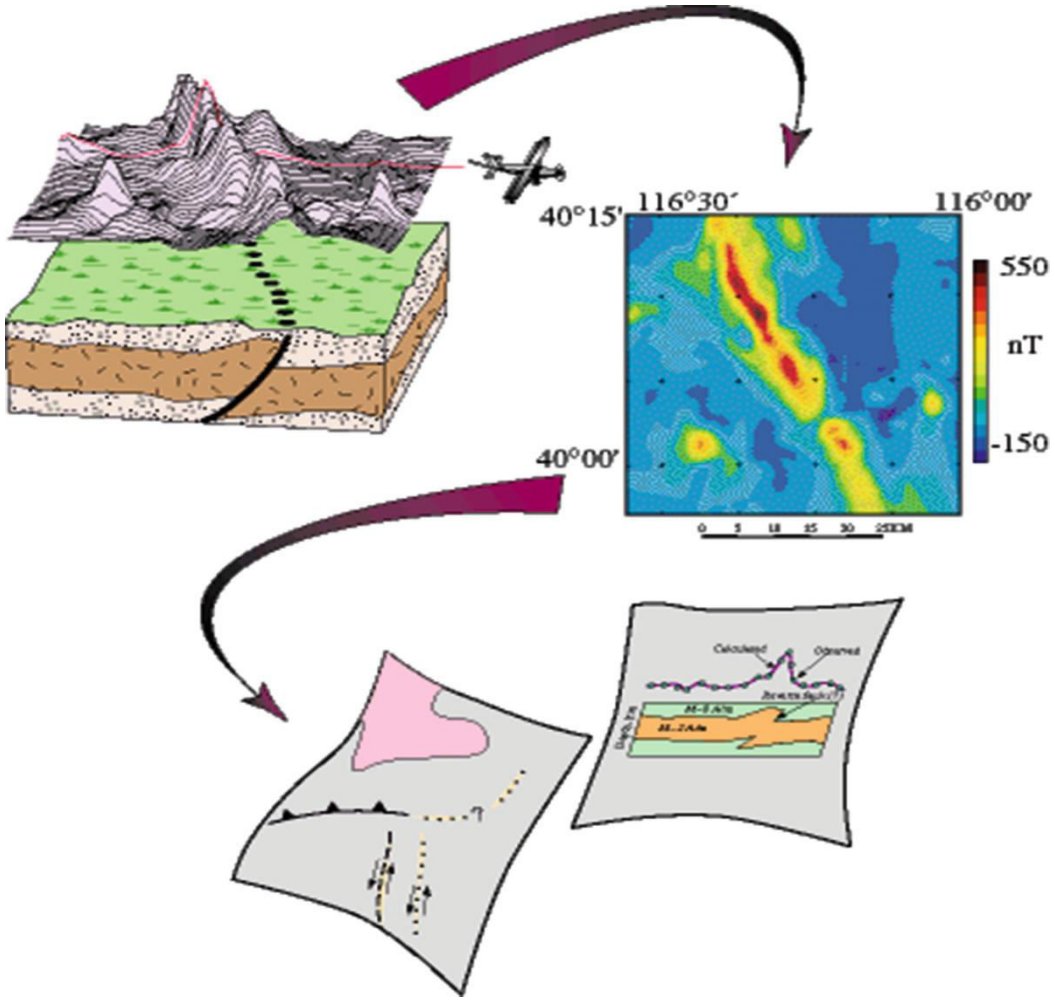

The flight height is typically 200 to 1,000s of feet, and should remain as constant as possible. For oil reconnaissance, the most interesting feature is generally deep basement structure. In this case, high surveys are flown, typically above 1000', to effectively filter out the signals from small, shallow bodies.

Diurnal drift and other errors, *e.g.*, variable flying height can be averaged out by:

• minimizing the RMS of the line crossover measurement differences, or

• fitting a high-order polynomial to each line and eliminating the differences completely. This procedure is similar to that applied to the SEASAT data and is a

technique used in geodetic surveys. A fixed ground magnetometer is used to monitor for magnetic storms.

Aeromagnetic surveys have the major advantages that they are very cheap, can cover huge areas, and can filter out shallow, high-frequency anomalies. This latter is also the major disadvantage of aeromagnetic surveying for prospecting for shallow bodies within mining range. Onboard computers for quasi-real time assessment of the data are becoming more common, as it is important to make sure the data are satisfactory before demobilizing.

Sea Magnetic Surveys

The instrument is towed behind the ship at a distance of up to 500 m to avoid the magnetic effect of ship. It is then known as the *fish*. The instrument is made buoyant and a proton magnetometer is usually used. The sampling frequency is typically 4-20 s, giving measurements spaced at intervals of 8-16 m if the ship speed is 4-6 knots. GPS navigation is almost universally used now. Loran navigation was most common in the past. Sea magnetic surveys are generally conducted at the same time as a seismic survey. The ship's course is optimized for the seismic survey and it is thus usually non-optimal for the magnetic survey. There may also be problems making the diurnal correction if the ship is more than 100 km from land. Under these circumstances the diurnal correction may have to be done by tie-line analysis. Recently, the longitudinal gradient is frequently measured and used, and has caused great improvement in the usefulness of marine magnetic data for oil exploration.

Magnetic survey Data display

As with all geophysical data, outliers must be removed before turning to modeling and interpretation work. Algorithms are available for this, or the geophysicist can do it by brain. It may be desired to interpolate all the measurements onto a regular

grid in the case of aeromagnetic data which are not uniformly measured. It is critical to maintain the integrity of the data when this is done. For example, if contouring at 5 γ intervals, each data point should fit the raw measurements to within 2.5 γ. Contour maps are the most common, but generating them without degrading the data nor introducing statistically unsupported artifacts is not simple. Decisions that must be taken in designing the final map are:

• contour interval (*e.g.* 0.25 γ),
• sampling interval (*e.g.* 75 m),
• height (*e.g.*, mean-terrain clearance of 150 m),
• spacing of flight lines,
• geomagnetic reference surface to subtract,
• % of data samples to contour,
• interpolation method (*e.g.*, minimum curvature with bicubic spline refinement).

Aeromagnetic data

Displaying the data as offset profiles is common. High frequencies attenuate out at great height. Very quiet, smooth aeromagnetic maps characterize sedimentary basins with deep basement. A lot of high frequency anomalies indicate shallow anomalous bodies that may be ore or igneous rocks. It is important to find the depth of bodies in sedimentary regimes. An irregular basement is often truncated by erosion, and thus the depth corresponds to the thickness of the sedimentary sequence. Abrupt changes in magnetic character may reflect boundaries between magnetic provinces, or a basement fault. The strike of the magnetic trend indicates the structural trend of area.

Using processing methods such as upward and downward continuation, the magnetic field can be calculated at any height. It may be helpful to display the data

as they would look had the survey been made at a higher elevation, thereby filtering out high-frequency anomalies due to small, shallow bodies.

Data interpretation

1 -Problems and errors related to magnetic data interpretation:

a- Magnetization: This may not be uniform, but the interpreter is usually obliged to assume it is. Large anomalies tend not to reflect major lateral changes in structure, as they do in gravity, rather lateral changes in rock susceptibility. In the example illustrated below, a lateral change in susceptibility gives a 3000 γ anomaly. Elsewhere, a basement ridge 1000' high gives only a 120 γ anomaly. The basement ridge is important for assessing the oil potential of the sedimentary basement, but the change in susceptibility is of no consequence.

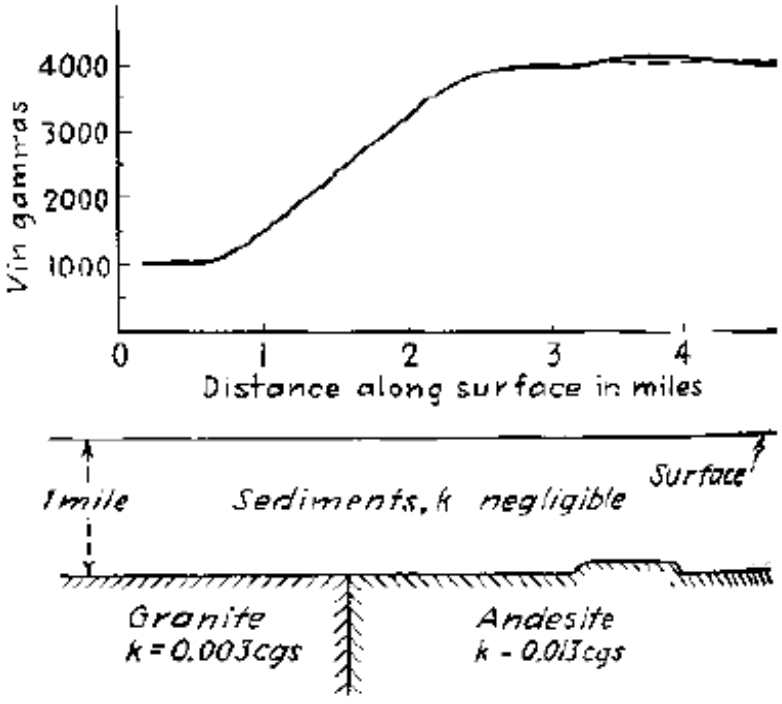

Comparison of magnetic effect of lateral susceptibility change in basement with effect of Structural feature on basement surface.

b- Ambiguity: The ambiguity problem is the same for magnetic surveying as it is for gravity. There is ambiguity between size and distance. In the case of magnetic the problem is much worse, as there are many other ambiguities, *e.g.*, between the direction of the body magnetization and the dip of the Earth's field.

Noise in ground magnetic surveys

Magnetic readings in populated areas are usually affected by stray fields from pieces of iron and steel (*cultural noise*). Even if no such materials are visible, profiles obtained along roads are usually very distorted compared to those obtained on parallel traverses through open fields only 10 or 20 m away.

Since the sources are often quite small and may be buried within a metre of the ground surface, the effects are very variable. One approach to the noise problem is to try to take all readings well away from obvious sources, noting in the field books where this has not been possible. Alternatively, the almost universal presence of ferrous noise can be accepted and the data can be filtered. For this method to be successful, many more readings must be taken than would be needed to define purely geological anomalies. The technique is becoming more popular with the increasing use of data loggers, which discourage note-taking but allow vast numbers of readings to be taken and processed with little extra effort, and is most easily used with alkali vapor and fluxgate instruments which read virtually continuously.

Simple Magnetic Interpretation

Field interpretation of magnetic data allows areas needing infill or checking to be identified and then revisited immediately and at little cost. Good interpretation requires profiles, which preserve all the detail of the original readings, and contour maps, which allow trends and patterns to be identified. Fortunately, the now almost

ubiquitous laptop PC has reduced the work involved in contouring (providing the necessary programs have been loaded).

Forms of magnetic anomaly

The shape of a magnetic anomaly varies dramatically with the dip of the Earth's field, as well as with variations in the shape of the source body and its direction of magnetization. Simple sketches can be used to obtain rough visual estimates of the anomaly produced by any magnetized body.

The following figure shows an irregular mass magnetized by induction in a field dipping at about 60◦. Since the field direction defines the direction in which a positive pole would move, the effect of the external field is to produce the distribution of poles shown. The secondary field due to these poles is indicated by the dashed lines of force. Field direction is determined by the simple rule that like poles repel.

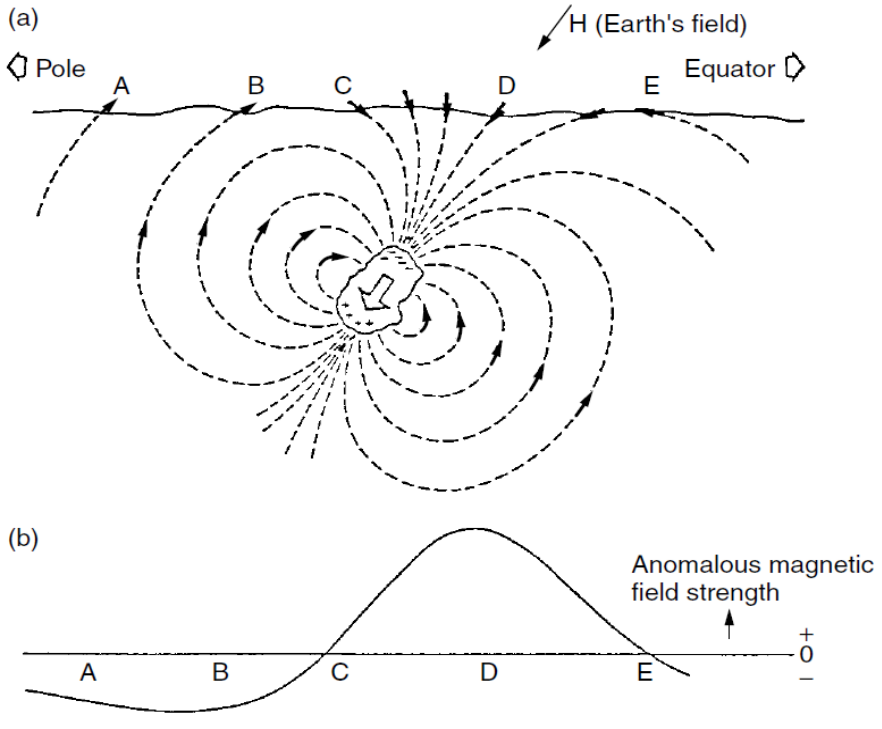

Mid-latitude total field anomaly due to induced magnetization.
(a) The induced field. (b) The anomaly profile, derived as described in the text.

If the secondary field is small, the directions of the total and background fields will be similar and no anomalous field will be detected near C and E. The anomaly will be positive between these points and negative for considerable distances beyond them. The anomaly maximum will be near D, giving a magnetic profile with its peak offset towards the magnetic equator (the previous figure). At the equator the total-field anomaly would be negative and centered over the body and would have positive side lobes to north and south, as can easily be verified by applying the method of the figure above to a situation in which the inducing field is horizontal. Because each positive magnetic pole is somewhere balanced by a negative pole, the net flux involved in any anomaly is zero. Over the central parts of a uniform magnetized sheet the fields from positive and negative poles cancel out, and only the edges are detected by magnetic surveys. Strongly magnetized but flat-lying bodies thus sometimes produce little or no anomaly.

‘Rule-of-thumb’ in depth estimation of magnetized subsurface bodies

Depth estimation is one of the main objectives of magnetic interpretation. Simple rules give depths to the tops of source bodies that are usually correct to within about 30%, which is adequate for preliminary assessment of field results. In the following Figure(part a) the part of the anomaly profile, on the side nearest the magnetic equator, over which the variation is almost linear is emphasized by a thickened line. The depths to the abruptly truncated tops of bodies of many shapes are approximately equal to the horizontal extent of the corresponding straight-line sections. This method is effective but is hard to justify since there is actually no straight segment of the curve and the interpretation relies on an optical illusion.

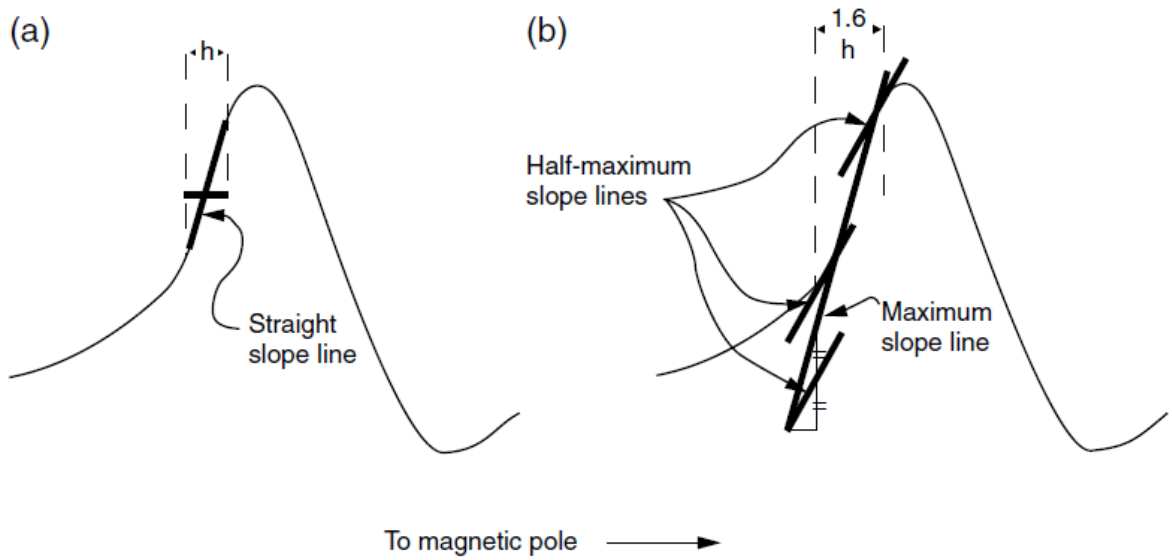

\Simple depth estimation: (a) Straight slope method. The distance over which the variation appears linear is (very) roughly equal to the depth to the top of the magnetized body. (b) Peters' method. The distance between the contact points of the half-slope tangents is (very) roughly equal to 1.6 times the depth to the top of the magnetized body.

In the slightly more complicated *Peters' method*, a tangent is drawn to the profile at the point of steepest slope, again on the side nearest the equator, and lines with half this slope are drawn using the geometrical construction of the above figure (part b). The two points at which the half-slope lines are tangents to the anomaly curve are found by eye or with a parallel ruler, and the horizontal distance between them is measured. This distance is divided by 1.6 to give a rough depth to the top of the source body. Peters' method relies on model studies that show that the true factor generally lies between about 1.2 and 2.0, with values close to 1.6 being common for thin, steeply dipping bodies of considerable strike extent. Results are usually very similar to those obtained using the straight slope. In both cases the profile must either be measured along a line at right angles to the strike of the anomaly or else the depth estimate must be multiplied by the cosine of the intersection angle (A in the following figure).

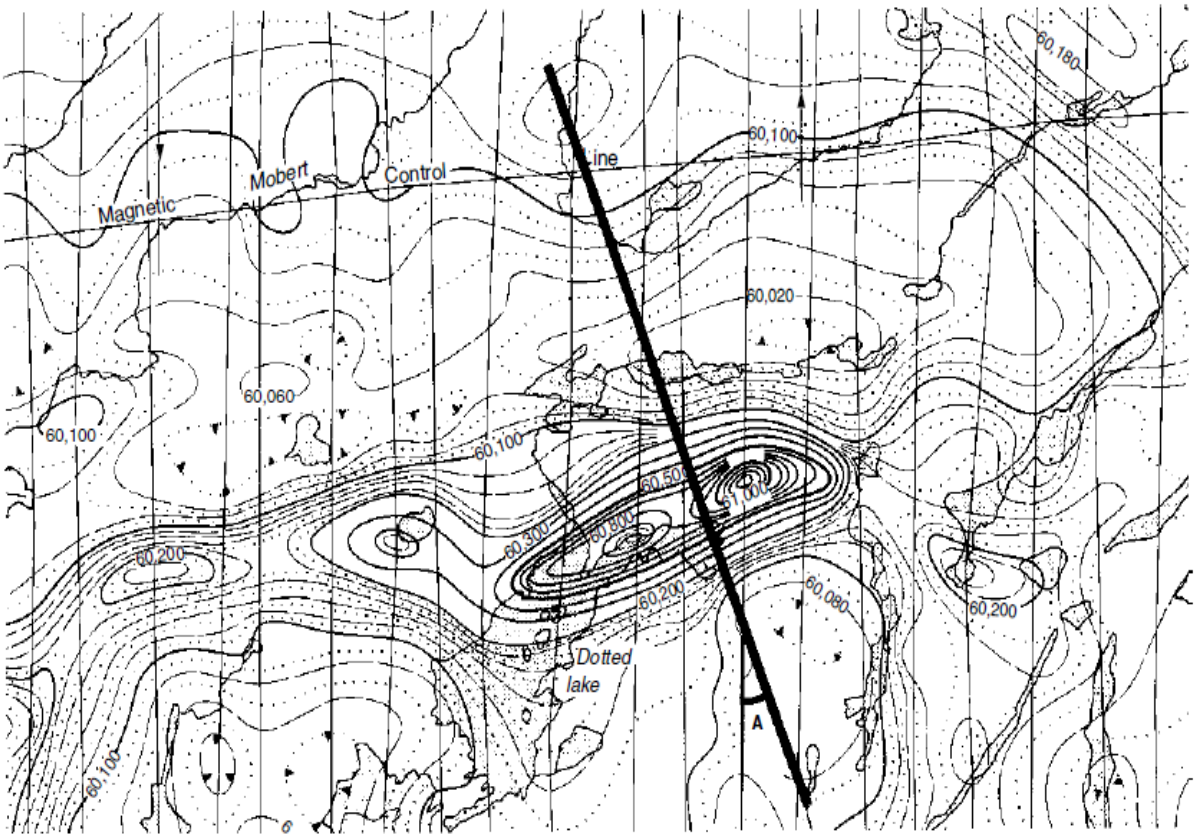

Effect of strike. A depth estimate on a profile recorded along a traverse line (i.e. one of the set of continuous, approximately straight lines) must be multiplied by the cosine of the angle A made with the line drawn at right angles to the magnetic contours. The example is from an aeromagnetic map (from northern Canada) but the same principle applies in ground surveys.

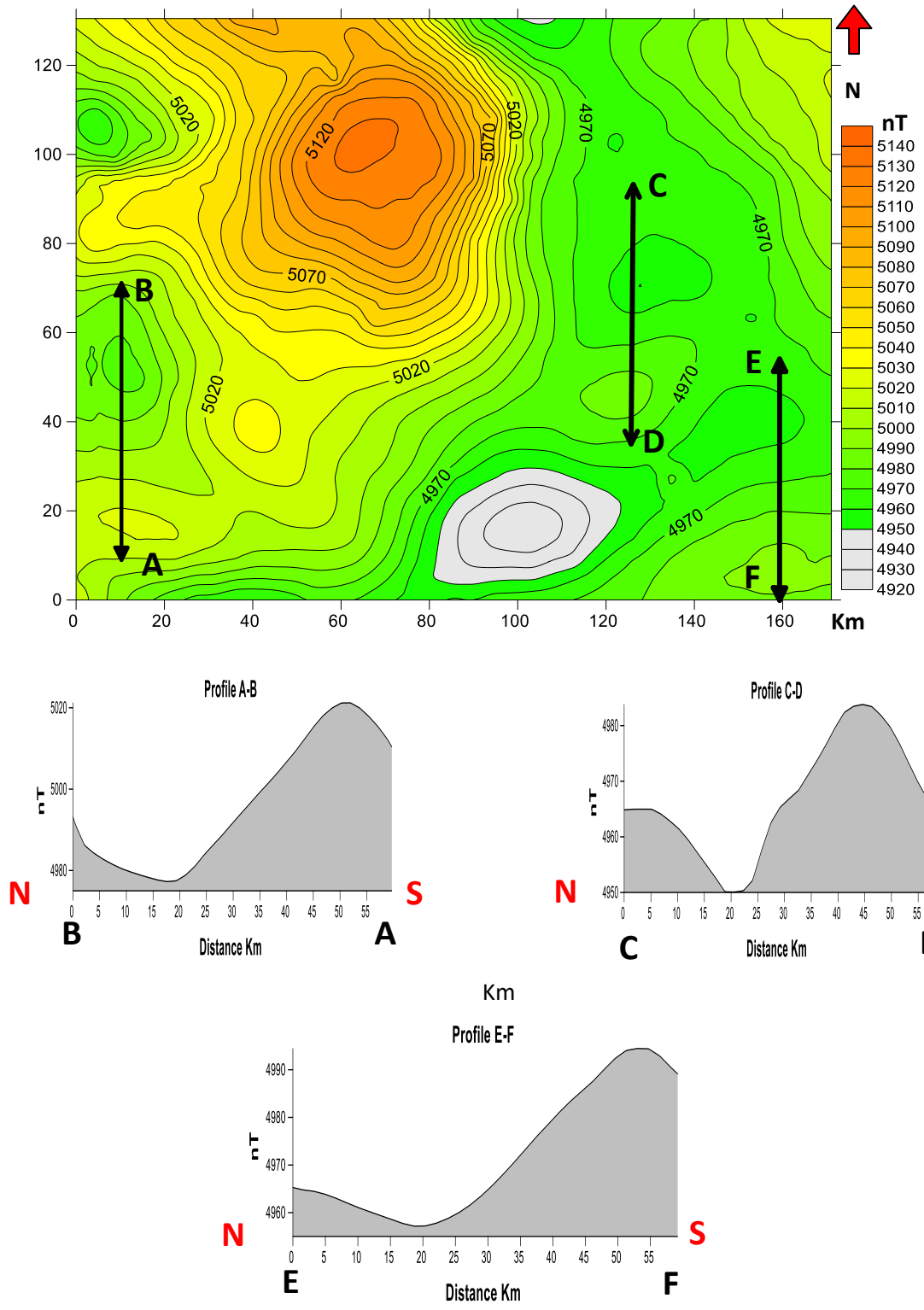
N
nT
5140
5130
5120
5110
5100
5090
5080
5070
5060
5050
5040
5030
5020
5010
5000
4990
4980
4970
4960
4950
4940
4930
4920
5020
5120
5070
4970
A
B
C
D
E
F
Km
Profile A-B
Profile C-D
Profile E-F
Distance Km
nT
N
S

Seismic reflection and refraction methods

Seismic reflection/refraction imaging has successfully been used in the oil industry to detect buried hydrocarbon traps for about 85 years (Dobrin, 1976). Use of surface reflection/refraction methods to characterize the near surface, generally the upper 100 m, is a much younger application, but is still based on about two decades of concentrated research refining these techniques in field and lab studies. As summarized by Steeples (1998), high quality images of the upper 100 m of ground using reflection/refraction imaging methods have been described in dozens of papers since the early 1980's. For high-resolution P-wave seismic-reflection data acquired with much shorter geophone intervals than used in this study, minimum imaging depths have decreased and resolution limits of thin beds have increased to where layers as shallow as 1 m and beds as thin as 0.1 m can be detected under the right conditions (Steeples, 1998). Because similar seismic sources and sensors are used, minimum imaging depths and resolution limits for seismic-refraction data are comparable to those of seismic-reflection data. Also, in many reflection/refraction studies the interpreted layer boundaries have been corroborated by the Stratigraphy interpreted from borehole data (e.g., Luzietti et al., 1992; Miller et al., 1995; Liberty, 1998). These studies show that reflection/refraction data have become a valuable tool in near-surface studies.

The seismic survey is one form of geophysical survey that aims at measuring the earth's (geo-) properties by means of physical (-physics) principles such as magnetic, electric, gravitational, thermal, and elastic theories. It is based on the theory of elasticity and therefore tries to deduce elastic properties of materials by measuring their response to elastic disturbances called seismic (or elastic) waves. Figure 22, showing a Schem of overall field setup for a seismic survey.

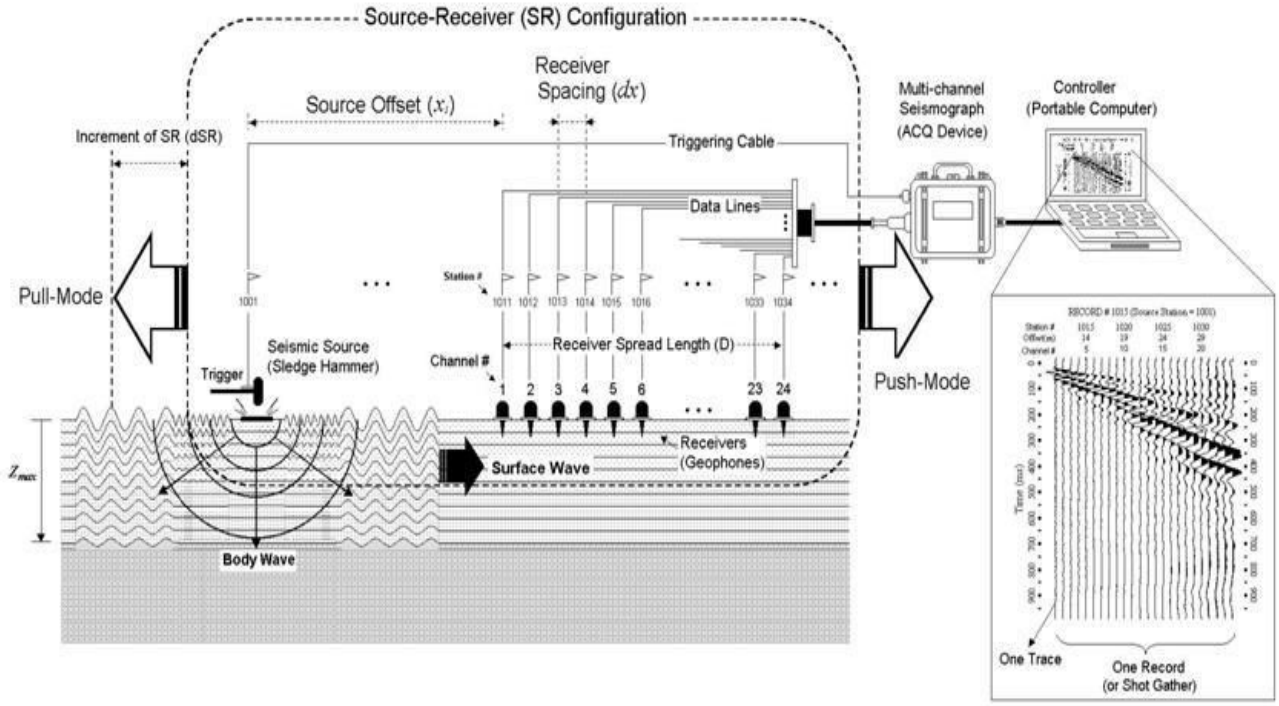

Figure (22): Schematic of overall field setup for a seismic survey..

A seismic source-such as sledgehammer-is used to generate seismic waves, sensed by receivers deployed along a preset geometry (called receiver array), and then recorded by a digital device called seismograph (**Fig. 22**). Based on a typical propagation mechanism used in a seismic survey, seismic waves are grouped primarily into direct, reflected, refracted, and surface waves (**Fig.23**).

There are three major types of seismic surveys: refraction, reflection, and surface-wave, depending on the specific type of waves being utilized. Each type of seismic survey utilizes a specific type of wave (for example, reflected waves for (reflection survey) and its specific arrival pattern on a multichannel record (**Fig. 24**). The **figure 25** shows the active and passive seismic sources which recorded during a seismic surveying.

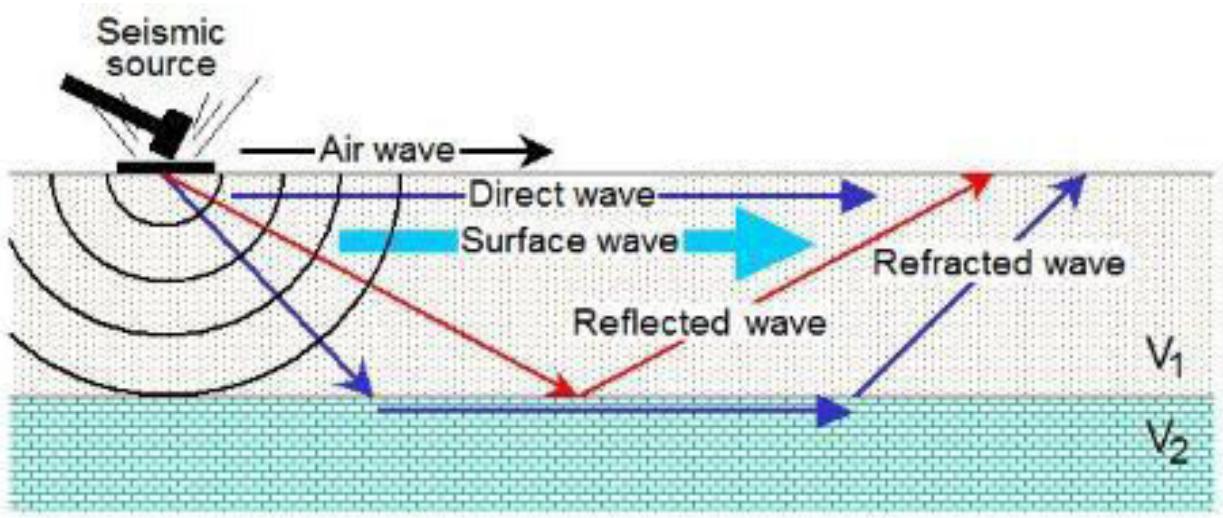

Figure (23): Major types of seismic waves based on propagation characteristics.

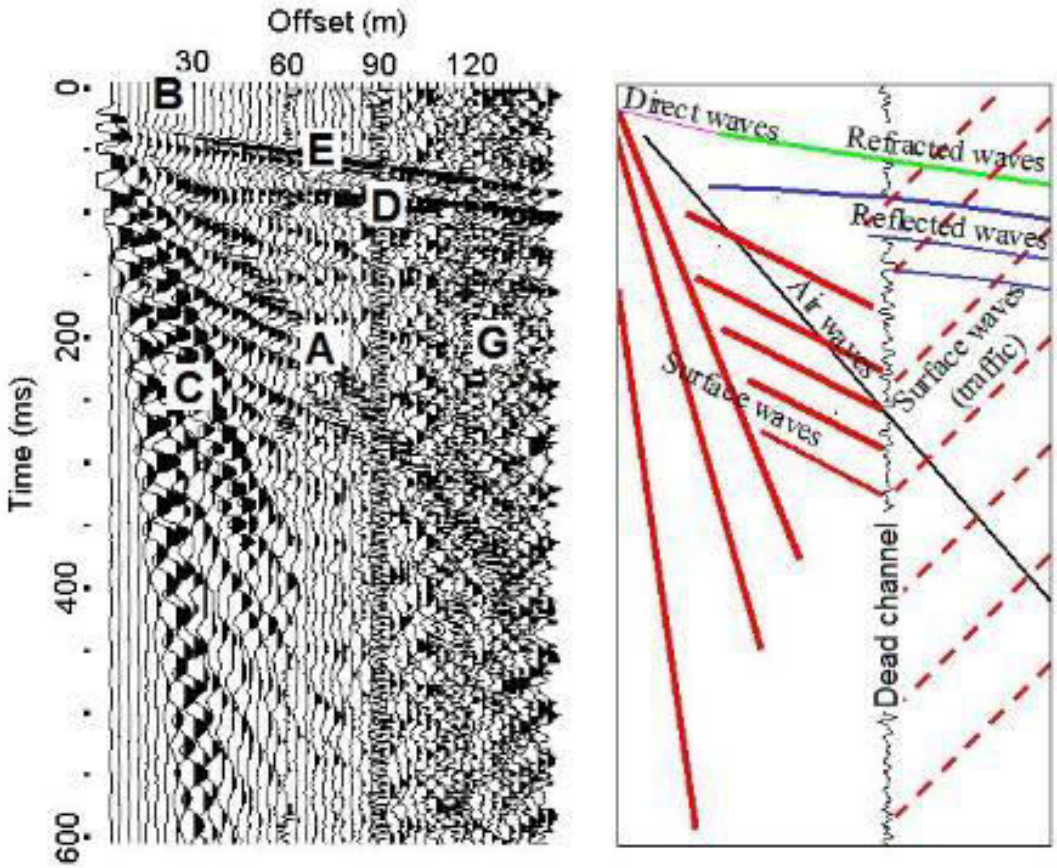

Figure (24): A field record and interpretation of different seismic events based on the arrival pattern.

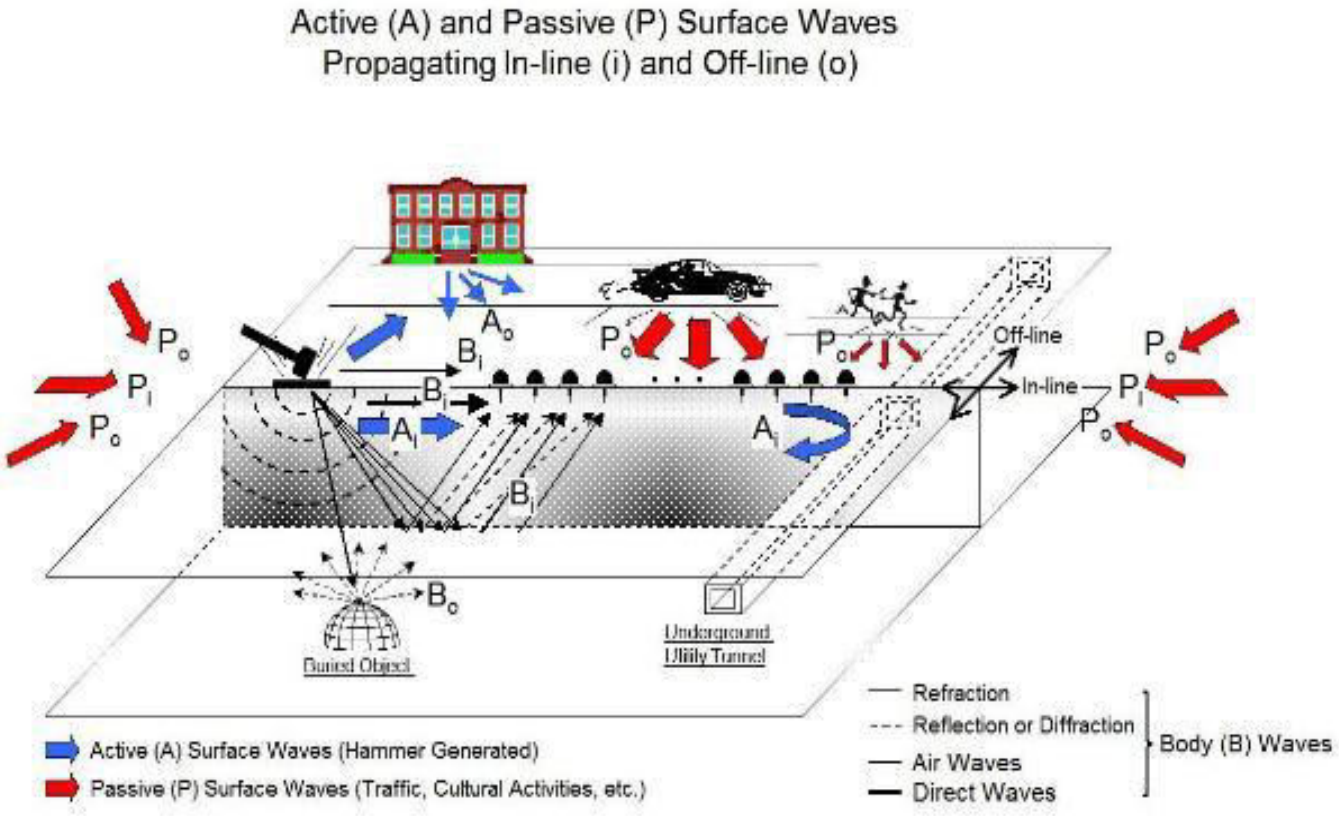

Figure (25): Illustration of active versus passive waves and inline versus offline waves.

Seismic Refraction Survey

A refraction survey uses refracted (or head) waves to deduce velocities of the layered-earth model. So-called first arrival information is used for the analysis (**Fig.26**). More generalized methods based on the turning waves from an arbitrary velocity model have also been used in recent days. This is called seismic refraction tomography. Historically the refraction method has been commonly used to map depth and velocity of bedrock.

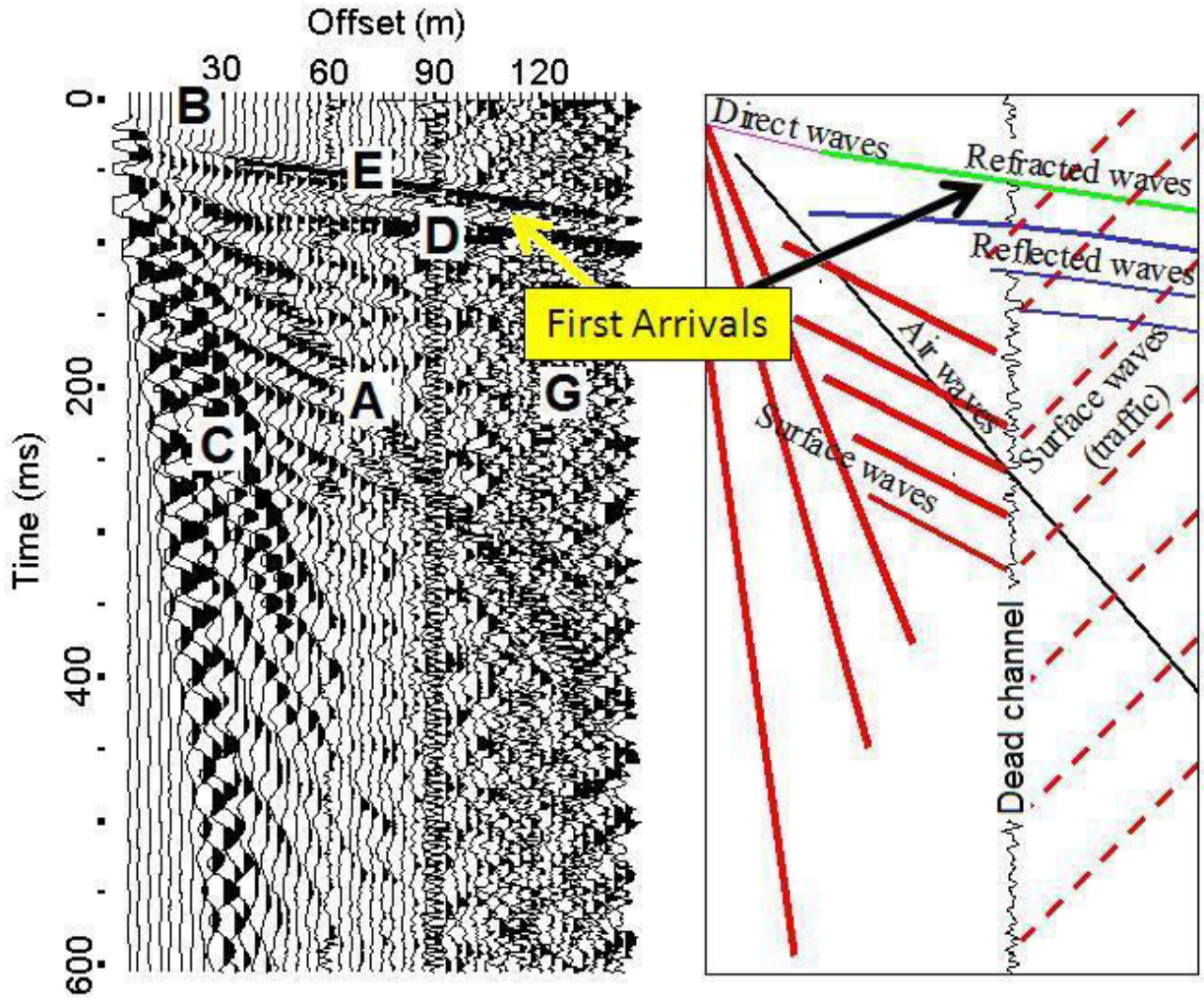

Figure (26): A field record showing that refraction waves constitute the first arrivals.

Seismic reflection method

Reflected waves from the interfaces between materials of significant different elastic properties (density and seismic velocity) are used for this type of survey. More specifically, a special acquisition and processing method called the "CDP (common-depth-point) method" is used and the final product from this survey is a section that depicts a cross-sectional image of the subsurface below the surveyed line. This method was invented and has been used traditionally in exploration for natural resources (oil, coal, etc.). Since the early 1980s, it has been

used mostly for shallow geotechnical engineering projects. Comparing these types of reflection surveys together, they are different in dimensions surveyed and resolution achieved. Field acquisition and data processing procedures are normally much more costly than with the other types of seismic survey.

The new technology has come with very easy and powerful instrumentation that reveals the subsurface features quite clear , figure 28. Instruments for seismic refraction survey try to show the data and the results directly on the instrument screen. It gives the operator a real chance to see the data and results before moving to another location. In some of these instruments the operator can do the filtering directly in the field and the picking for the first seismic wave arrivals and even to calculate the subsurface layers velocities and thicknesses.

Figure (28) : The modern instrument of seismic refraction – refraction surveying.

The seismic refraction instruments come with 12, 24, 48 channels. Usually each cable of 12 geophones takes out come on one reel. The spacing between one geophone and another depends on the instrument and the manufacturer. ABEM for

example makes the inter-distance of 12.5 meters. In this case the operator can work with inter-distance of 1 to 12.5 meters.

For the survey itself you can choose the suitable method, but the new technology permit the surveyor for 2D and 3D. For example you can use the 24 channel for roll along survey method. In this method the total spreading line move certain distance, which usually two third of the spreading distance. This will give a continuous survey with 1/3 overlap. The overlap depends on the type of the survey and the details wanted. In this roll along method the survey section length can be unlimited. The limitation however will depend on the interpretation software. The software here is very important to take all the data and connected to produce one cross section. The depth of the survey is mainly depending on the distance between the energy source and the geophones. In roll along survey method this distance always kept constant.

For 3D survey the geophone spreading can be arranged to cover the whole area. The data of this survey can be handled by sophisticated software. With this software you can do the filtering and connection for all spreading and get the 3D results. Some of this software is:

REFLEXW 1	**GPR / Reflection seismic 2D** **containing 2D data - analysis**
REFLEXW 2	**GPR / Reflection seismic 2D / 3D** **- containing 2D data analysis** **- 3D data interpretation**
REFLEXW 3	**Refraction / Reflection seismic& GPR 2D** **- containing 2D data analysis** **- modeling with wave field simulation** **- travel time inversion**

REFLEXW 4	**Complete reflection / refraction 2D / 3D** **containing 2D data - analysis** **- refraction travel time analysis** **- CMP processing, 3D data interpretation** **- FD forward modeling / tomography**

GROUND PENETRATING RADAR

Measurement principles

GPR is a geophysical technique which is particularly appropriate to image the soil in two or three dimensions with a high spatial resolution, up to a depth of several meters. GPR operates by transmitting high frequency (VHF-UHF, i.e., 10-2000 MHz) electromagnetic waves into the soil (see Figure 29). Wave propagation is governed by the frequency-dependent soil dielectric permittivity ε (determining wave velocity), electric conductivity σ (determining wave attenuation), magnetic permeability μ (determining wave velocity, affects attenuation), and their spatial distribution.

Electromagnetic contrasts create partial wave reflections and transmissions that are measured by a receiving antenna, depending on the mode of operation (reflection or transmission). For non-magnetic materials as prevalent in the environment, μ is equal to the free space magnetic permeability μ_0 and, thereby, does not affect wave Propagation compared to free space conditions.

The main characteristic of a GPR system is its operating frequency (centre frequency), determining resolution (typically considered as one quarter the wavelength) and penetration depth. Penetration depth is also determined by the electrical losses in the ground and scattering phenomena. The choice of an operating frequency is always a trade-off between resolution and penetration depth, as higher frequencies permit higher resolution but lower penetration depth. When

the antennas a coupled with the ground, dipole- and bowtie-type antennas are commonly used. For off-ground GPR, horn antennas a mostly used as they are more directive. Finally, antennas can be lowered in boreholes for both transmission and reflection measurements. Dipoles are then used as they geometrically extend in one dimension only. A radar system can use a single antenna as transmitter and receiver (mono static mode), both a transmitting and a receiving antenna (bi static mode, the most used), or several transmitters and receivers (multichannel systems). This last mode can be emulated by a bi static system and by performing measurements with different antenna separations or positions. In that case, measurements are more time consuming. Multi-offset measurements provide more information compared to single offset measurements. There are two families of GPR: The time domain systems, also called pulse radars, and the frequency domain systems. The time domain radars are by far the most commonly used. They are based on the transmission of a pulse in the time domain. The frequency domain systems transmit stepped-frequency continuous-waves and are increasingly used nowadays, not only because electronic components become more affordable, but also because it presents a series of advantages compared to pulse radars.

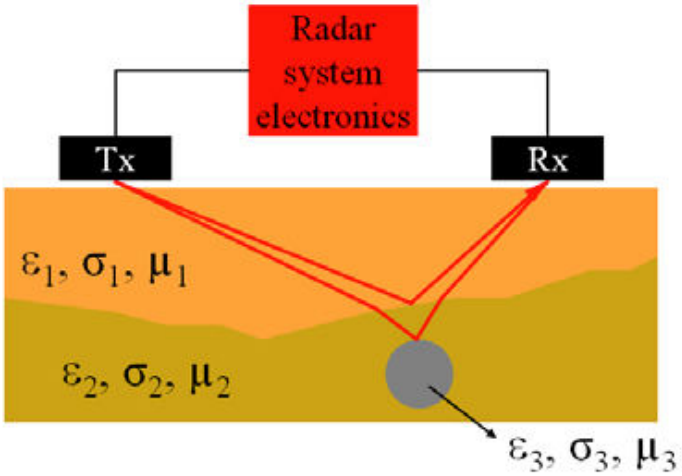

Figure (29) : Ground penetrating radar (GPR) basic principles. Tx is the transmitting antenna. Rx is the receiving antenna. Slid lines represent wave propagation paths (straight-ray approximation).

First GPR applications started in the 60s, mainly for geological surveys. In the 70s, the first commercial GPR systems were available and introduced in civil and military engineering, as well as in archaeology. In the 80s, GPR was introduced in forensic investigations. In the 90s, first researches and applications were initiated in agricultural and environmental engineering. Most GPR surveys were mainly focused on qualitative imaging of the subsurface. During the last decade, considerable efforts have been devoted to GPR for more quantitative analyses, thereby providing information regarding the soil properties and their spatial distribution. Progress in the technology itself has been made by progressively improving the dynamic range of the systems and efficiency of the antennas, speed of acquisition, and real-time user interfaces including visualization and basic processing of the radar images. Modern systems also include multi-channel acquisition.Figure 30 illustrates a GPR image of the subsurface, where measurements have been made along a transect. The profile is recorded with a Puls Ekko 1000 system (Sensors & Softwares Inc.) using fixed offset 250 MHz centre frequency shielded antennas with a transmitter-receiver separation of 25 cm. The horizontal step size was 5 cm and a time step of 0.2 ns was used. The recording is made in the central part of the Netherlands in a partial consolidated sand environment with an unconsolidated top layer.

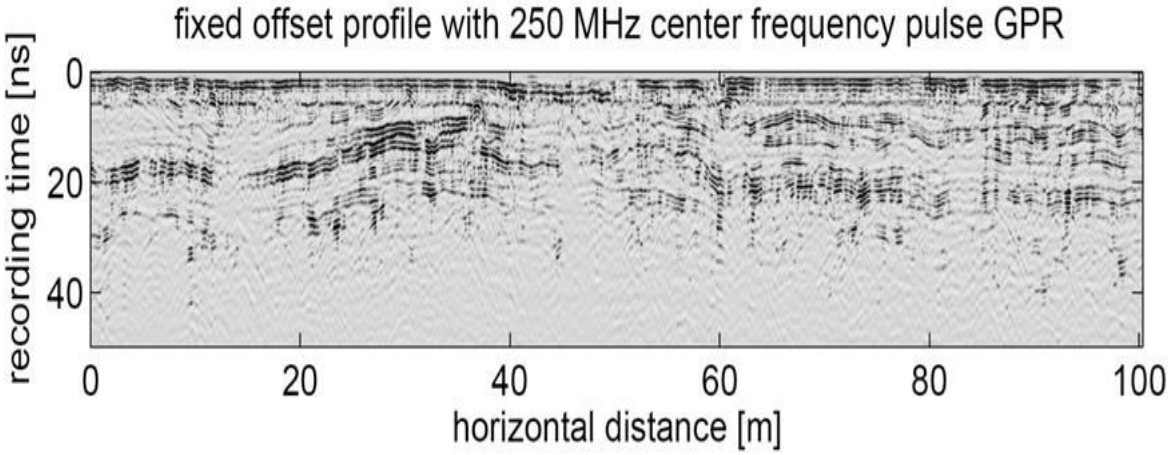

Figure (30) : GPR image of the subsurface, illustrating soil Stratigraphy up to a depth of about 5meters (Courtesy Evert Slob).

The choice of a particular GPR system or setup depends on the application, information that is intended to be retrieved , and processing algorithm that is intended to be used. Generally, GPR signal analysis is performed using ray-tracing approximations (see Figure 29 and Figure 31) and tomographic inversion. Several methodologies are generally adopted for determining wave propagation velocity and retrieve corresponding soil dielectric permittivity and correlated water content from the GPR data (Huisman et al., 2003) :

- Determination of the wave propagation time to a known interface using single-offset surface GPR (Grote et al., 2003; Lunt et al., 2005; van Overmeeren et al., 1997; Weiler et al., 1998);
- Detection of the velocity-dependent reflecting hyperbola of a buried object using single-offset surface GPR along a transect (Vellidis et al., 1990; Windsor et al., 2005);
- Extraction of stacking velocity fields from multi-offset radar soundings at a fixed central location (common midpoint method) (Garambois et al., 2002; Greaves et al., 1996);
- Determination of the ground-wave velocity for surface water content retrieval using multi- and single-offset surface GPR (Chanzy et al., 1996; Du and Rummel, 1994; Galagedara et al., 2003; Galagedara et al., 2005a; Galagedara et al., 2005b; Grote et al., 2003; Huisman et al., 2002; Huisman et al., 2001);
- Determination of the surface reflection coefficient using single-offset off-ground GPR (Chanzy et al., 1996; Redman et al., 2002; Serbin and Or, 2003; Serbin and Or, 2004);
- Determination of the two-dimensional spatial distribution of water between boreholes using transmission tomography (Alumbaugh et al., 2002; Binley et al., 2001; Rucker and Ferré, 2005; Zhou et al., 2001).

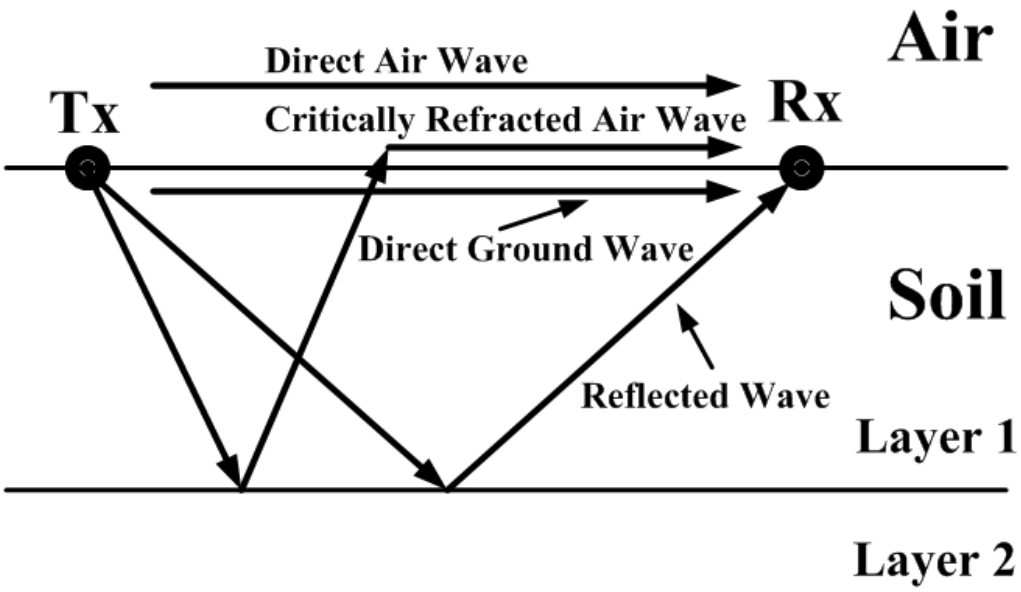

Figure (31) : Propagation paths of GPR waves in a two-layered soil.

Several manufacturers commercialize GPR systems nowadays. The oldest company is GSSI, which is the most important one present on the market, for both applications and research. All manufacturers propose a range of different antennas operating at different frequencies, from a few MHz to the GHz frequencies. Table 2 presents a list of the main GPR manufacturers, including the name of their radar products, and some key notes (not exhaustive list). The GSSI, Sensors & Software's, and Mala equipments are the most used in research by universities and research institutions and for agricultural/environmental engineering applications. Other companies are more dedicated to civil engineering applications (e.g., concrete inspection, buried pipe detection, etc.). All available GPR systems are time domain radars (pulse radars), except for 3d_Radar who proposes two stepped-frequency continuous-wave systems.

Frequency domain radars can be readily set up using vector network analyzer (VNA) technology. A series of VNA manufacturers exist and the two main ones

are Rohde & Schwarz and HP Agilent, each proposing a series of different systems. These systems are not listed here as they cannot yet be considered as GPR systems (their scope is not initially intended for such applications and they are presently used in GPR research only).

Table (2) : List of GPR manufacturers and commercial products

Manufacturer	Radar system	Key characteristics
GSSI	SIR-20	Antennas in the range 15-2600 MHz 2 channels
	SIR-3000	1 channel
Sensors & Software Inc	PulseEKKO PRO	Antennas: 12.5-1000 MHz 1 channel
	Noggin	Antennas: 250-1000 MHz
MALA GeoScience	RAMAC (X3M, ProEx, CX)	Antennas in the range 25-1000 MHz
	MIRA	Antenna array: 200, 400, 1300 MHz Up to 16 channels
IDS	RIS ONE	Antennas: 25-2000 MHz
	RIS MF Hi-Mod	Multi-frequency array
3D-Radar AS	3d-Radar Antenna arrays	Frequency domain radar Antenna array : 100-2000 MHz
	GeoScope	Antennas: 30-2000 MHz
Utsi Electronics	Groundvue	Antennas : 30-4000 MHz
RASCAN Systems LLC	Rascan	Investigation depths : 15-35 cm
PipeHawk	PipeHawk II	

References

1- P- and S-wave Seismic Reflection and Refraction Measurements at CCOC By Robert A. Williams, William J. Stephenson, Jack K. Odum, and David M. Worley2005, U.S. Geological Survey, Denver Federal Center, MS 966, Box 25046, Denver, CO 80225.

2- S.Lambot, G.Grandjean, K.Samyn, I.Cousin, J.Thiesson, A.Stevens, L.Chiarantini, T.Dahlin, 2009. Technical specifications of the system of geophysical sensors. Report N° FP7-DIGISOILD1.1,ages.

3-Orellana and Mooney H.M., 1966,"Master Curves For Schlumberger Arrangement", Madrid, P.34.

4- Keller G.V. and Frischknecht F.C., 1966, "Electrical methods in Geophysical Prospecting", Pergamon press , New York , reprinted ed., Chapt.3 , pp.89-180.

5-Sharma P.V., 1986, "Geophysical Methods in Geology" , 2nd Ed. ,Elsevier Science Publishing Co., Inc., Amestrdam , The Netherlands.442 pages.

6-Zohdy A. A. R., Eaton G. P., and Mabey D. R., 1990,"*Application Of Surface Geophysics To Ground-Water Investigations"*, P.123,Techniques of Water-Resources Investigations of the United States Geological Survey , 4th Ed., U.S. Geological Survey, Denver.

7- Griffiths D H and King R F ,1981, " Applied Geophysics fo Geologists and Engineers" the elements of geophysical prospecting, 2nd Ed. , Pergamon Press, 201 pages.

8-Kunetz G. , 1966 , "principles of direct current resistivity prospecting" ,Gebruder Borntraeger, Brlin-Nikolasse, 103 pages .

9-Todd D.K. , 1959,"Groundwater Hydrology", Jhon Wiley & Sons , Inc. , New York , Toppan Printing Company, Ltd. Japan, 336 pages.

10-Al-Khafaji W.M.S. 2014. A Geophysical Study to Evaluate the Groundwater Reserve and Structural Situation of South Sinjar Anticline Region NW-Iraq, PhD. Dissertation, University of Baghdad, College of Science, Department of Geology, 171

11-Kearey P. , Brooks M. , Hill I.,2002,"An Introduction to Geophysical Exploration", 3rd ed., Blackwell Science Ltd., USA, 281 pages.

12-Eric C. , 2015, Gravity and the figure of the Earth, Purdue University, Department of Earth and Atmospheric Sciences, West Lafayette, IN 47907-1397.

13-Dobrin M.B. and Savit C.H., 1988, Introduction to Geophysical prospecting, (4th Ed.), McGraw Hill, New York.

14-Park C. , 2015 , PARK SEISMIC LLC , seismic refraction and reflection method , http://parkseismic.com/Whatisseismicsurvey.html

15-Prof. Dr. Basim R. Hijab , 2011, Engineering Geophysics Lectures, University of Baghdad, College of Science , Department of Geology.

16- Valenta J., 2015, Introduction to Geophysics – Lecture Notes, Czech Republic development cooperation, 72 pages

17-Hammer S., 1939. Terrain corrections for gravimeter stations. Geophysics, 4 (3), 184–194.